		Transfection efficency (%)	% Infected cells
Mock			**30**
Rab1a wildtype myc	**Expressing**	45	38
	Non-expressing	55	30
Rab1a S25N myc	**Expressing**	37	45
	Non-expressing	63	22

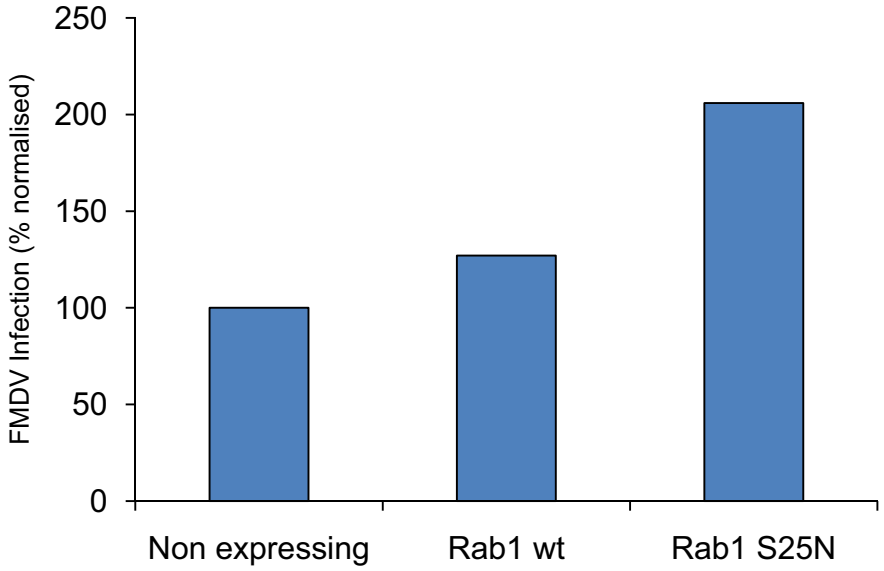


Figure 6.3(B): Experiment 2. The effects of dominant-negative Rab1 on FMDV infection of IBRS-2 cells
IBRS-2 cells were transfected to express wt Rab1a-myc or dn Rab1a S25N-myc for 14 hours and then infected with FMDV. *Upper Table*: For each transfection, the frequency of infection (% infected cells) was determined for the cells expressing the Rab1 transgene (i.e. green expressing cells) and for the non-expressing cell population (Non-expressing cells). The percentage of cells expressing a transgene is also shown (Transfection efficiency). *Lower Figure*: For each transfection, the frequency of infection of cells expressing Rab1 was normalised to the results for the non-expressing cell population.

		Transfection efficency (%)	% Infected cells
Mock			**40**
Rab1a wildtype myc	**Expressing**	36	42
	Non-expressing	64	30
Rab1a S25N myc	**Expressing**	21	59
	Non-expressing	79	33

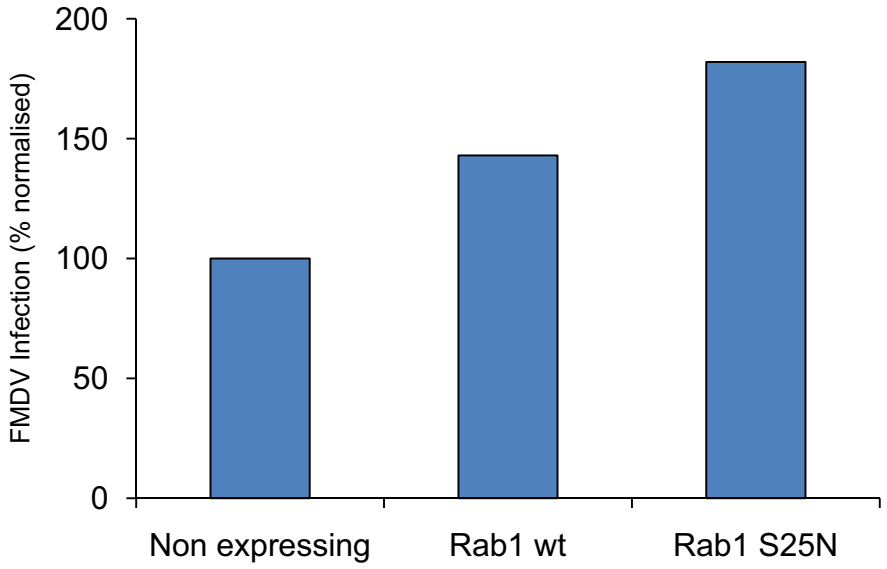


Figure 6.3(C): Experiment 3. The effects of dominant-negative Rab1 on FMDV infection of IBRS-2 cells
IBRS-2 cells were transfected to express wt Rab1a-myc or dn Rab1a S25N-myc for 14 hours and then infected with FMDV. *Upper Table*: For each transfection, the frequency of infection (% infected cells) was determined for the cells expressing the Rab1 transgene (i.e. green expressing cells) and for the non-expressing cell population (Non-expressing cells). The percentage of cells expressing a transgene is also shown (Transfection efficiency). *Lower Figure*: For each transfection, the frequency of infection of cells expressing Rab1 was normalised to the results for the non-expressing cell population.

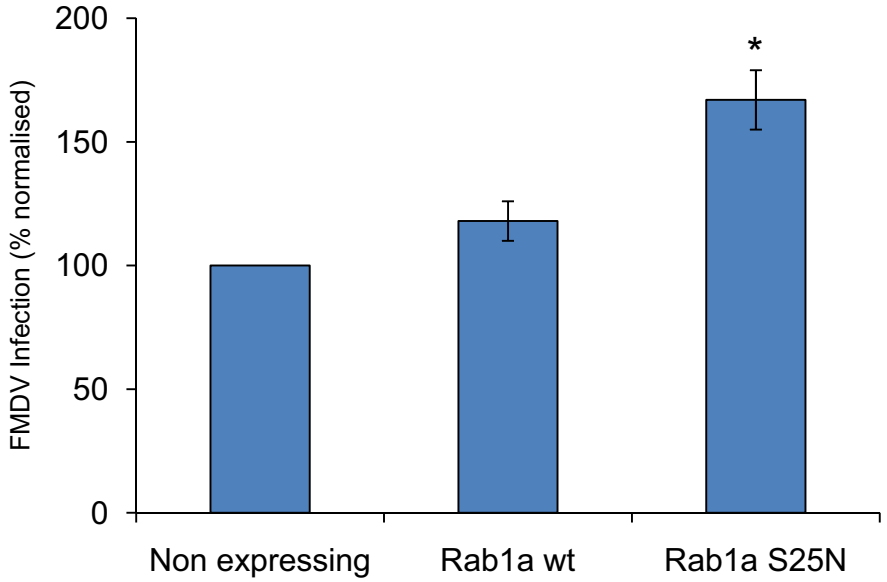


Figure 6.3(D): The effects of dominant-negative Rab1 on FMDV infection of IBRS-2 cells
Shown is the mean ± SD for the experiments shown in figure 6.3 (A-C). For each transgene (wt, dn S25N) the frequency of infection of cells expressing Rab1 was normalised to the results for the non-expressing cell population (*P* value: $* < 0.05$).

shows expression of wt Rab1a-myc increases infection by ~20%, in contrast expression of dn Rab1a S25N-myc increases infection by ~100%. Figure 6.3(C) also shows an increase to FMDV infection in cells expressing both wt and dn Rab1a proteins. An increase of ~40% is seen in cells expressing the wt Rab1a-myc and a ~75% increase is seen in cells expressing the dn Rab1a S25N-myc.

The mean level of infection for the three experiments is shown in Figure 6.3(D). Overall, it appears wt Rab1a-myc slightly increased the frequency of FMDV infection by ~20%, and dn Rab1a S25N-myc by ~70%. The apparent increase of FMDV infection caused by dn Rab1a S25N-myc indicates that Rab1 activity is not required for successful FMDV replication and the inactivation of Rab1 function appears to be enhanced FMDV infection.

6.3 Rab2

Rab2 is a resident protein in the ERGIC and necessary for ER to Golgi transport (Tisdale et al., 1992). Rab2 has also been found to recruit COPI onto the ERGIC membrane through Arf1 and is thought to be involved in the recycling of proteins back to the ER and onto the Golgi (Tisdale, 1999; Tisdale and Jackson, 1998) (see section 1.9.3). To determine if Rab2 has a part to play in FMDV infection the dn Rab2 S20N myc was used, which has a mutation that renders it unable to bind GTP, and is therefore inactive (Tisdale et al., 1992).

6.3.1 The effects of dominant-negative Rab2 on membranes in the early secretory pathway

As previously described in the above experiments for Rab1, the effects of dn Rab2 on membranes of the early secretory pathway was investigated by confocal microscopy by labelling membranes for the Golgi. Figure 6.4 shows

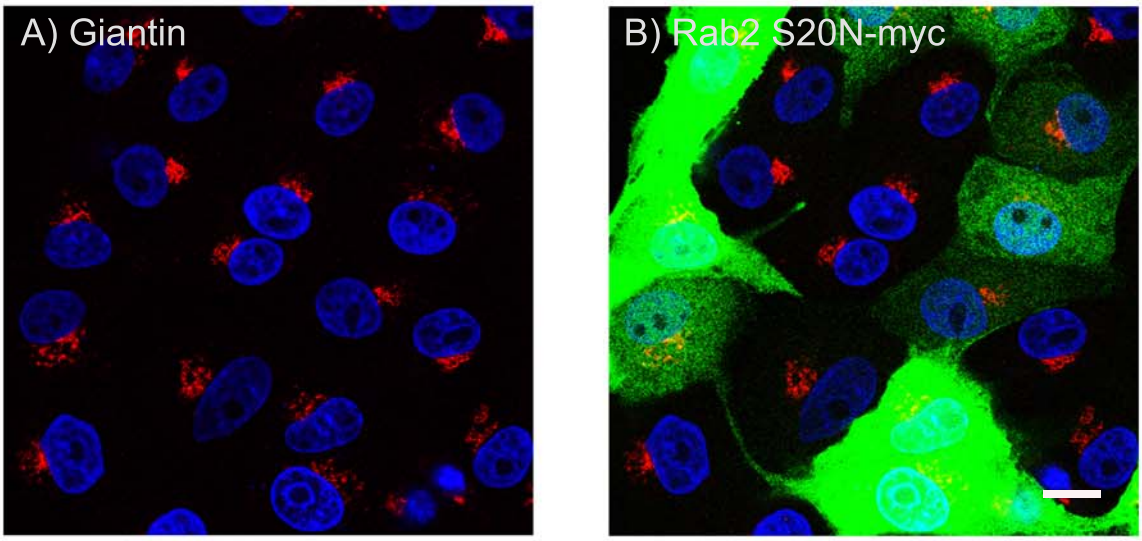


Figure 6.4 The effects of dn Rab2 expression on the Golgi
IBRS-2 cells were transfected to express dn Rab2 S20N-myc for 14 hours and labelled for the Golgi (Giantin panels A-B). Cells expressing Rab2 are shown as green; the Golgi is shown in red Panel B shows a merged image for red and green fluorescence. The cell nuclei were stained with DAPI and are shown as blue. Scale bar = 10 μm.

cells expressing dn Rab2 S20N-myc (shown in green, panel B) and labelled for the Golgi (Giantin, shown in red panels A-B). Although Golgi labelling remains in cells expressing the dn Rab2 S20N-myc the peri-nuclear labelling appears to become fragmented when the protein is over-expressed (Fig 6.4 A-B).

6.3.2 The effect of dominant-negative Rab2 on FMDV infection

In the next experiment the effect of dn Rab2 on FMDV infection was investigated. IBRS-2 cells were transfected with either wt Rab2-myc or dn Rab2 S20N-myc for 14 hours. The transfected cells were then infected with FMDV $O1Kcad_2$ at a low MOI (MOI. of 0.5) for four hours. Cells were processed for IFCM as previously described (see section 4.2.2). Infected cells are shown in red.

Figure 6.5 shows cells expressing wt Rab2-myc or dn Rab2 S20N-myc (shown as green panels A and D) and infected with FMDV (shown as red, panels B and E). Expression of both wt Rab2-myc and dn Rab2 S20N-myc appear to increase the frequency of FMDV infection compared to cells in the non-expressing population.

The above experiments were repeated three times and the effect of the dn Rab2 proteins on infection quantified. The frequency of infection was calculated for the cells expressing a Rab2 transgene (wt Rab2, dn Rab2 S20N) and the data normalised to the results for the non-expressing cell population of the same cover-slip. Figure 6.6(A-C) shows data for three independent experiments. The mean of the three experiments is shown in figure 6.6(D). Figure 6.6(A) shows that expression of wt Rab2-myc reduced the frequency of infected cells by ~10% when compared to cells of the non-expressing population. In contrast, the frequency of infection increased by ~70% in cells

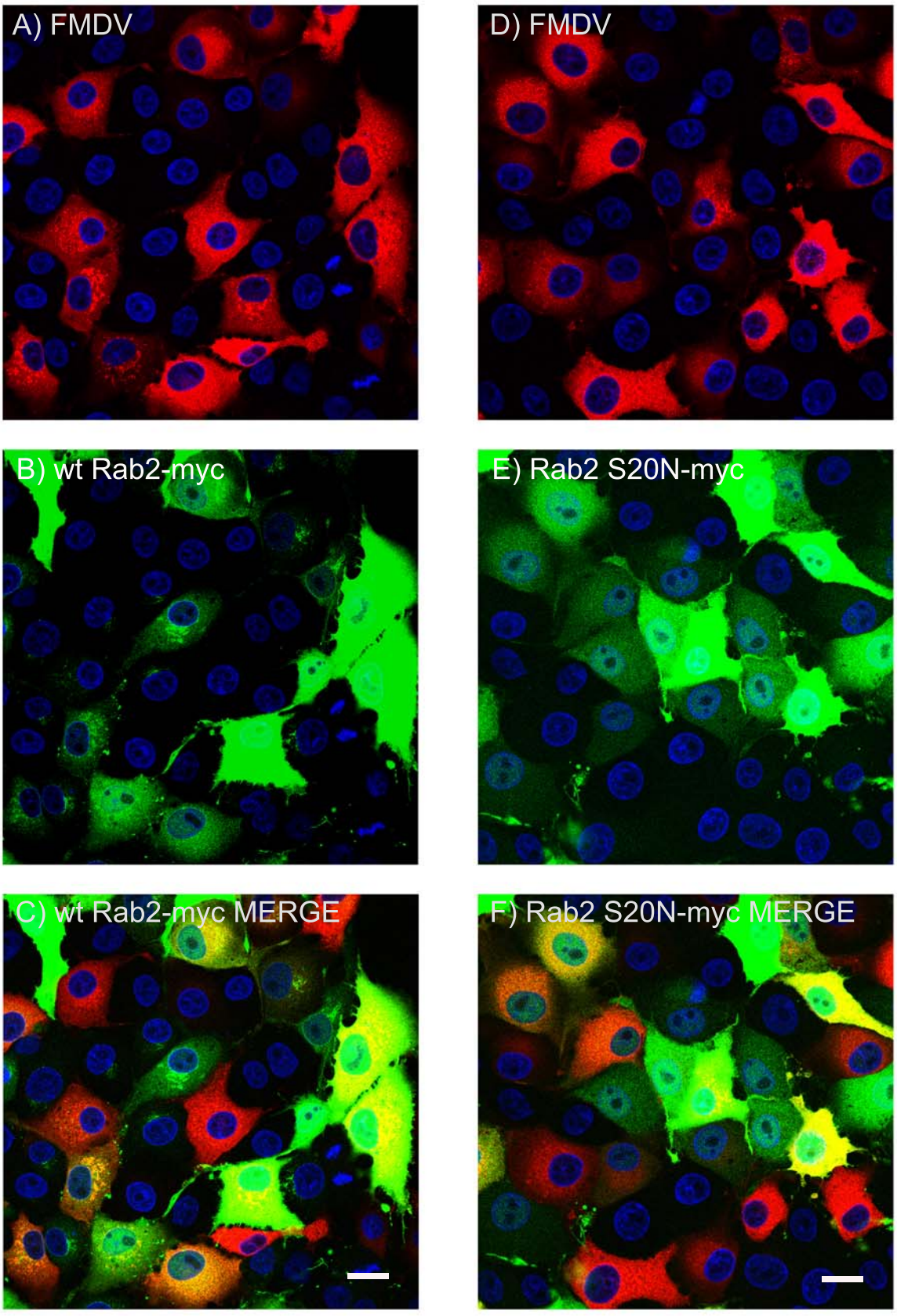


Figure 6.5 FMDV Infection of cells expressing wt or dn Rab2 (S20N)
IBRS-2 cells were transfected to express wt Rab2-myc (A-C) or dn Rab2 S20N-myc (D-F) for 14 hours and then infected with FMDV. Cells expressing Rab2 are shown as green. Infected cells are shown as red. Panels A and D show labelling for FMDV. Panels B and E show the signal for Rab2-myc. Panels C and F showed merged images for red and green fluorescence. The cell nuclei were stained with DAPI and are shown as blue. Scale bar = 10 μm.

expressing the dn Rab2 S20N-myc. In the next experiment (Figure 6.6B) an increase in FMDV infection was observed for both wt Rab2-myc and dn Rab2 S20N-myc. Over a 2.5 fold increase was observed in cells expressing the wt Rab2-myc protein, whereas a 2 fold increase was seen in cells expressing the dn Rab2 S20N-myc. Similarly, the third experiment (Figure 6.6C) shows an apparent increase in FMDV infection of ~50% in cells expressing either of the Rab2 proteins.

The mean level of infection for the three experiments is shown in Figure 6.6(D). Overall, it appears wt Rab2-myc increased the frequency of FMDV infection by ~60%, and dn Rab2 S20N-myc by ~75%. The observed increase in FMDV infection caused by expression of wt Rab2-myc may be due to the over-expression of the protein having a dominant-negative effect on endogenous Rab2. Expression of dn Rab2 is thought to prevent the fusion of ERGIC vesicles and the recruitment of COPI to ERGIC membranes. The apparent increase of FMDV infection observed in cells expressing dn Rab2 S20N-myc may indicate that the inactivation of Rab2 activity is advantageous to FMDV replication.

6.4 Rab6

Rab6 is associated with the Golgi and located on TGN membranes (Antony et al., 1992) and the medial and *trans* cisternae (Goud et al., 1990). The localisation and use of dn proteins of Rab6 suggests it may be involved in intra-Golgi transport (Martinez et al., 1994). Expression of wt Rab6 and the constituently active version of the protein reduce transport between Golgi compartments without effecting ER to Golgi transport. In contrast over expression of the dn Rab6 results in an accumulation of protein in late Golgi compartments and a delay in protein secretion (Martinez et al., 1994). The

		Transfection efficency (%)	% Infectied cells
Mock			**27**
Rab2 wildtype myc	**Expressing**	44	29
	Non-expressing	56	31
Rab2 S20N myc	**Expressing**	39	41
	Non-expressing	61	22

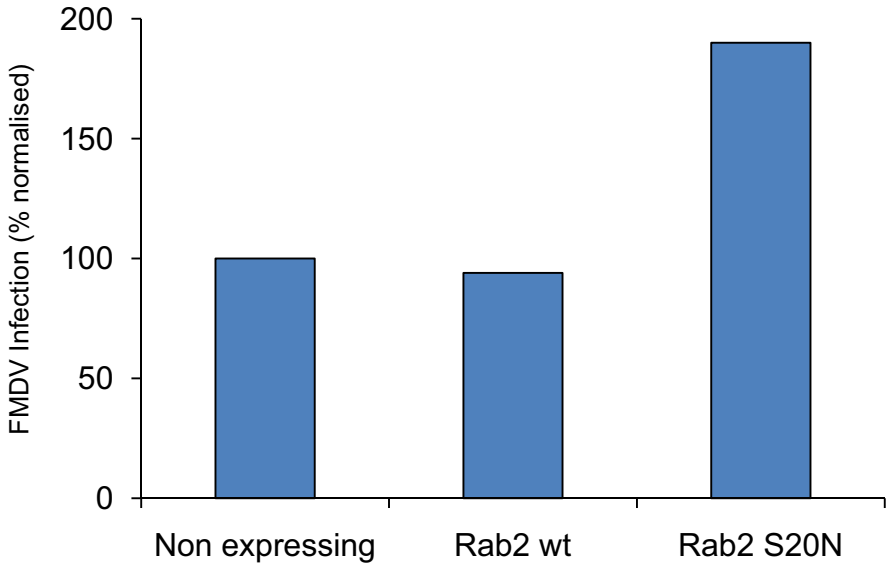


Figure 6.6(A): Experiment 1. The effects of dominant-negative Rab2 on FMDV infection of IBRS-2 cells
IBRS-2 cells were transfected to express wt Rab2-myc or dn Rab2 S20N-myc for 14 hours and then infected with FMDV. *Upper Table*: For each transfection, the frequency of infection (% infected cells) was determined for the cells expressing the Rab2 transgene (i.e. green expressing cells) and for the non-expressing cell population (Non-expressing cells). The percentage of cells expressing a transgene is also shown (Transfection efficiency). *Lower Figure*: For each transfection, the frequency of infection of cells expressing Rab2 was normalised to the results for the non-expressing cell population.

		Transfection efficency (%)	% Infected cells
Mock			**30**
Rab2 wildtype myc	**Expressing**	51	41
	Non-expressing	49	18
Rab2 S20N myc	**Expressing**	44	44
	Non-expressing	56	22

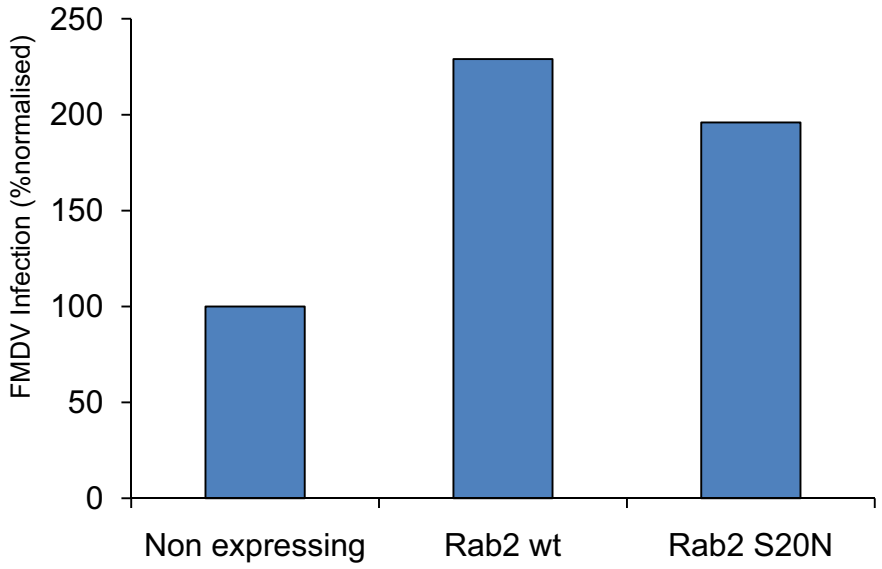


Figure 6.6(B): Experiment 2. The effects of dominant-negative Rab2 on FMDV infection of IBRS-2 cells
IBRS-2 cells were transfected to express wt Rab2-myc or dn Rab2 S20N-myc for 14 hours and then infected with FMDV. *Upper Table*: For each transfection, the frequency of infection (% infected cells) was determined for the cells expressing the Rab2 transgene (i.e. green expressing cells) and for the non-expressing cell population (Non-expressing cells). The percentage of cells expressing a transgene is also shown (Transfection efficiency). *Lower Figure*: For each transfection, the frequency of infection of cells expressing Rab2 was normalised to the results for the non-expressing cell population.

		Transfection efficency (%)	% Infected cells
Mock			**40**
Rab2 wildtype myc	**Expressing**	33	47
	Non-expressing	67	32
Rab2 S20N myc	**Expressing**	33	45
	Non-expressing	67	30

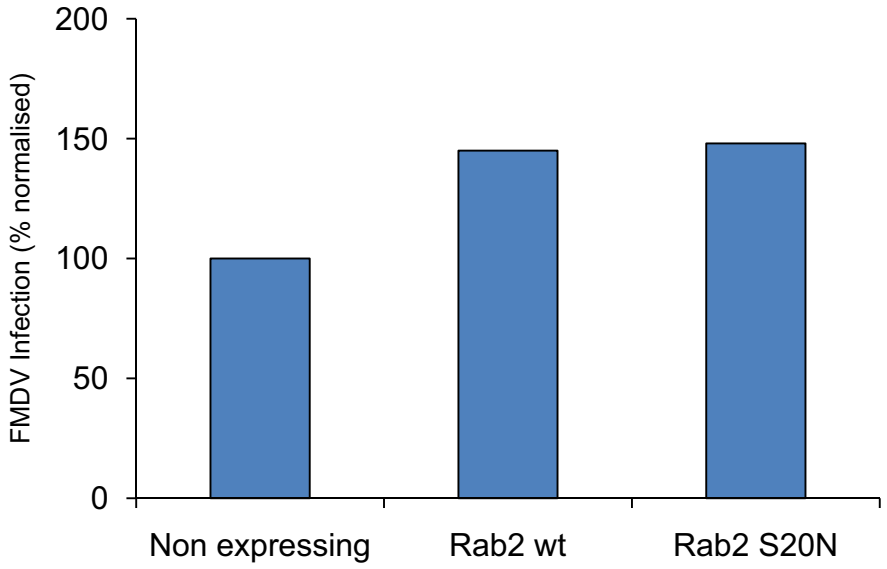


Figure 6.6(C): Experiment 3. The effects of dominant-negative Rab2 on FMDV infection of IBRS-2 cells
IBRS-2 cells were transfected to express wt Rab2-myc or dn Rab2 S20N-myc for 14 hours and then infected with FMDV. *Upper Table*: For each transfection, the frequency of infection (% infected cells) was determined for the cells expressing the Rab2 transgene (i.e. green expressing cells) and for the non-expressing cell population (Non-expressing cells). The percentage of cells expressing a transgene is also shown (Transfection efficiency). *Lower Figure*: For each transfection, the frequency of infection of cells expressing Rab2 was normalised to the results for the non-expressing cell population.

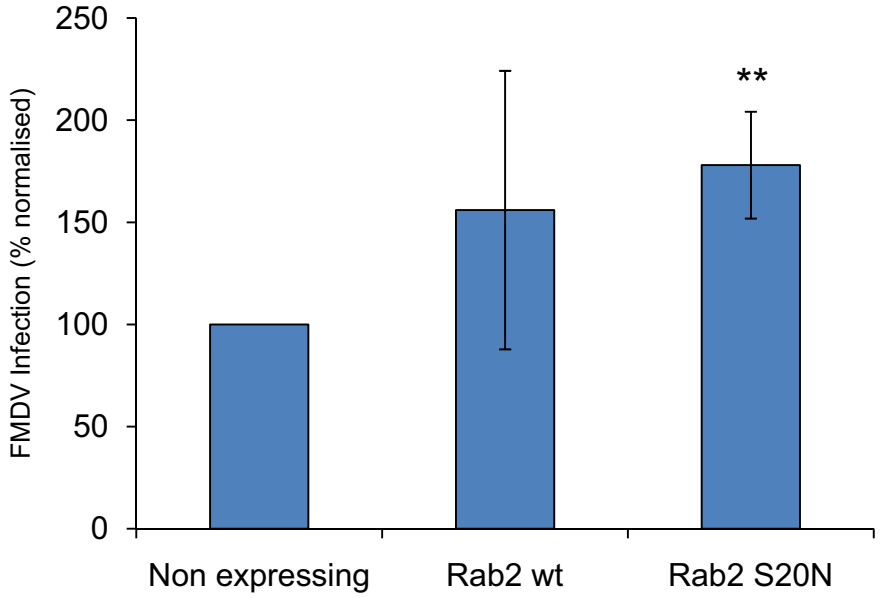


Figure 6.6(D): The effects of dominant-negative Rab2 on FMDV infection of IBRS-2 cells
Shown is the mean ± SD for the experiments shown in figure 6.6 (A-C). For each transgene (wt, dn S20N) the frequency of infection of cells expressing Rab2 was normalised to the results for the non-expressing cell population (*P* value: ** < 0.01).

Previously characterised dominant negative Rab6 T27N myc was used to investigate the role of Rab6 and intra-Golgi transport in FMDV infection.

6.4.1 The effects of dominant-negative Rab6 on membranes in the early secretory pathway

The effect of dn Rab6 on membranes of the early secretory pathway was investigated by immunofluorescence confocal microscopy as previously described (see section 6.2.1). Figure 6.7 shows cells expressing wt Rab6-myc or dn Rab6 T27N-myc (shown in green, panels B and D) and labelled for the Golgi (Giantin shown in red, panels A-D). Co-localisation of Golgi labelling and wt Rab6-myc was observed, however expression of wt Rab6-myc and dn Rab6 T27N-myc did not appear to have any effect on Golgi as it remained intact (Fig 6.7 A-D).

6.4.2 The effect of dominant-negative Rab6 on FMDV infection

The next experiment investigated the effect of dn Rab6 on FMDV infection. IBRS-2 cells were transfected with either wt Rab6-myc or dn Rab6 T27N-myc for 14 hours. The transfected cells were then infected with FMDV O1Kcad$_2$ at a low MOI (MOI. of 0.5) for four hours. Cells were processed for IFCM as previously described (see section 4.2.2). Infected cells are shown in red in figures.

Figure 6.8 shows cells expressing wt Rab6-myc or dn Rab6 T27N-myc (shown in green, panels B and E) and infected with FMDV (shown in red, panels A and D). The frequency of infection did not appear to be affected in cells expressing either wt Rab6-myc or dn Rab6 T27N-myc when compared to cells in the non-expressing population.

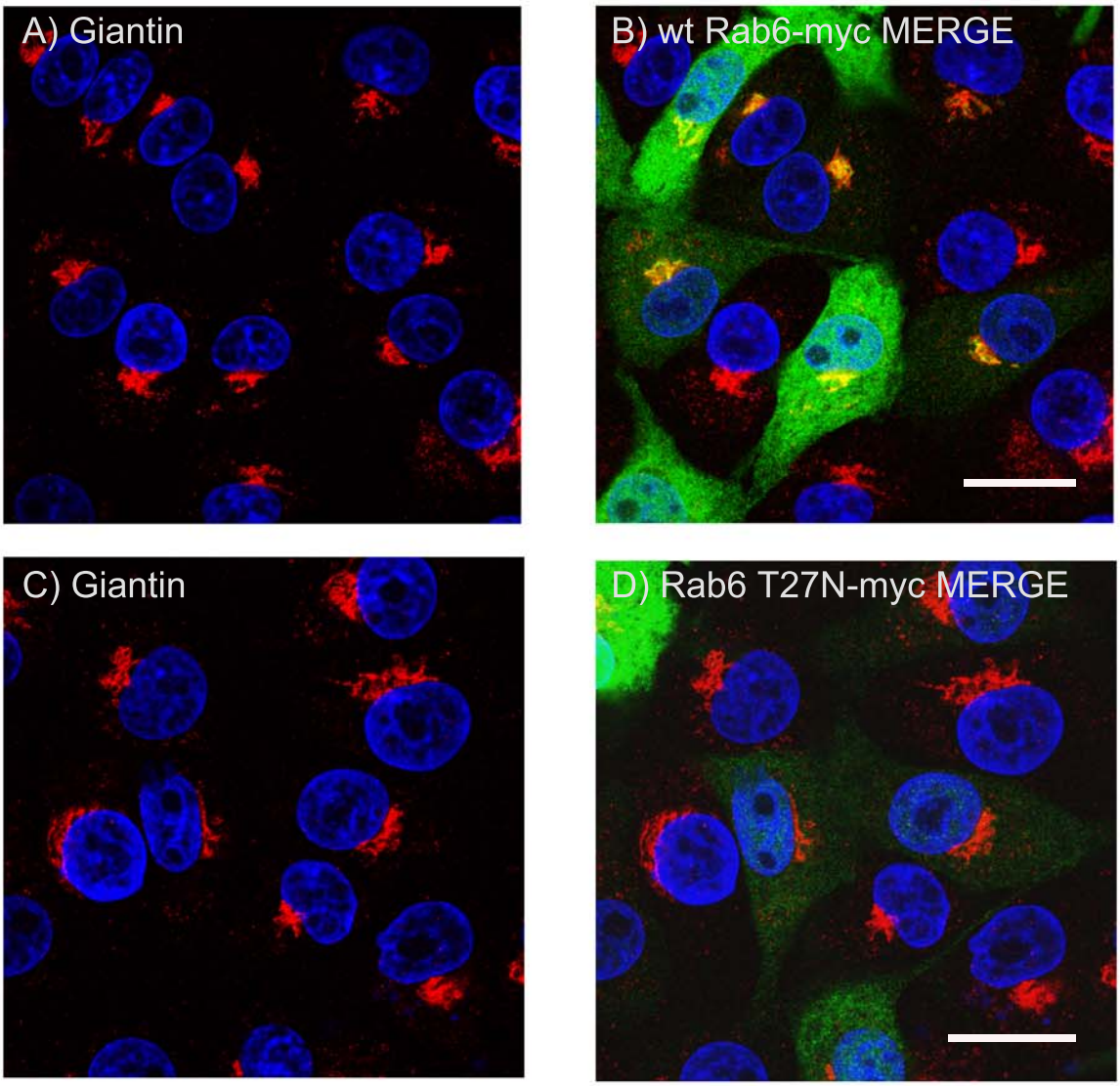


Figure 6.7 The effects of Rab6 expression on the Golgi
IBRS-2 cells were transfected to express wt Rab6-myc (panels A-B) or dn Rab6 T27N-myc (panels C-D) for 14 hours and labelled for the Golgi (Giantin panels A-D). Cells expressing Rab6 are shown as green; the Golgi is shown in red. Panels B and D showed merged images for red and green fluorescence. The cell nuclei were stained with DAPI and are shown as blue. Scale bar = 10 μm.

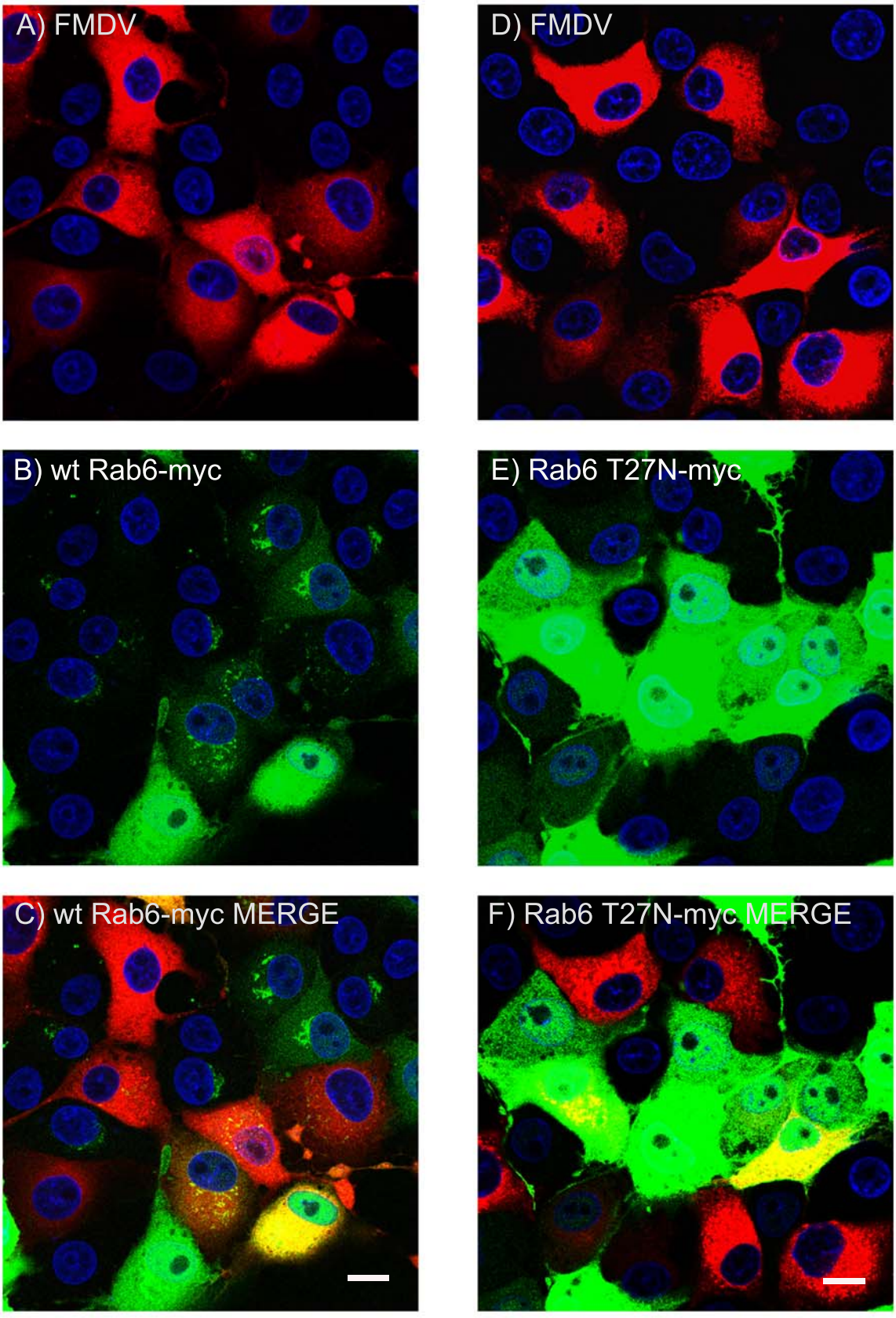


Figure 6.8 FMDV Infection of cells expressing wt or dn Rab6 (T27N)
IBRS-2 cells were transfected to express wt Rab6-myc (A-C) or dn Rab6 T27N-myc (D-F) for 14 hours and then infected with FMDV. Cells expressing Rab6 are shown as green. Infected cells are shown as red. Panels A and D show labelling for FMDV. Panels B and E show the signal for Rab6-myc. Panels C and F showed merged images for red and green fluorescence. The cell nuclei were stained with DAPI and are shown as blue. Scale bar = 10 μm.

The above experiment was repeated twice and the effect of the dn Rab6 proteins on infection quantified. The frequency of infection was calculated for the cells expressing a Rab6 transgene (wt Rab6, dn Rab6 T27N) and the data normalised to the results for the non-expressing cell population of the same cover-slip. Figure 6.9(A-B) show two experiments carried out independently, with figure 6.9(C) showing the mean of the experiments. The first experiment (Figure 6.9 A) shows an increase (~20%) in the frequency of infection in cells expressing wt Rab6-myc, whereas expression of dn Rab6 T27N-myc did not affect the frequency of infection when compared to cells of the non-expressing population. The second experiment (Figure 6.9 B) showed similar results with wt Rab6-myc increasing infection by ~20% and dn Rab6 T27N-myc having no effect on infection levels.

The mean level of infection for the two experiments is shown in Figure 6.9(C). Overall, it appears wt Rab6-myc only slightly increased the frequency of FMDV infection by ~20%, whereas dn Rab6 T27N-myc did not have any effect on FMDV infection. The observed increase in FMDV infection caused by expression of wt Rab6-myc was only 20% which may be due to biological variance and therefore was not considered significant. Expression of dn Rab6 T27N-myc had no effect on FMDV infection and is therefore inter-golgi transport is unlikely to be involved in infection.

6.5 Rab34

Rab34 has two known effector molecules: Rab-interacting lysosomal protein (RLIP), which is involved in Rab34 interaction with Dynein microtubule motors (Wang and Hong, 2002), and hmunc13, a protein kinase linked to the induction of apoptosis (Speight and Silverman, 2005). In addition Rab34 has also been implicated in macropinocytosis (Sun et al., 2003) and the

		Transfection efficency (%)	% Infected cells
Mock			**24**
Rab6 wildtype myc	**Expressing**	30	33
	Non-expressing	70	28
Rab6 T27N myc	**Expressing**	21	25
	Non-expressing	79	25

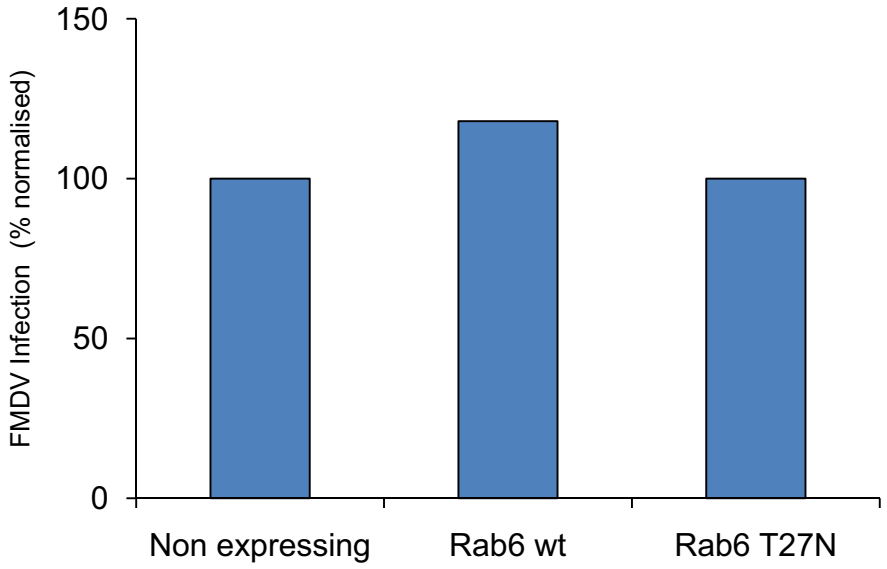


Figure 6.9(A): Experiment 1. The effects of dominant-negative Rab6 on FMDV infection of IBRS-2 cells
IBRS-2 cells were transfected to express wt Rab6-myc or dn Rab6 T27N-myc for 14 hours and then infected with FMDV. *Upper Table*: For each transfection, the frequency of infection (% infected cells) was determined for the cells expressing the Rab6 transgene (i.e. green expressing cells) and for the non-expressing cell population (Non-expressing cells). The percentage of cells expressing a transgene is also shown (Transfection efficiency). *Lower Figure*: For each transfection, the frequency of infection of cells expressing Rab6 was normalised to the results for the non-expressing cell population.

		Transfection efficency (%)	% Infected cells
Mock			**35**
Rab6 wildtype myc	**Expressing**	51	40
	Non-expressing	49	30
Rab6 T27N myc	**Expressing**	41	32
	Non-expressing	59	30

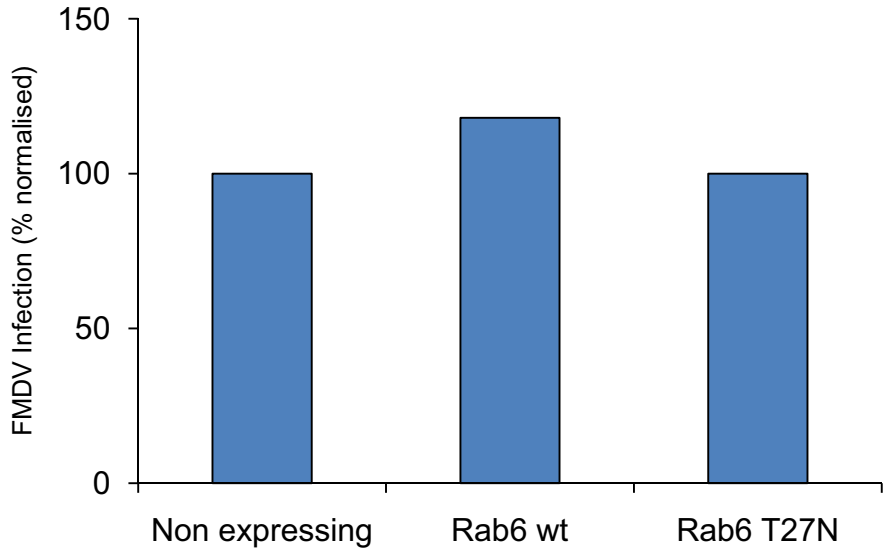


Figure 6.9(B): Experiment 2. The effects of dominant-negative Rab6 on FMDV infection of IBRS-2 cells
IBRS-2 cells were transfected to express wt Rab6-myc or dn Rab6 T27N-myc for 14 hours and then infected with FMDV. *Upper Table*: For each transfection, the frequency of infection (% infected cells) was determined for the cells expressing the Rab6 transgene (i.e. green expressing cells) and for the non-expressing cell population (Non-expressing cells). The percentage of cells expressing a transgene is also shown (Transfection efficiency). *Lower Figure*: For each transfection, the frequency of infection of cells expressing Rab6 was normalised to the results for the non-expressing cell population.

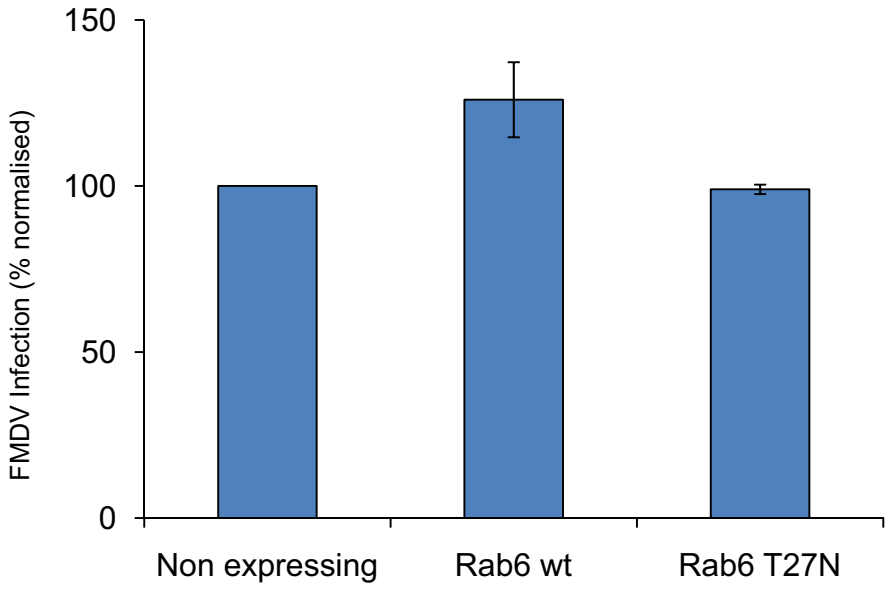


Figure 6.9(C): The effects of dominant-negative Rab6 on FMDV infection of IBRS-2 cells
Shown is the mean ± SD for the experiments shown in figure 6.9 (A-B). For each transgene (wt or dn T27N) the frequency of infection of cells expressing Rab6 was normalised to the results for the non-expressing cell population.

translocation of lysosomes to the microtubule organising centre (MTOC) (Wang and Hong, 2002). More recently Rab34 has been shown to localise to the Golgi and is believed to be involved in the early secretory pathway. The use of dn Rab34 proteins has indicated that Rab34 is required for export of proteins from the Golgi to the plasma membrane, upstream of the trans-Golgi-network (TGN), but not for ER to Golgi transport (Goldenberg et al., 2007).

In this study, the dominant negative Rab34 T66N-GFP (Goldenberg et al., 2007) was used to investigate whether a block in intra-Golgi transport and secretion of proteins to the cell surface would have any effects on FMDV infection.

6.5.1 The effects of dominant-negative Rab34 on membranes in the early secretory pathway

The effect of dn Rab34 on membranes of the early secretory pathway was investigated by immunofluorescence confocal microscopy as previously described (see section 6.2.1). Figure 6.10 shows cells expressing wt Rab34-GFP (shown in green, panels B, D and F) and labelled for the ER (shown in red, panels A-B), the ERGIC (shown in red, panels C-D) or the Golgi (shown in red, panels E-F). Expression of wt Rab34-GFP does not appear to alter ER (Fig 6.10 A-B) or Golgi labelling (Fig 6.10 C-D). In comparison, ERGIC labelling appears diffuse in a number of cells expressing the protein; however this is not seen in all cells expressing wt Rab34-GFP (Fig 6.10 E-F). Figure 6.11 shows cells expressing dn Rab34 T66N-GFP (shown in green, panels B, D and F) and labelled for the ER (shown in red, panels A-B), the ERGIC (shown in red, panels C-D) or the Golgi (shown in red, panels E-F). In cells expressing dn

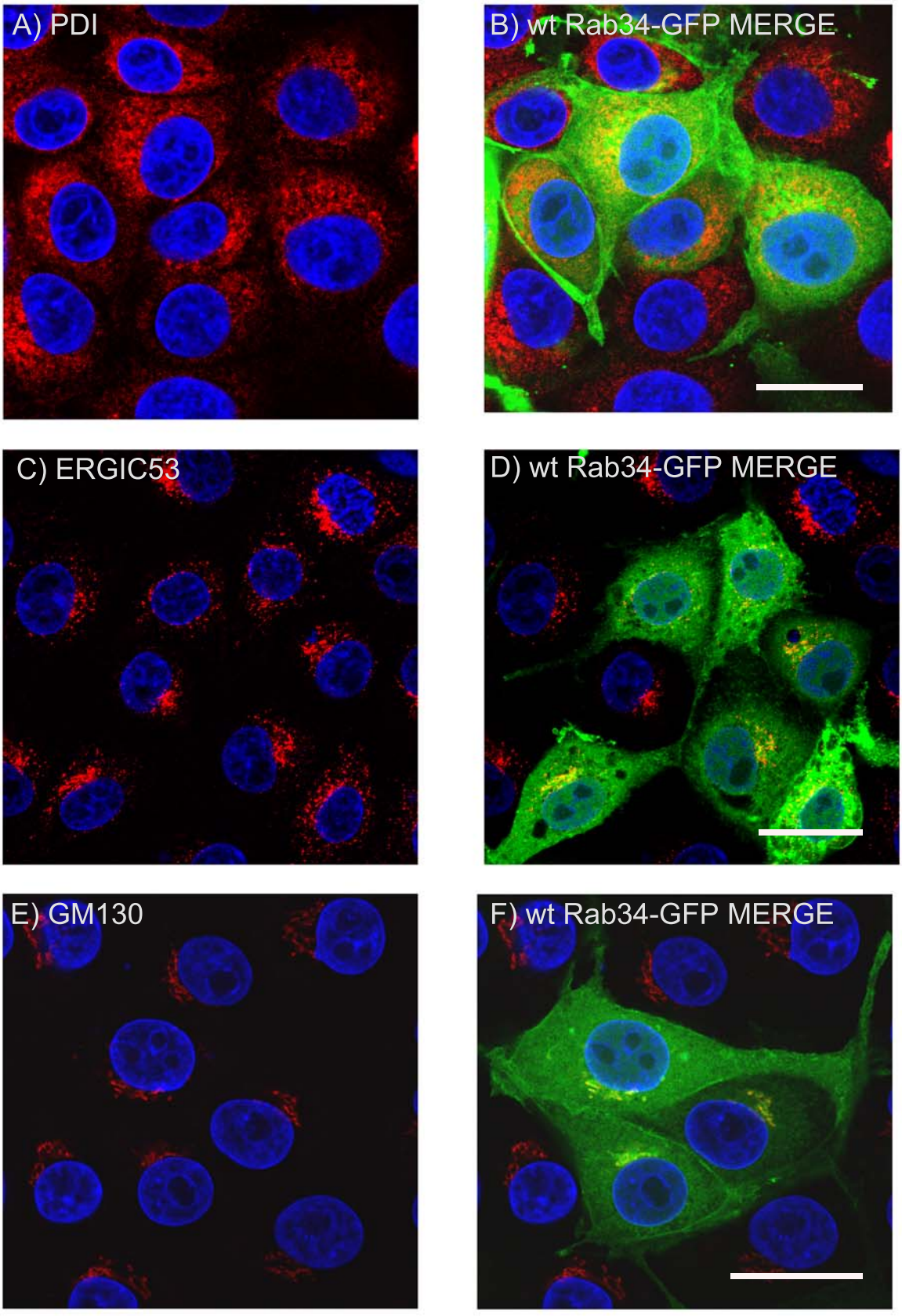


Figure 6.10 The effects of wt Rab34 expression on the ER, ERGIC and Golgi
IBRS-2 cells were transfected to express wt Rab34-GFP for 14 hours and labelled for the ER (PDI; panels A & B), the ERGIC (ERGIC53; panels C & D) or the Golgi (GM130; panels E & F). Cells expressing Rab34 are shown as green; the ER, ERGIC and Golgi are shown in red. Panels B, D & F show merged images for red and green fluorescence. The cell nuclei were stained with DAPI and are shown as blue. Scale bar = 10 μm.

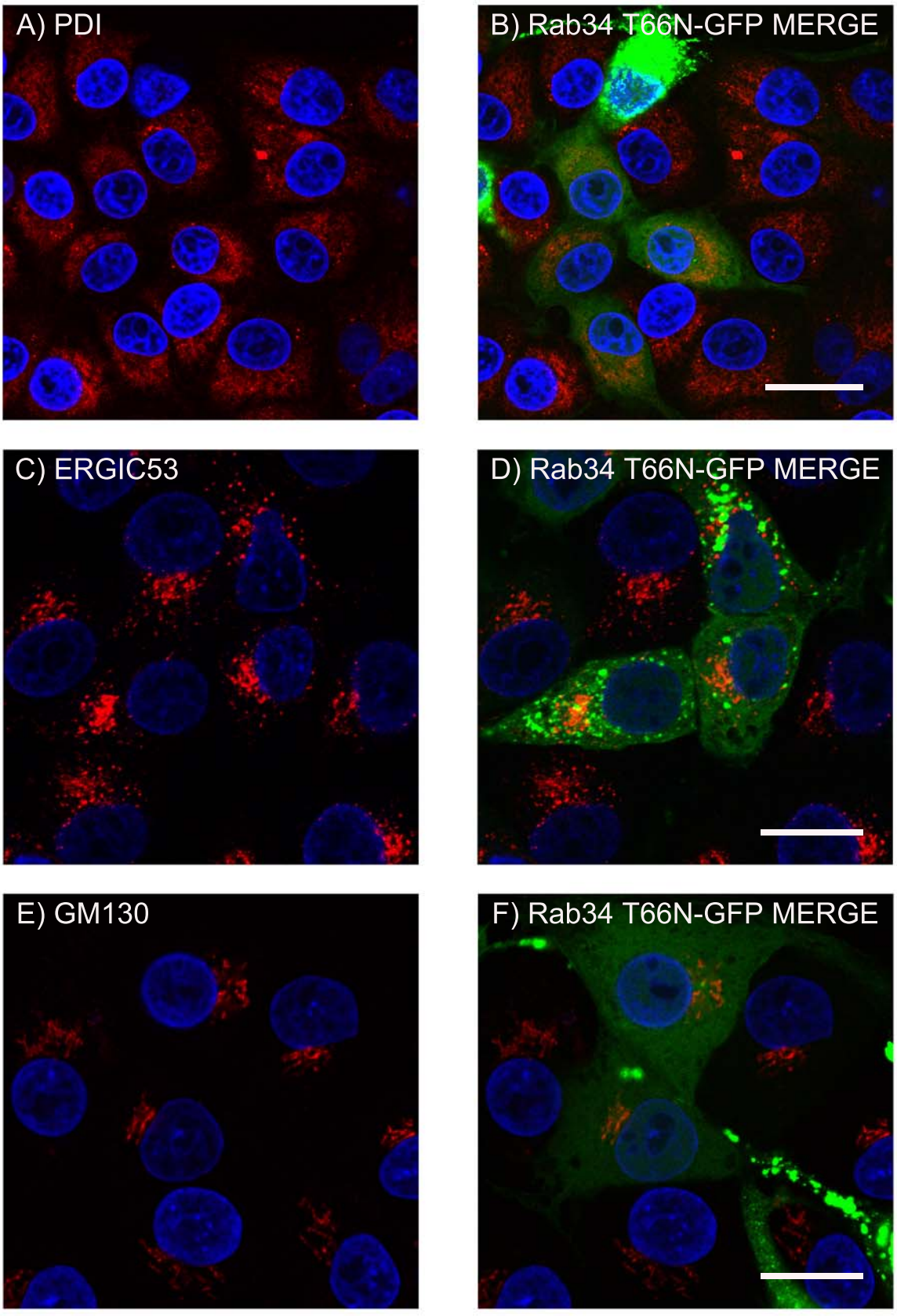


Figure 6.11 The effects of dn Rab34 (T66N) expression on the ER, ERGIC and Golgi
IBRS-2 cells were transfected to express dn Rab34 T66N-GFP for 14 hours and labelled for the ER (PDI; panels A & B), the ERGIC (ERGIC53; panels C & D) or the Golgi (GM130; panels E & F). Cells expressing Rab34 are shown as green; the ER, ERGIC and Golgi are shown in red. Panels B, D & F show merged images for red and green fluorescence. The cell nuclei were stained with DAPI and are shown as blue. Scale bar = 10 μm.

Rab34 T66N-GFP ER, ERGIC and Golgi labelling appears to remain unaltered, confirming this particular dn does not affect ER to Golgi transport (Fig 6.11 A-F).

6.5.2 The effect of dominant-negative Rab34 on FMDV infection

The next experiment investigated the effect of dn Rab34 on FMDV infection. IBRS-2 cells were transfected with either wt Rab34-GFP or dn Rab34 T66N-GFP for 14 hours. Cells were then infected with FMDV and processed for IFCM as previously described (see section 4.2.2). Infected cells are shown in red in the figures.

Figure 6.12 shows cells expressing wt Rab34-GFP or dn Rab34 T66N-GFP (shown in green, panels B and E) and labelled for FMDV (shown in red, panels A and D). Expression of the wt did not appear to have any effect on the frequency of FMDV infection when compared to cells of the non-expressing population. Expression of dn Rab34 T66N-GFP appeared to have a slight inhibitory effect on the frequency of infection.

The above experiment was repeated three times and the effect of the dn Rab34 proteins on infection quantified. The frequency of infection was calculated for the cells expressing a Rab34 transgene (wt Rab34, dn Rab34 T66N) and the data normalised to the results for the non-expressing cell population of the same cover-slip. Figure 6.13 (A-C) shows three experiments carried out independently, the mean of the experiments is shown in figure 6.13(D). The first experiment (Figure 6.13 A) shows a ~10% reduction in the frequency of infection in cells expressing wt Rab34-GFP and a 30% reduction in cells expressing dn Rab34-GFP. The second experiment (Figure 6.13 B) shows a very similar pattern; expression of wt Rab34-GFP reduces infection by 10% and dn Rab34 T66N-GFP by 30%. Figure 6.13(C) shows the third

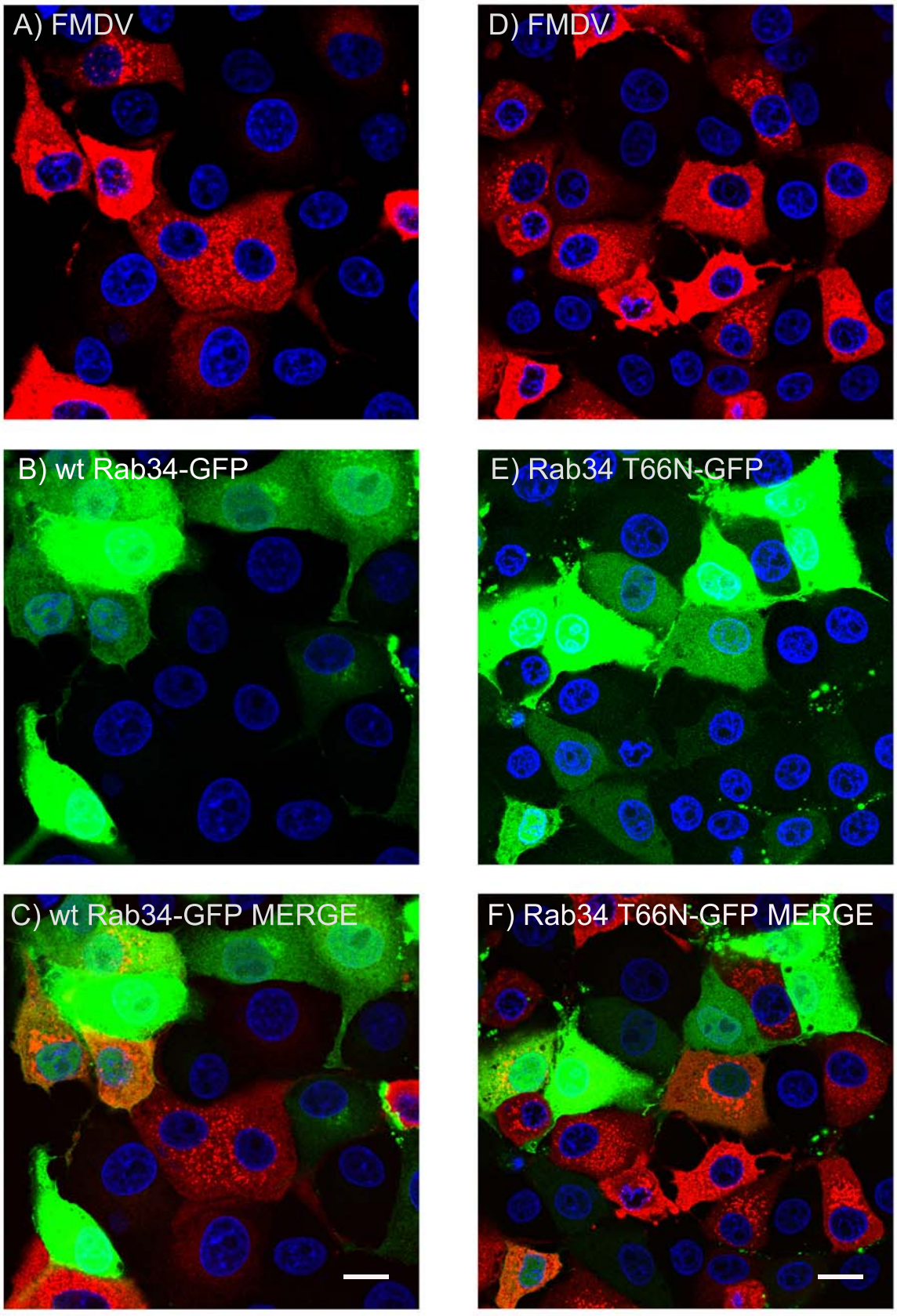


Figure 6.12 FMDV Infection of cells expressing wt or dn Rab34 (T66N)
IBRS-2 cells were transfected to express wt Rab34-GFP (A-C) or dn Rab34 T66N-GFP (D-F) for 14 hours and then infected with FMDV. Cells expressing Rab34 are shown as green. Infected cells are shown as red. Panels A and D show labelling for FMDV. Panels B and E show the signal for Rab34-GFP. Panels C and F showed merged images for red and green fluorescence. The cell nuclei were stained with DAPI and are shown as blue. Scale bar = 10 μm.

		Transfection efficency (%)	% Infected cells
Mock			**32**
Rab34 wildtype GFP	**Expressing**	35	35
	Non-expressing	65	36
Rab34 T66N GFP	**Expressing**	38	29
	Non-expressing	63	41

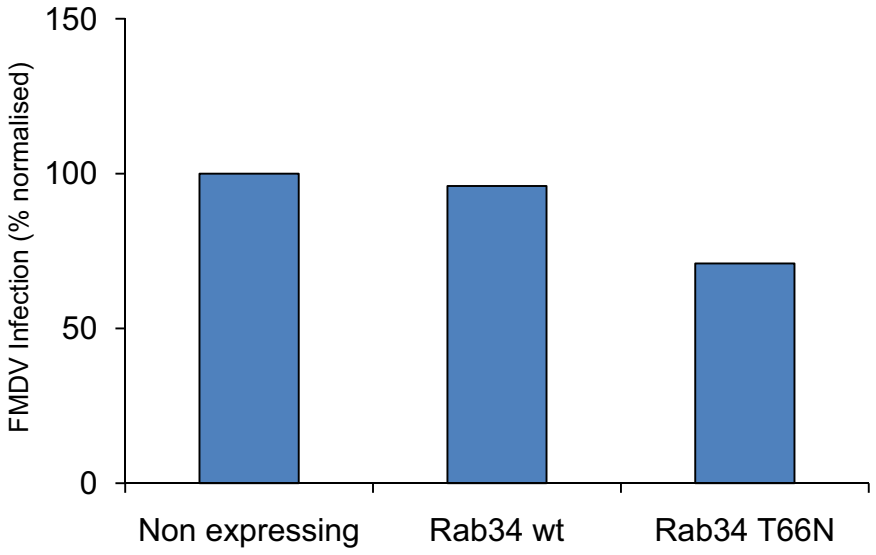


Figure 6.13(A): Experiment 1. The effects of dominant-negative Rab34 on FMDV infection of IBRS-2 cells
IBRS-2 cells were transfected to express wt Rab34-GFP or dn Rab34 T66N-GFP for 14 hours and then infected with FMDV. *Upper Table*: For each transfection, the frequency of infection (% infected cells) was determined for the cells expressing the Rab34 transgene (i.e. green expressing cells) and for the non-expressing cell population (Non-expressing cells). The percentage of cells expressing a transgene is also shown (Transfection efficiency). *Lower Figure*: For each transfection, the frequency of infection of cells expressing Rab34 was normalised to the results for the non-expressing cell population.

		Transfection efficency (%)	% Infected cells
Mock			**32**
Rab34 wildtype GFP	**Expressing**	35	35
	Non-expressing	65	36
Rab34 T66N GFP	**Expressing**	38	29
	Non-expressing	63	41

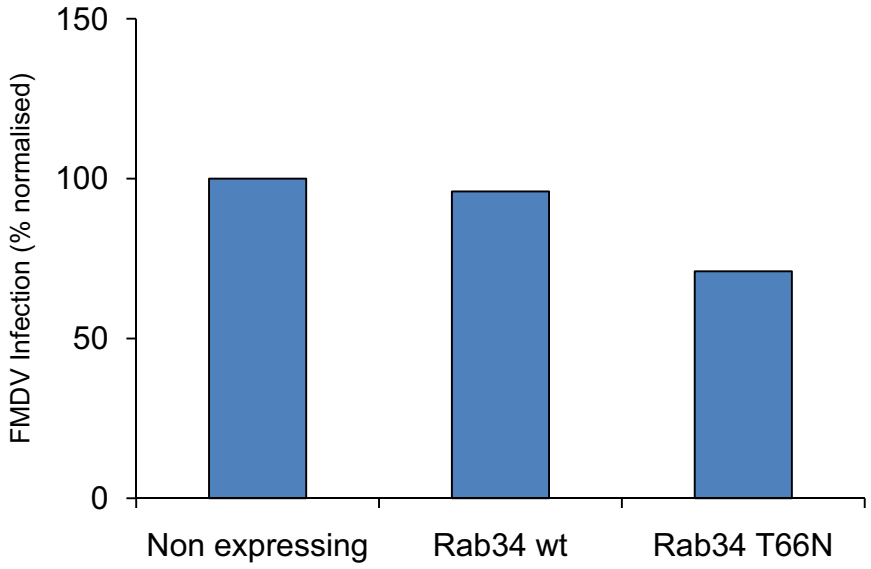


Figure 6.13(B): Experiment 2. The effects of dominant-negative Rab34 on FMDV infection of IBRS-2 cells
IBRS-2 cells were transfected to express wt Rab34-GFP or dn Rab34 T66N-GFP for 14 hours and then infected with FMDV. *Upper Table*: For each transfection, the frequency of infection (% infected cells) was determined for the cells expressing the Rab34 transgene (i.e. green expressing cells) and for the non-expressing cell population (Non-expressing cells). The percentage of cells expressing a transgene is also shown (Transfection efficiency). *Lower Figure*: For each transfection, the frequency of infection of cells expressing Rab34 was normalised to the results for the non-expressing cell population.

		Transfection efficency (%)	% Infected cells
Mock			**35**
Rab34 wildtype myc	**Expressing**	43	34
	Non-expressing	57	38
Rab34 T66N myc	**Expressing**	34	27
	Non-expressing	66	34

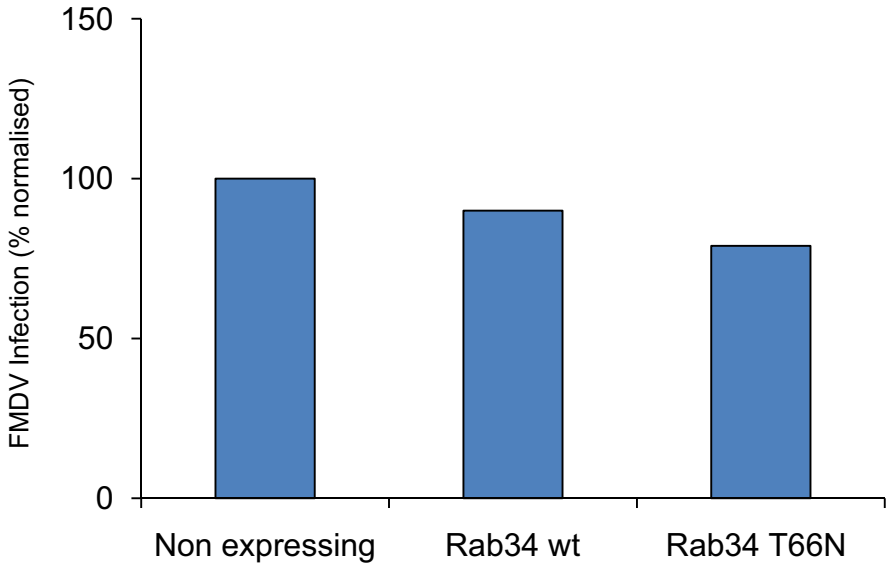


Figure 6.13(C): Experiment 3. The effects of dominant-negative Rab34 on FMDV infection of IBRS-2 cells
IBRS-2 cells were transfected to express wt Rab34-GFP or dn Rab34 T66N-GFP for 14 hours and then infected with FMDV. *Upper Table*: For each transfection, the frequency of infection (% infected cells) was determined for the cells expressing the Rab34 transgene (i.e. green expressing cells) and for the non-expressing cell population (Non-expressing cells). The percentage of cells expressing a transgene is also shown (Transfection efficiency). *Lower Figure*: For each transfection, the frequency of infection of cells expressing Rab34 was normalised to the results for the non-expressing cell population.

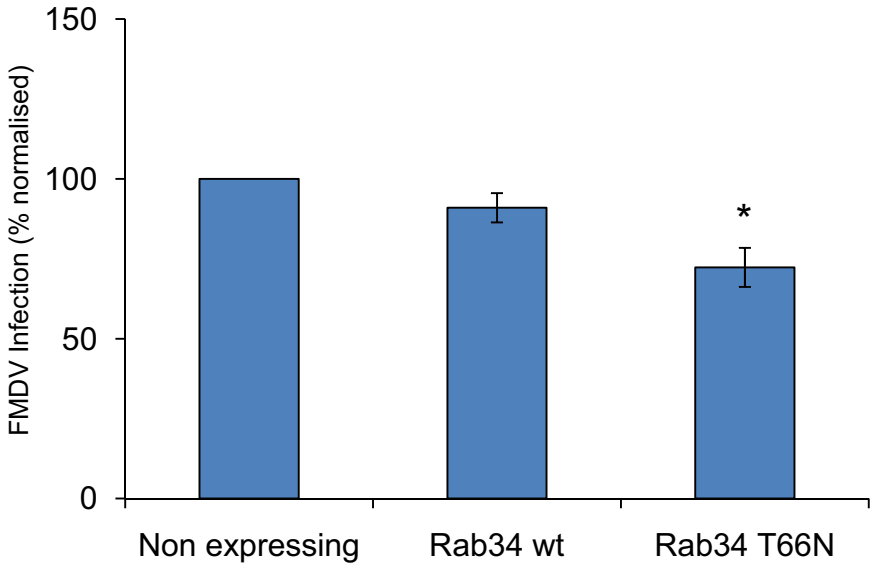


Figure 6.13(D): The effects of dominant-negative Rab34 on FMDV infection of IBRS-2 cells
Shown is the mean ± SD for the experiments shown in figure 6.13 (A-C). For each transgene (wt or dn T66N) the frequency of infection of cells expressing Rab34 was normalised to the results for the non-expressing cell population (*P* value: $* < 0.05$).

experiment where a 10% and 25% reduction to FMDV infection is seen in cells expressing wt Rab34-GFP and dn Rab34 T66N-GFP respectively.

The mean level of infection for the three experiments is shown in figure 6.13(D). Overall, expression of wt Rab34-GFP reduced the frequency of infection by 10%, and dn Rab34 T66N-GFP by ~25%. These effects were considered a biological variance.

6.6 TBC1D20

Rab proteins cycle between an active GTP-bound and an inactive GDP-bound state, which is controlled by guanine nucleotide exchange factors (GEFs) and GTPase-activating proteins (GAPs). GAPs activate GTP hydrolysis which results in inactivation and extraction of the Rab from the membrane (see section 1.9.5). TBC1D20 contains a Tre2, Bub2 and Cdc16 domain, which are present in most GAPs, and is reported to be the first known GAP for Rab1 (see section 6.2). Over-expression of TBC1D20 has been reported to block transport from the ER suggesting this protein plays a role in protein transport, possibly through the regulation of Rab1 (Sklan et al., 2007a; Sklan et al., 2007b).

To determine if TBC1D20-GFP has any effect on protein transport in the early secretory system and/or FMDV infection, the protein was expressed in cells. Over-expression of this protein is thought to cause a dominant negative effect on endogenous TBC1D20. The catalytically inactive mutant of TBC1D20 (R105A-GFP) was also expressed in cells as a control.

6.6.1 The effects of TBC1D20 on membranes in the early secretory pathway

The effect of TBC1D20 on membranes of the early secretory pathway was investigated by ICFM as previously described (see section 1.9). Figure 6.14

shows cells expressing the catalytically inactive TBC1D20 R105A-GFP (shown in green, panels B, D and F) and labelled for the ER (shown in red, panels A-B), the ERGIC (shown in red, panels C-D) or the Golgi (shown in red, panels E-F). The over-expression of TBC1D20 R105A-GFP appears to reduce ER (Fig 6.14 A-B) and disperse ERGIC labelling (Fig 6.14 C-D). The Golgi labelling remains but appears fragmented in the cells over-expressing the protein (Fig 6.14 E-F). Figure 6.15 shows cells expressing TBC1D20-GFP (shown in green, panels B, D and F) and labelled for the ER (shown in red, panels A-B), the ERGIC (shown in red, panels C-D) or the Golgi (shown in red, panels E-F). In cells expressing TBC1D20-GFP the ER labelling appears to become more punctuate (Fig 6.15, panels A-B) and the characteristic peri-nuclear labelling of the ERGIC is more dispersed than in non-expressing cells (Fig 6.15, panels C-D). Golgi labelling is also dispersed in cells expressing the protein. The above observations suggest that the over-expression of both TBC1D20-GFP and TBC1D20 R105A-GFP block transport through the early secretory pathway (see discussion 6.7)

6.6.2 The effect of TBC1D20 on FMDV infection

The next experiment investigated the effect of TBC1D20 on FMDV infection. IBRS-2 cells were transfected with either TBC1D20 R105A-GFP or TBC1D20-GFP for 14 hours. Cells were infected with FMDV and processed for IFCM as previously described (see section 4.2.2). Infected cells are shown in red in the figures.

Figure 6.16 shows cells expressing TBC1D20 R105A-GFP or TBC1D20-GFP (shown in green, panels B and E) and labelled for FMDV (shown in red, panels A and D). Expression of both the TBC1D20 R105A-GFP mutant and TBC1D20-GFP appeared to reduce the frequency of infection when compared to cells of the non-expressing population (Fig 6.16, merge panels C and F).

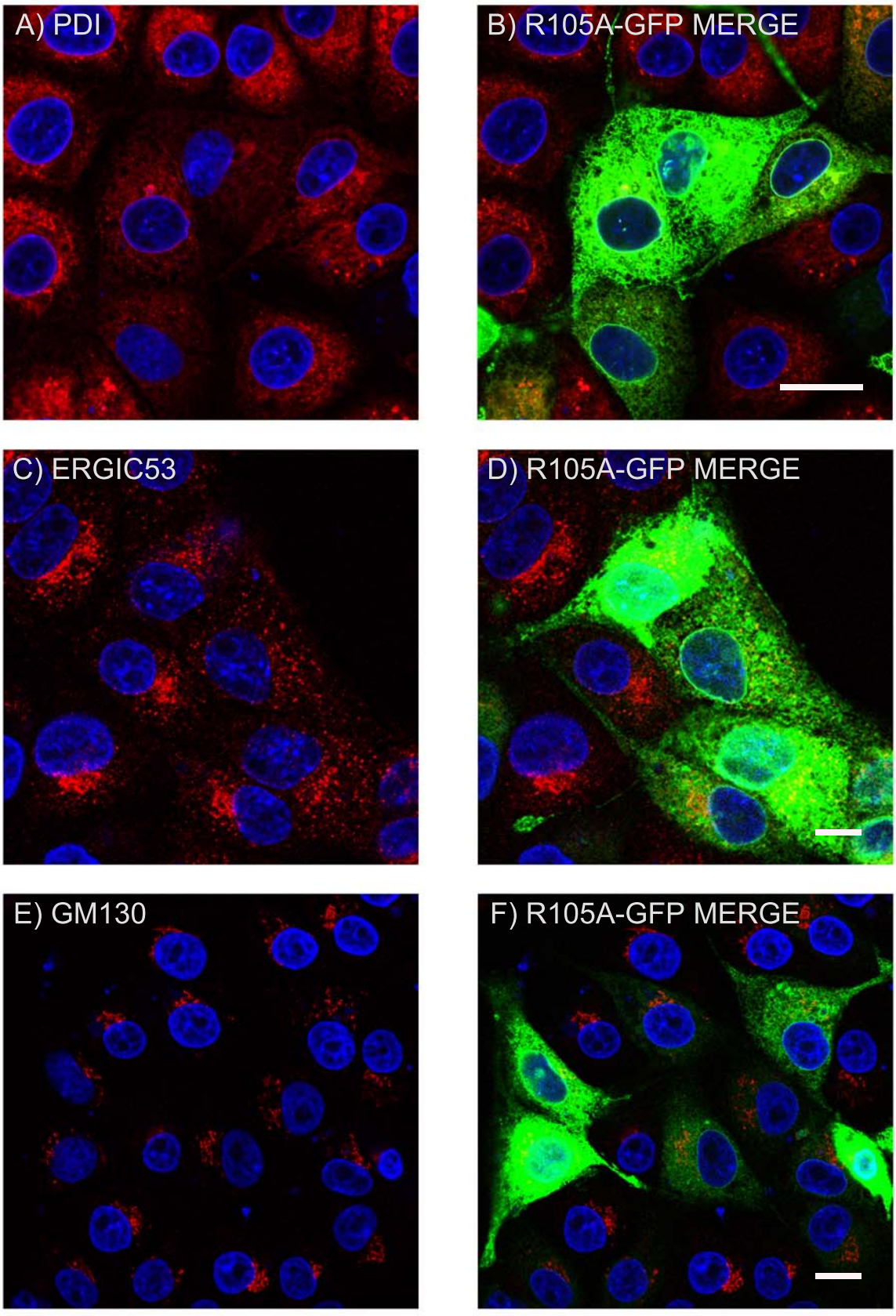


Figure 6.14 The effects of TBC1D20 R105A expression on the ER, ERGIC and Golgi
IBRS-2 cells were transfected to express the inactive mutant TBC1D20 R105A-GFP for 14 hours and labelled for the ER (PDI; panels A & B), the ERGIC (ERGIC53; panels C & D).or the Golgi (GM130; panels E & F). Cells expressing R105A are shown as green; the ER, ERGIC and Golgi are shown in red. Panels B, D & F showed merged images for red and green fluorescence. The cell nuclei were stained with DAPI and are shown as blue. Scale bar = 10 μm.
.

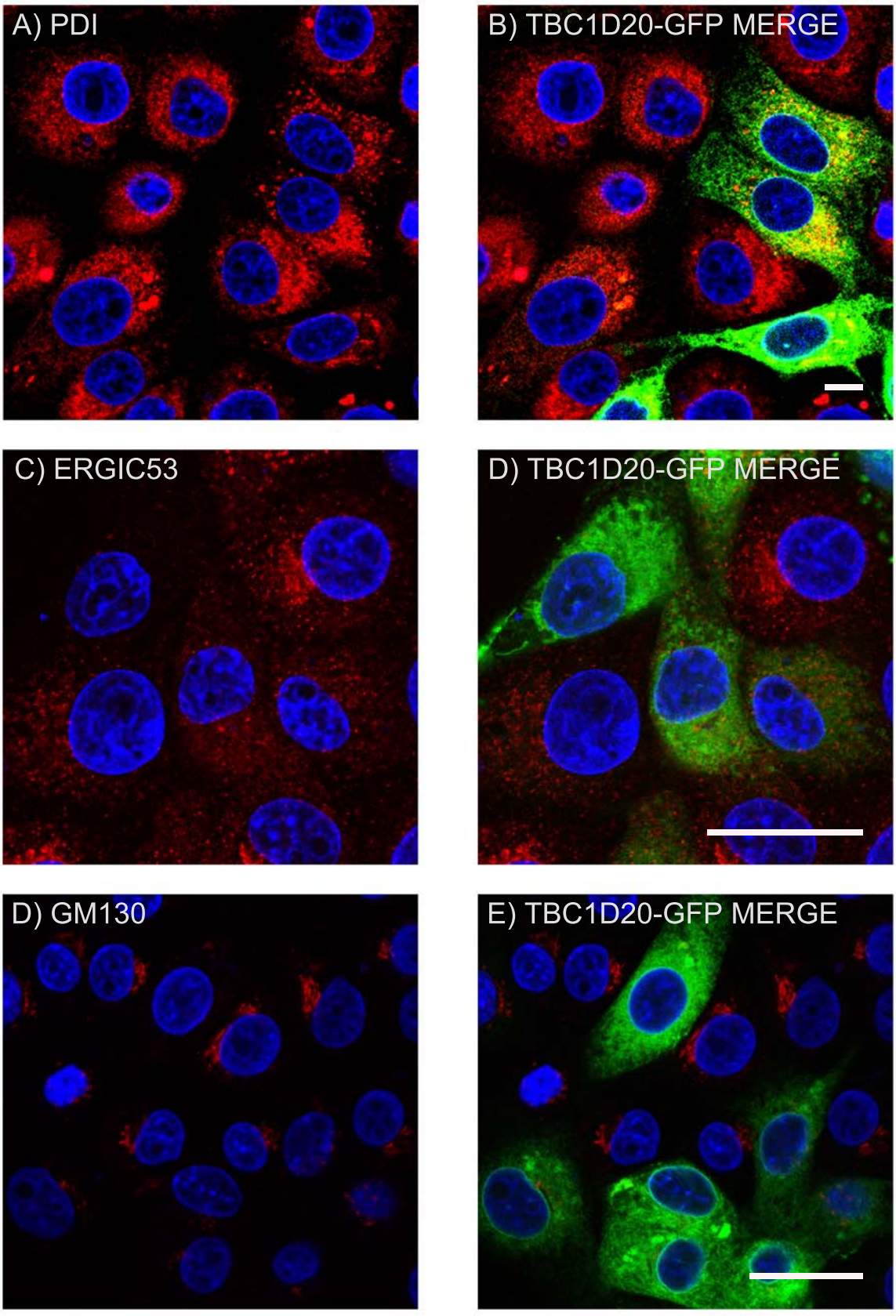


Figure 6.15 The effects of TBC1D20 expression on the ER, ERGIC and Golgi
IBRS-2 cells were transfected to express TBC1D20-GFP for 14 hours and labelled for the ER (PDI; panels A & B), the ERGIC (ERGIC53; panels C & D) or the Golgi (GM130; panels E & F). Cells expressing TBC1D20 are shown as green; the ER, ERGIC and Golgi are shown in red. Panels B and D showed merged images for red and green fluorescence. The cell nuclei were stained with DAPI and are shown as blue. Scale bar = 10 μm.

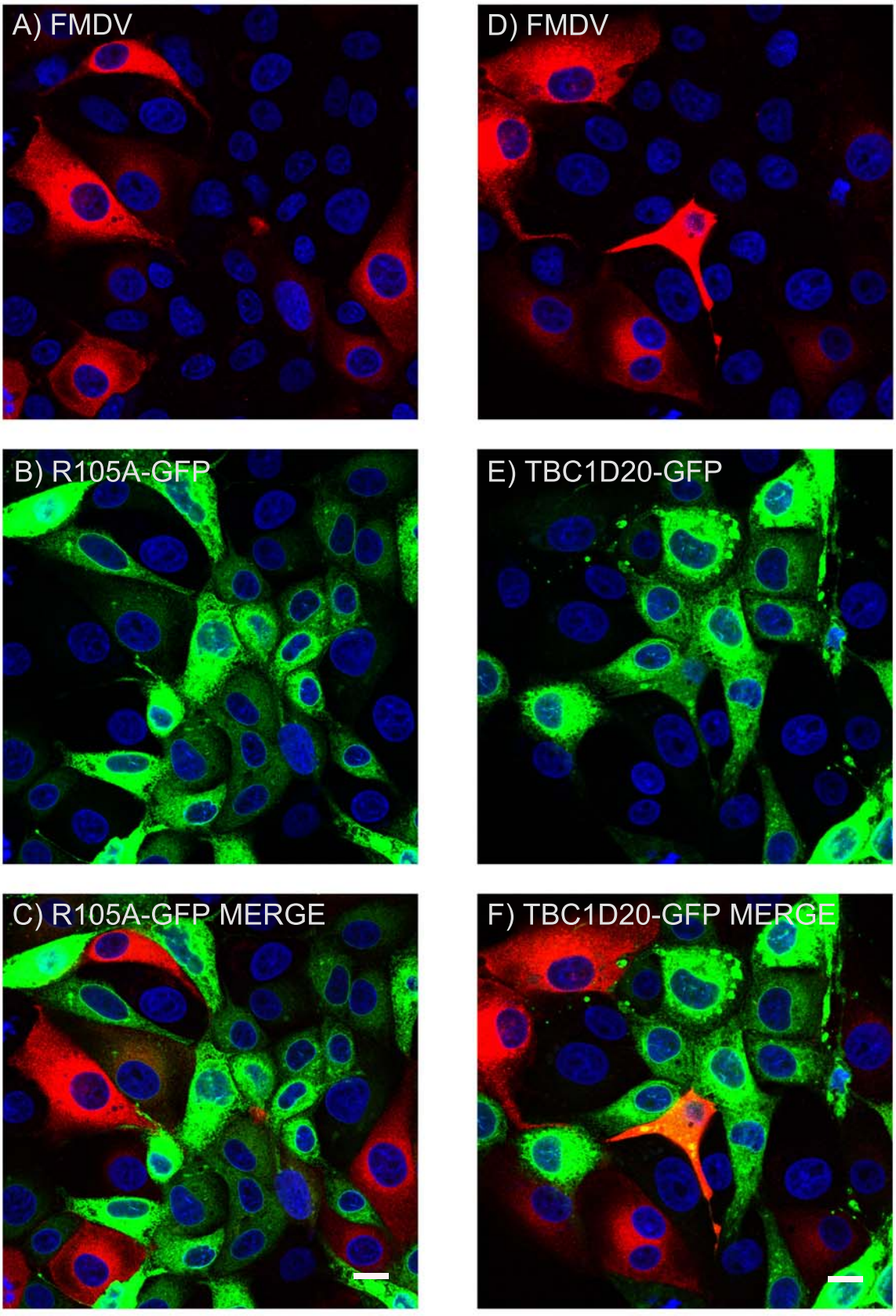


Figure 6.16 FMDV Infection of cells expressing R105A or TBC1D20
IBRS-2 cells were transfected to express TBC1D20 R105A-GFP (A-C) or TBC1D20-GFP (D-F) for 14 hours and then infected with FMDV. Cells expressing TBC1D20 are shown as green. Infected cells are shown as red. Panels A and D show labelling for FMDV. Panels B and E show the signal for TBC1D20-GFP. Panels C and F showed merged images for red and green fluorescence. The cell nuclei were stained with DAPI and are shown as blue. Scale bar = 10 μm.

The above experiment was repeated three times and the effect of the TBC1D20 proteins on infection quantified. The frequency of infection was calculated for the cells expressing a transgene (R105A, TBC1D20) and the data normalised to the results for the non-expressing cell population of the same cover-slip. Figure 6.17 (A-C) shows three experiments carried out independently, the mean of the experiments is shown in figure 6.17(D). The first experiment (Figure 6.17 A) shows ~80% reduction in the frequency of infection in cells expressing TBC1D20 R105A-GFP and ~50% reduction in infection for cells expressing TBC1D20-GFP. The second experiment (Figure 6.17 B) also shows a reduction in FMDV infection in cells expressing the TBC1D20 proteins by 40-45%. Figure 6.17(C) shows ~50% reduction to infection in cells expressing TBC1D20 R105A-GFP and ~25% reduction in cells expressing TBC1D20-GFP.

The mean level of infection for the three experiments is shown in figure 6.17(D). Overall, expression of TBC1D20 R105A-GFP reduced the frequency of infection by ~60%, and TBC1D20-GFP by ~40%. The reduction in the frequency of infection in cells expressing the catalytically inactive TBC1D20 (R105A) maybe due to the protein exerting a dominant-negative effect on the cells endogenous TBC1D20, blocking an essential interaction with down-stream effectors.

6.6.3 The effect of TBC1D20 on BEV infection

The above experiments were repeated using BEV-1 in place of FMDV. Cells were transfected to express TBC1D20 R105A-GFP or TBC1D20-GFP for 14 hours and then infected with BEV-1 at an MOI of 0.5. After 4 hours cells were fixed in 4% PFM and labelled for infection with an anti-BEV-1 primary

		Transfection efficency (%)	% Infected cells
Mock			**36**
TBC1D20 R015A GFP	**Expressing**	45	9
	Non-expressing	55	36
TBC1D20 GFP	**Expressing**	46	20
	Non-expressing	54	36

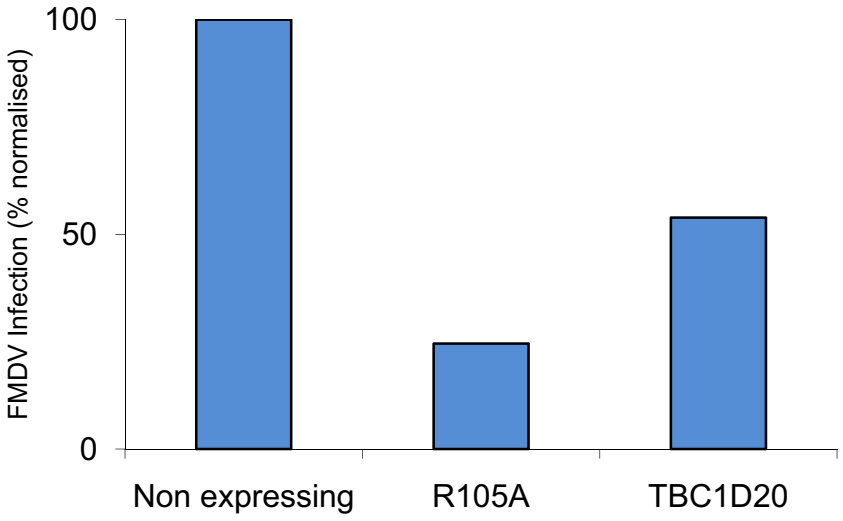


Figure 6.17(A): Experiment 1. The effects of TBC1D20 on FMDV infection of IBRS-2 cells
IBRS-2 cells were transfected to express the inactive mutant TBC1D20 R105A-GFP or TBC1D20-GFP for 14 hours and then infected with FMDV. *Upper Table*: For each transfection, the frequency of infection (% infected cells) was determined for the cells expressing the TBC1D20 transgene (i.e. green expressing cells) and for the non-expressing cell population (Non-expressing cells). The percentage of cells expressing a transgene is also shown (Transfection efficiency). *Lower Figure*: For each transfection, the frequency of infection of cells expressing TBC1D20 was normalised to the results for the non-expressing cell population.

		Transfection efficency (%)	% Infected cells
Mock			**34**
TBC1D20 R015A GFP	**Expressing**	51	9
	Non-expressing	49	19
TBC1D20 GFP	**Expressing**	54	16
	Non-expressing	46	37

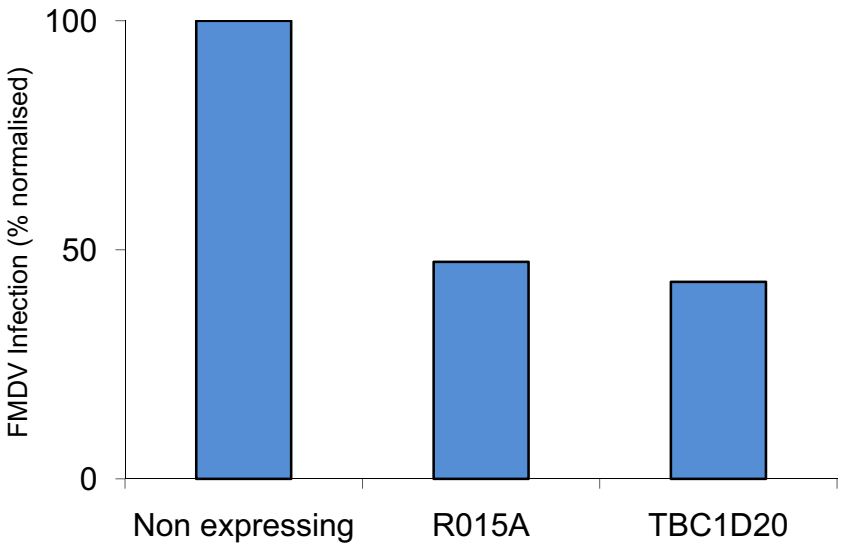


Figure 6.17(B): Experiment 2. The effects of TBC1D20 on FMDV infection of IBRS-2 cells
IBRS-2 cells were transfected to express the inactive mutant TBC1D20 R105A-GFP or TBC1D20-GFP for 14 hours and then infected with FMDV. *Upper Table*: For each transfection, the frequency of infection (% infected cells) was determined for the cells expressing the TBC1D20 transgene (i.e. green expressing cells) and for the non-expressing cell population (Non-expressing cells). The percentage of cells expressing a transgene is also shown (Transfection efficiency). *Lower Figure*: For each transfection, the frequency of infection of cells expressing TBC1D20 was normalised to the results for the non-expressing cell population.

		Transfection efficency (%)	% Infected cells
Mock			**57**
TBC1D20 R015A GFP	**Expressing**	52	48
	Non-expressing	48	65
TBC1D20 GFP	**Expressing**	61	35
	Non-expressing	39	65

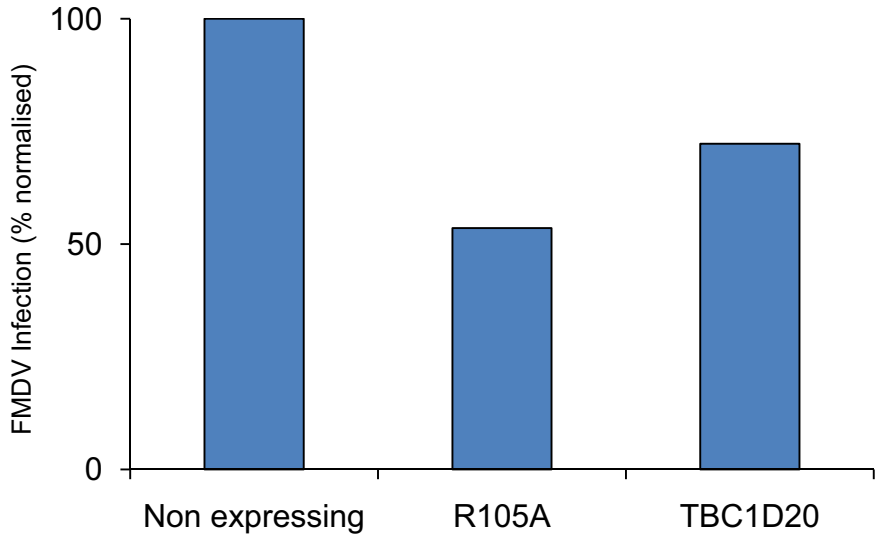


Figure 6.17(C): Experiment 3. The effects of TBC1D20 on FMDV infection of IBRS-2 cells
IBRS-2 cells were transfected to express the inactive mutant TBC1D20 R105A-GFP or TBC1D20-GFP, for 14 hours and then infected with FMDV. *Upper Table*: For each transfection, the frequency of infection (% infected cells) was determined for the cells expressing the TBC1D20 transgene (i.e. green expressing cells) and for the non-expressing cell population (Non-expressing cells). The percentage of cells expressing a transgene is also shown (Transfection efficiency). *Lower Figure*: For each transfection, the frequency of infection of cells expressing TBC1D20 was normalised to the results for the non-expressing cell population.

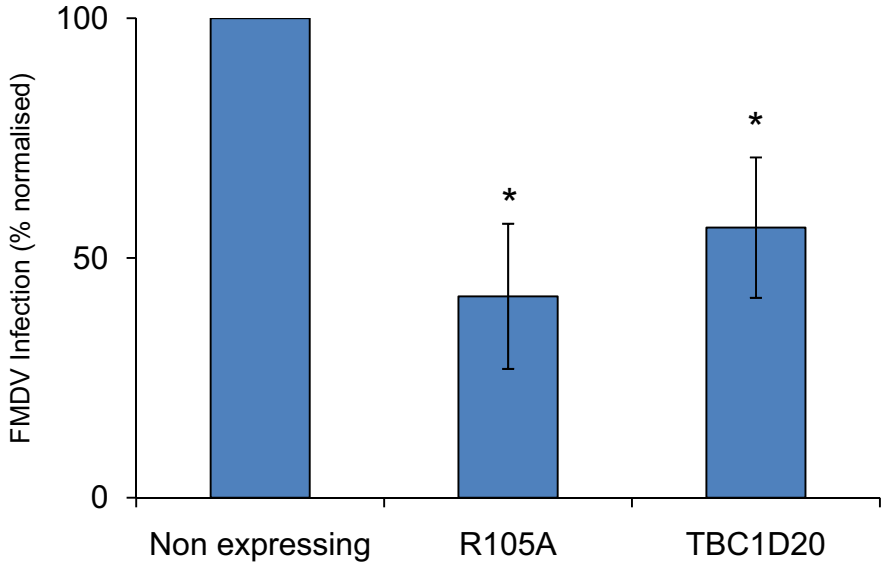


Figure 6.17(D): The effects of TBC1D20 on FMDV infection of IBRS-2 cells
Shown is the mean ± SD for the experiments shown in figure 6.17(A-C). For each transgene (R105A or TBC1D20) the frequency of infection of cells expressing TBC1D20 was normalised to the results for the non-expressing cell population (*P* value: $*$ < 0.05).

antibody and an anti-Guinea pig Alexa 568 secondary antibody. BEV-1 infected cells are shown in red on the figures.

Figure 6.18 shows cells expressing TBC1D20 R105A-GFP or TBC1D20-GFP (shown in green, panels B and D) and infected with BEV-1 (shown in red, panels A and D). As seen in FMDV infected cells (see figure 6.19), expression of either TBC1D20 R105A-GFP or TBC1D20-GFP appeared to reduce the frequency of BEV infected cells in comparison to cells of the non-expressing population.

The above experiment was repeated twice and the effect of the TBC1D20 proteins on BEV infection quantified. Data was normalised as previously described (see section 6.6.2). Figure 6.19(A-B) shows two experiments carried out independently, the mean of the experiments is shown in figure 6.19(C). The first experiment (Figure 6.19A) shows ~40% reduction in the frequency of infection in cells expressing TBC1D20 R105A-GFP and a ~50% reduction in cells expressing TBC1D20-GFP. Similarly, the second experiment (Figure 6.19B) shows ~40% reduction to infection levels in cells expressing either of the TBC1D20 proteins.

The mean level of infection for the above experiments is shown in figure 6.19(C). Overall, expression of TBC1D20 R105A-GFP reduced the frequency of infection by ~45%, and TBC1D20-GFP by ~40%. Expression of the catalytically inactive TBC1D20 R105A inhibits infection to a similar level as TBC1D20-GFP, suggesting the mutant version is producing a dominant-negative effect in cells expressing the protein.

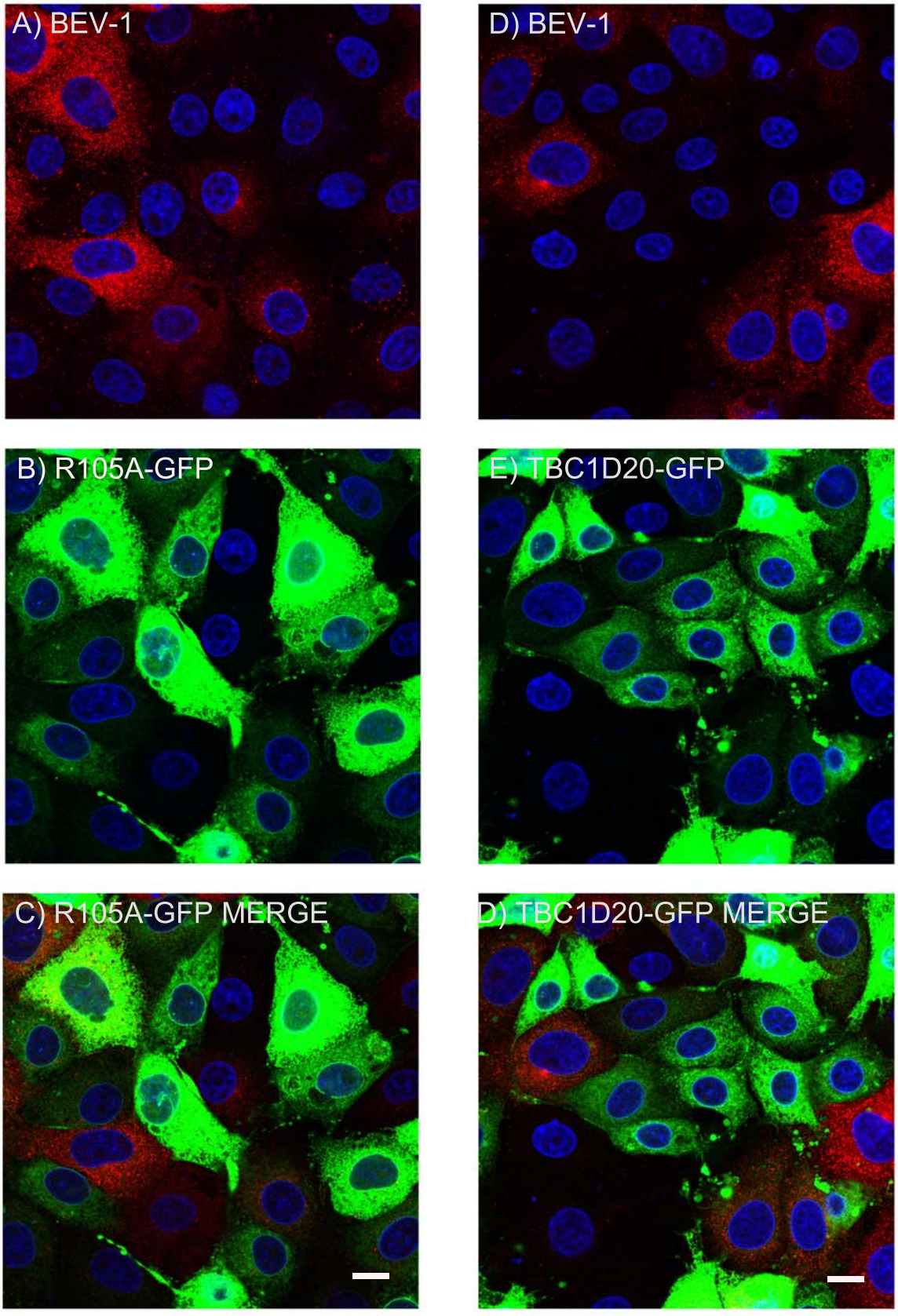


Figure 6.18 BEV Infection of cells expressing R105A or TBC1D20
IBRS-2 cells were transfected to express TBC1D20 R105A-GFP (A-C) or TBC1D20-GFP (D-F) for 14 hours and then infected with BEV. Cells expressing TBC1D20 are shown as green. Infected cells are shown as red. Panels A and D show labelling for BEV. Panels B and E show the signal for TBC1D20-GFP. Panels C and F showed merged images for red and green fluorescence. The cell nuclei were stained with DAPI and are shown as blue. Scale bar = 10 μm.

		Transfection efficency (%)	% Infected cells
Mock			**48**
TBC1D20 R015A GFP	**Expressing**	55	20
	Non-expressing	45	44
TBC1D20 GFP	**Expressing**	55	24
	Non-expressing	45	44

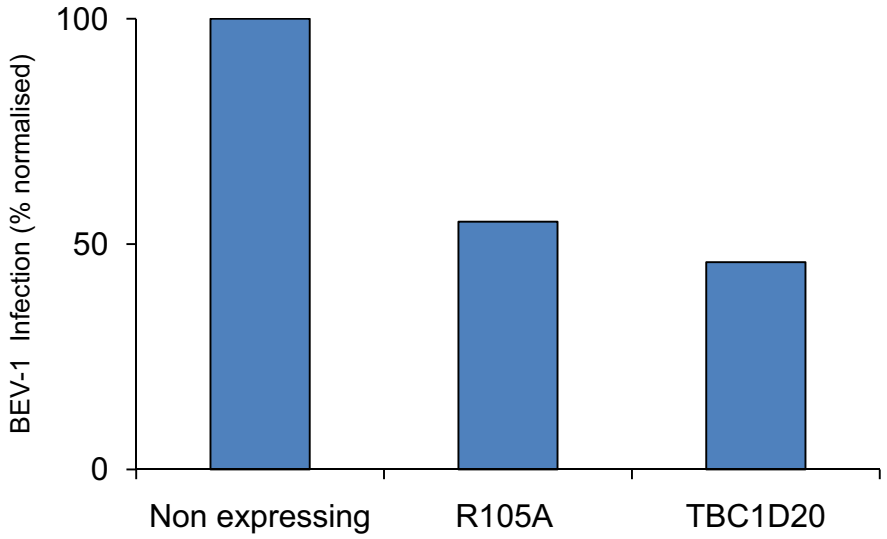


Figure 6.19(A): Experiment 1. The effects of TBC1D20 on BEV infection of IBRS-2 cells
IBRS-2 cells were transfected to express the inactive mutant TBC1D20 R105A-GFP or TBC1D20-GFP for 14 hours and then infected with BEV. *Upper Table*: For each transfection, the frequency of infection (% infected cells) was determined for the cells expressing the TBC1D20 transgene (i.e. green expressing cells) and for the non-expressing cell population (Non-expressing cells). The percentage of cells expressing a transgene is also shown (Transfection efficiency). *Lower Figure*: For each transfection, the frequency of infection of cells expressing TBC1D20 was normalised to the results for the non-expressing cell population.

		Transfection efficency (%)	% Infected cells
Mock			**51**
TBC1D20 R015A GFP	**Expressing**	68	26
	Non-expressing	32	50
TBC1D20 GFP	**Expressing**	42	20
	Non-expressing	58	31

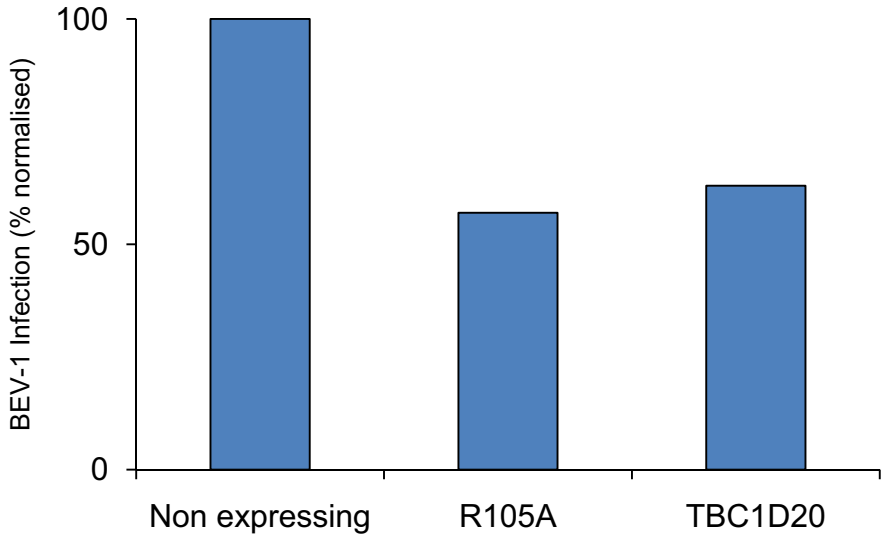


Figure 6.19(B): Experiment 2. The effects of TBC1D20 on BEV infection of IBRS-2 cells
IBRS-2 cells were transfected to express the inactive mutant TBC1D20 R105A-GFP or TBC1D20-GFP for 14 hours and then infected with BEV. *Upper Table*: For each transfection, the frequency of infection (% infected cells) was determined for the cells expressing the TBC1D20 transgene (i.e. green expressing cells) and for the non-expressing cell population (Non-expressing cells). The percentage of cells expressing a transgene is also shown (Transfection efficiency). *Lower Figure*: For each transfection, the frequency of infection of cells expressing TBC1D20 was normalised to the results for the non-expressing cell population.

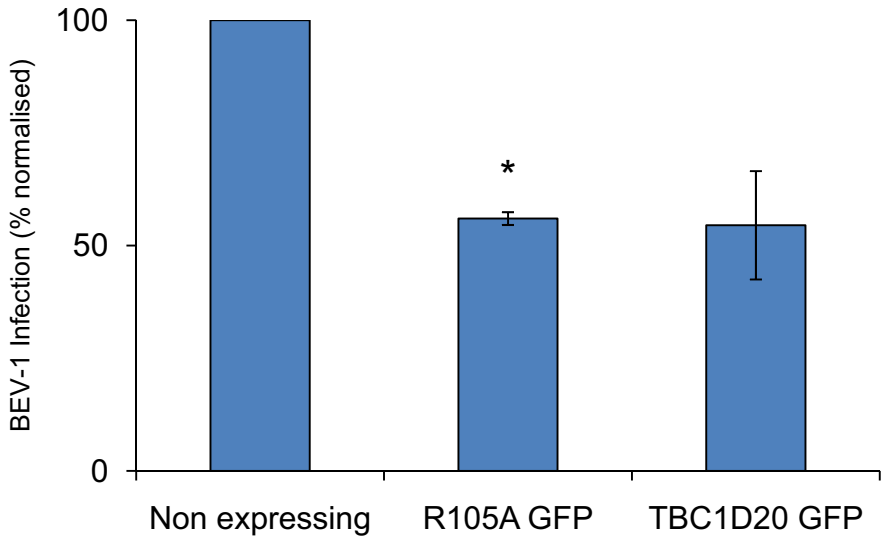


Figure 6.19(C): The effects of TBC1D20 on BEV infection of IBRS-2 cells
Shown is the mean ± SD for the experiments shown in figure 6.19 (A-B). For each transgene (R105A or TBC1D20) the frequency of infection of cells expressing TBC1D20 was normalised to the results for the non-expressing cell population (*P* value: $*$ < 0.05).

6.7 Discussion

This chapter investigated the role of Rab proteins in FMDV infection. The first protein to be investigated was Rab1, which is essential for ER to Golgi transport (Haas et al., 2007) as it is required for membrane recruitment of GBF1 and hence Arf1 activation (Monetta et al., 2007). Consistent with previous studies (Alvarez et al., 2003; Tisdale et al., 1992), expression of the dn Rab1 S25N-myc resulted in fragmentation of Golgi membranes suggesting that this dn is blocking transport within the early secretory pathway. Infection studies showed an increased frequency of FMDV infection in cells expressing dn Rab1. This apparent increase suggests that Rab1 activity is not essential for FMDV replication and that inactivation of Rab1 may enhance infection. It is thought that expression of dn Rab1a S25N-myc inhibits the tethering of COPII vesicles and recruitment of COPI to the ERGIC (Alvarez et al., 2003; Tisdale et al., 1992). Therefore, FMDV infection could be enhanced in cells expressing dn Rab1 as COPII vesicles may not be able to fuse with the ERGIC. In addition, as Rab1 is required for Arf1-mediated formation of COPI coats, the observation that dn Rab1 increases FMDV infection is consistent with the increase in infection observed with dn Arf1 T31N, as both dn proteins would be expected to have the same effect on formation of COPI coats.

In IBRS-2 cells, expression of dn Rab2 only appeared to fragment the Golgi when over-expressed. As Rab2 localises to the ERGIC (Tisdale, 1999; Tisdale and Balch, 1996; Tisdale and Jackson, 1998) this disruption suggests a block to transport is occurring between the ERGIC and the Golgi. Expression of both wt Rab2-myc and dn Rab2 S20N-myc increased the frequency of FMDV infection. The observed increase in cells expressing wt Rab2-myc may be due to over-expression of the protein producing a dominant-negative effect.

Expression of dn Rab2 is thought to prevent homotypic fusion of ERGIC vesicles and the recruitment of COPI (by Arf1) to ERGIC membranes (Tisdale, 1999; Tisdale and Jackson, 1998). This suggests that the apparent increase of FMDV infection observed in cells expressing dn Rab2 S20N-myc may result from a block to ERGIC maturation, and that a block to ERGIC-Golgi (and/or ERGIC to ER) transport is in some way advantageous for FMDV replication. In addition, as dn Rab2 is reported not to interfere with COPII vesicle formation, the observed increase of FMDV infection suggests that COPII vesicles may be utilised for FMDV replication. Furthermore, as both dn Rab1 and dn Rab2 increased FMDV infection, these two proteins may have similar effects on membrane flow to the ERGIC.

Expression of dn Rab6 is thought to slow inter-Golgi transport but does not interfere with ER to Golgi transport (Martinez et al., 1994). The activity of Rab6 has also been implicated in the transport of proteins through the early secretory pathway by a COPI independent pathway (Kano et al., 2009). Expression of dn Rab6 T27N-myc did not affect Golgi labelling or the frequency of FMDV infection and is therefore unlikely to play a role in virus replication. These observations are in agreement with the insensitivity of FMDV to BfA as they imply that the Golgi is not required for FMDV replication. The role of a second Rab protein (Rab34) that is also involved in inter-Golgi transport was also investigated. Expression of dn Rab34 T66N-GFP did not appear to alter the ER, ERGIC or Golgi labelling which suggests that membrane flow between these compartments was not affected. This is different to other published reports which showed that ER to Golgi transport was disrupted (Goldenberg et al., 2007). However, expression of wt Rab34-GFP did cause dispersal of the peri-nuclear region of the ERGIC but did not affect the Golgi. This phenotype was

also observed in cells expressing dn Rab6 T27N-myc (see Fig 6.8) which suggests that the wt protein may have a dn effect. However expression of wt Rab34 did not appear to have any effect on FMDV infection as only a 10% difference was observed in cells expressing the protein and cells of the non-expressing population. Similarly, only a mild inhibition (25%) of FMDV infection was seen in cells expressing dn Rab34 T66N-GFP (Fig 6.12). Over-expression of dn Rab34 may slow transport through the early secretory system due to an accumulation of protein in late Golgi compartments. This effect on membrane flow may cause a slight reduction in infection, however such a small decrease suggests this does not appear to be essential for replication. Overall, it can be suggested that inter-Golgi transport and the Golgi itself are not involved in FMDV replication, however perhaps an accumulation of proteins in the Golgi can indirectly slow ER to Golgi transport.

The Rab1 GAP TBC1D20 was also investigated. GAP proteins hydrolyse GTP thereby releasing the Rab from the membrane and returning it to the cytosol. Over-expression of TBC1D20 therefore inhibits Rab1 by maintaining the GDP-bound inactive state (Haas et al., 2007). It appeared that over-expression of TBC1D20-GFP in IBRS-2 cells blocked transport through the early secretory pathway, as ER labelling became punctuate and both the ERGIC and Golgi were dispersed. Surprisingly, expression of the catalytically inactive TBC1D20 mutant, R105A-GFP, also reduced ER labelling and fragmented the ERGIC and Golgi in cells over-expressing the protein, although the effects were not as dramatic as in cells expressing active TBC1D20-GFP. These observations suggest the catalytically inactive version of the protein is also having an inhibitory effect on the secretory system when over-expressed (see Fig 6.14).

A decrease in the frequency of both FMDV and BEV infection was observed in cells expressing TBC1D20-GFP. It has been reported that TBC1D20 localises to the ER by binding to the ER resident protein reticulon and when over-expressed, blocks protein transport out of the ER (Haas et al., 2007). Therefore, it may be possible that expression of TBC1D20 is interfering with normal transport out of the ER which is affecting FMDV replication. It should also be considered that the majority of Rab proteins along with GAPs and GEFs tend to interact with multiple effectors, therefore there is a possibility that TBC1D20 may have many functions other than serving as a GAP for Rab1 and 2. The inhibition of BEV infection could be due to an indirect effect caused by expression of TBC1D20, such as a block to the flow of membranes to the Golgi which therefore may affect its integrity.

In addition, expression of TBC1D20 R105A-GFP reduced the frequency of infection of both FMDV and BEV. This reduction may be due to the protein exerting a dominant-negative effect on TBC1D20. Over-expression of the inactive mutant may block an essential interaction of TCB1D20 with down-stream effectors. For example R105A could potentially bind to Rab1-GTP on the membrane, blocking the proteins interaction with p115 or alternatively endogenous TBC1D20, therefore Rab1 may become constituently active.

In summary, it appears blocking the secretory pathway before the Golgi with dn Rab1 and dn Rab2 may be advantageous to FMDV replication, whereas expression of the Rab1 GAP TBC1D20 that is reported to block ER export reduces FMDV replication levels. In contrast, a block to inter-Golgi or post-Golgi transport did not appear to have any significant effect on FMDV infection. Overall, the data suggests that FMDV replication may require functioning ERES and COPII vesicle formation, but does not require the membranes from the

ERGIC or Golgi and a block to COPI transport maybe an advantage for FMDV replication.

Chapter 7: Investigating the effect of Rab RNAi on FMDV infection

7.1 Introduction

The experiments carried out in the previous chapter (Chapter 6) show that inhibition of Rab1 and Rab2 activity, through the expression of dominant negative, proteins appears to enhance FMDV infection. A Rab RNAi (RNA interference) library was used to target Rab1, Rab2, Rab5, Rab6, Rab34 (including all isoforms). The effects of Rab knockdown on FMDV replication was measured using a quantitative PCR (QPCR) assay. These experiments were conducted to confirm the findings from the experiments that used dominant-negative proteins.

The Rab RNAi library (a generous gift from Ian Goodfellow at Imperial College) is designed to target the human genes, therefore the human cancer cell line HeLa was used for all subsequent experiments.

7.2 Characterisation of FMDV infection in HeLa cells

HeLa cells are not infected by field-strains of FMDV (such as O1Kcad$_2$) therefore the tissue-culture adapted heparan-sulphate binding virus (FMDV O1BFS) was used to carry out infection studies. Virtually all cells express heparan sulphate on their surfaces and therefore O1BFS should be able to enter HeLa cells to allow infection to proceed. Several experiments were carried out to determine if HeLa cells could be infected with O1BFS and successfully replicate to produce progeny virus.

In the first experiment, HeLa cells were infected with O1BFS to determine if infection would produce a cytopathic effect (CPE). A confluent monolayer of HeLa cells was infected with a serial dilution of O1BFS (10^7, 10^6 and 10^5 pfu/ml)

and incubated at 37°C for 1 hour to allow virus uptake. Cells were washed once in serum-free media prior to the addition of virus growth media and incubated at 37°C for a further 24 hours. Cells were observed via a light microscope at regular intervals for evidence of cytopathic effect (CPE). Cells started to show signs of CPE at seven hours post infection (pi) in cells treated with 10^7 pfu/ml. At 24 hours, cells were stained with methylene blue to determine the extent of the CPE. Figure 7.1 shows the CPE in HeLa cells infected with O1BFS at 24 hours. Complete cell death was observed in cells treated with 10^7 pfu/ml of virus and extensive CPE was seen in cells infected with 10^6 pfu/ml. Little or no CPE was observed in cells treated with 10^5 pfu/ml. These results are characteristic of a normal FMDV infection; however the apparent time taken for CPE to develop showed a delay when compared to the normal time expected for CPE to develop for non-primate cell lines (e.g. BHK cells).

The next experiment attempted to recover productive virus from infected HeLa supernatants, which would indicate if infectious progeny was being produced. Cells were infected with O1BFS (10^6 pfu/ml) for one hour to allow virus uptake. Cells were then subjected to a brief acid wash, to inactivate any remaining external virus, and infection allowed to continue for a further eight hours. Samples of cell supernatants were collected immediately after the acid wash (0hrs) and at eight hours pi (8hrs). The supernatants were then serially diluted in PBS and titrated onto BHK21 cells (see methods 2.2.3). After 48 hours, plaques were stained with methylene blue and counted. Figure 7.2 shows the result of the assay and that new virus is produced from FMDV infected HeLa cells at 8 hours pi. Very little virus was evident in supernatants collected at 0 hours (<1 $x10^1$pfu/ml), whereas ~ 4 $x10^4$pfu/ml was produced in supernatants collected from infected cells at 8 hours pi. The above experiments

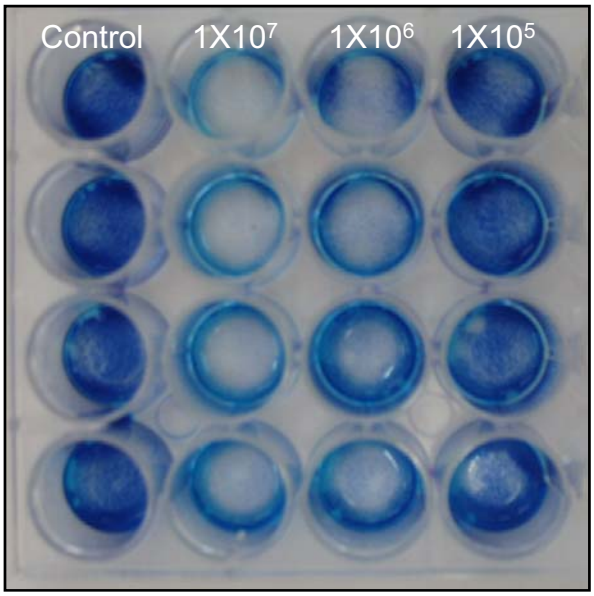


Figure 7.1 FMDV causes a cytopathic effect in HeLa cells
HeLa cells were infect with serial dilutions of O1BFS for 24 hours and stained with methylene blue to determine the extent of the cytopathic effect. The control lane contains no FMDV.

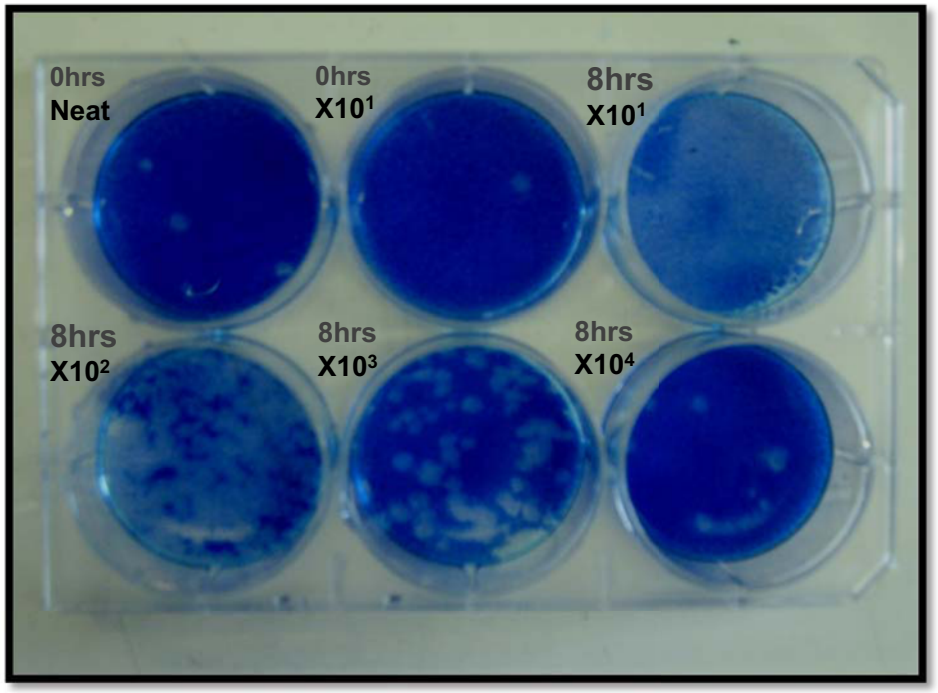


Figure 7.2 FMDV produces productive virus in HeLa cells
The supernatants collected from O1BFS infected HeLa cells were serially diluted and titrated onto BHK-21 cells and incubated for 48 hours in eagles overlay. Plaques were visualised by staining with methylene blue. The first two wells show background virus at 0 hours. The remaining four wells show serial dilutions of productive virus at 8 hours pi.

show that HeLa cells can be productively infected with O1BFS, although the rate of replication and virus yields are relatively low when compared to infection of non-primate cells.

To further characterise infection, HeLa cells were infected with O1BFS and processed for IFCM at 2, 4, 6 and 8 hours pi. Cells were permeabilised in 0.1% Triton-X and blocked using block buffer. Infected cells were identified using a rabbit anti-FMDV antibody and an Alexa-Fluor 568 labelled anti-rabbit secondary antibody. Infected cells are shown as red on Fig 7.3.

At 2 hours pi viral protein was not observed. At 4 hours pi a number of cells are clearly infected (shown in red, panel B), which is characterised by diffuse labelling throughout the cell. At 6 hours pi the number of infected cells was at a maximum (shown in red, panel C). At later time points (>8 hours pi or longer) many infected cells appeared dead, indicating the end of one infectious cycle (images not shown). These results indicate that the optimum time of virus replication would be between 5-6 hour pi.

In the next experiment, HeLa cells were infected with O1BFS and processed for TEM (see methods 2.10), to establish if host cell membrane rearrangements occurred in infected cells. Cells were infected with O1BFS for 6 hours (as above) and processed for TEM (Figure 7.4). A distinct clearing of the cytoplasm and concentration of the cytoplasmic contents to the peri-nuclear region can be observed in infected cells (Fig 7.4, panel A-B). Several membrane vesicles characteristic of FMDV infection can be seen (Fig 7.4, panel B). In addition, a small number of double membrane vesicles were evident (Fig 7.4, panel C). These results show that infection of HeLa cells by O1BFS induces membrane rearrangements.

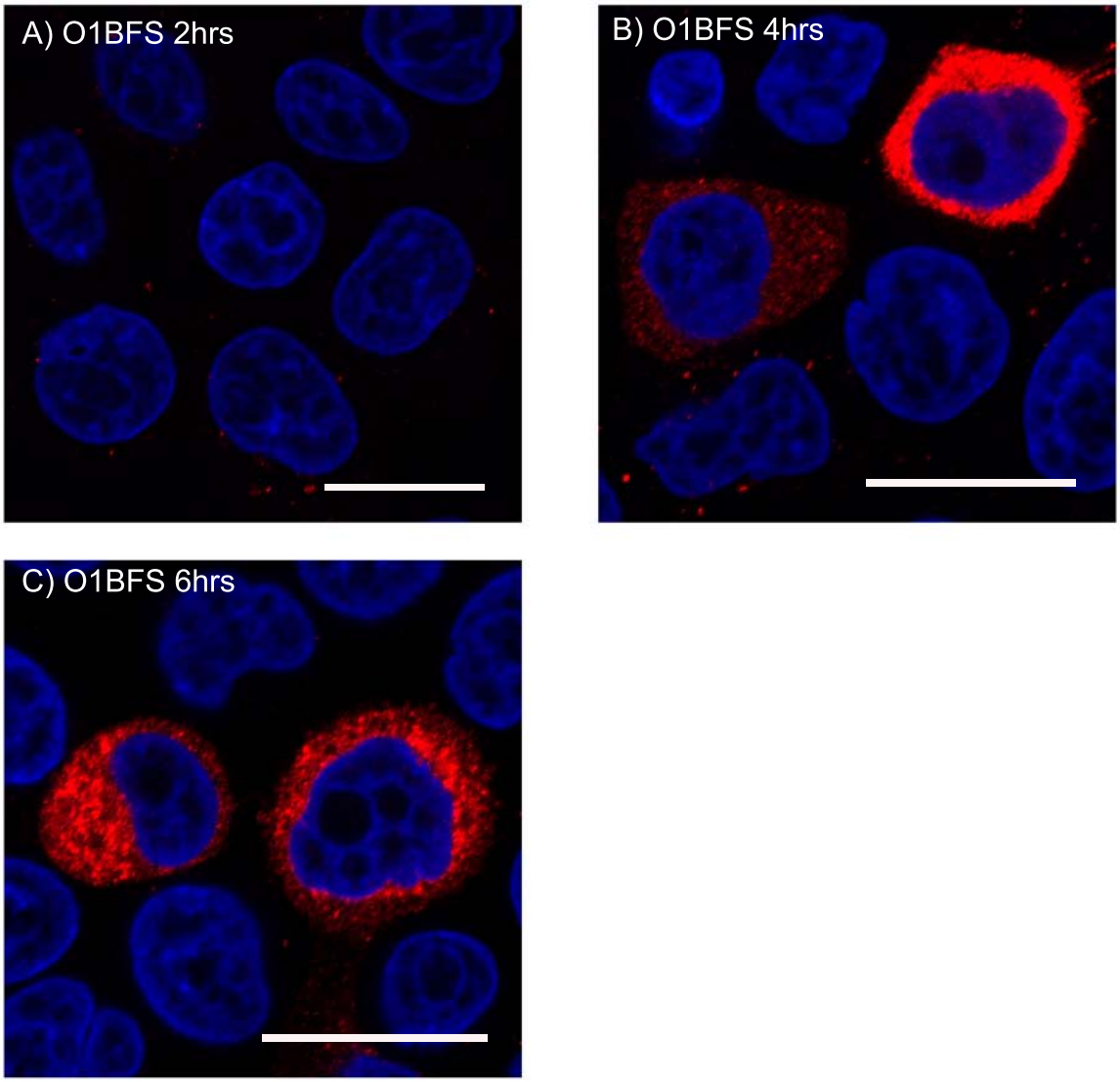


Figure 7.3 Time course of FMDV infection in HeLa cells
HeLa cells were infected with O1BFS FMDV and fixed at 2, 4 and 6 hours post infection. FMDV is shown in red (panels A-C). The cell nuclei were stained with DAPI and are shown as blue. Scale bar = 10 μm.

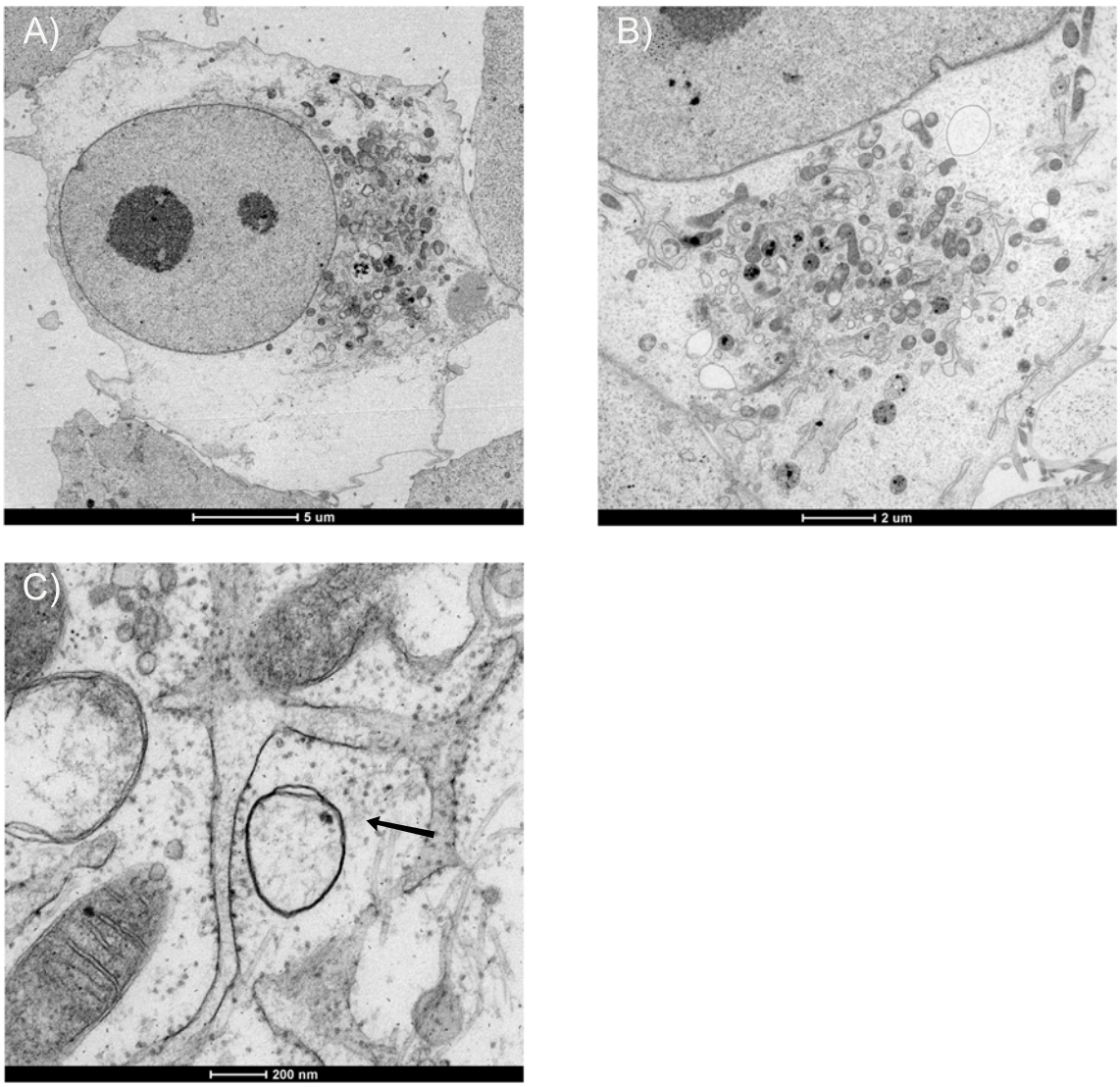


Figure 7.4 Membrane rearrangements in FMDV infected HeLa cells
HeLa cells were infected with FMDV (MOI 0.8) for 6 hours and processed for TEM. Panels A-B show membrane rearrangements in infected cells. Panel C shows a double membrane vesicle (black arrow). Scale bars shown at the bottom for each panel.

The above experiments establish that HeLa cells can be infected with O1BFS, and that infection is productive with maximum detection of viral proteins at 5-6 hours pi. In addition, infection resulted in host-cell membrane rearrangements characteristic of a normal infection. Taken together these findings confirm that HeLa cells can be infected with O1BFS FMDV, although infection levels are relatively low in comparison to the more susceptible cell lines (BHK21 or IBRS-2).

7.3 Optimisation of a QPCR assay for the detection of FMDV vRNA

A QPCR assay was developed to quantify levels of FMDV vRNA in infected cells. The QPCR assay is a standard assay used in the FMDV World Reference Laboratory (WRL) at the Institute for Animal Health, Pirbright for the detection of FMDV in field samples. As a control, the mRNA levels of the housekeeping gene GAPDH was also measured as they should not significantly alter during FMDV infection. The primers and probes for FMDV used in the assay were compared to published sequences of O1BFS. The primers and probe detect the 3D region of the genome and they have a 100% nucleotide match to O1BFS 3D. The primers and probe used for GAPDH mRNA detection were originally designed for bovine GAPDH, therefore an alignment of bovine and human GAPDH sequences were carried out. The comparison showed a 99% nucleotide match, with two nucleotide differences identified at the 5' end of the probe, therefore neither of the differences should interfere with the efficiency of the assay. The efficiencies for FMDV and GAPDH QPCR reactions were calculated from their respective standard curves using the MxPro v4.1 Stratagene software. The efficiency for the FMDV QPCR is 94.3% and the efficiency of the GAPDH QPCR is 95-100% (personal communication C. Wright, WRL, IAH).

An initial experiment was carried out with IBRS-2 cells, to establish the assay. IBRS-2 cells were infected with 1 x 10^6 or 0.5 x 10^6 pfu/ml of O1BFS. Cells were incubated at 37^{o}C to allow virus uptake. After one hour, the cells were subjected to an acid wash to inactivate any external virus before being incubated in virus growth media for a further 4 hours. Infected cells were lysed at 0 and 4 hours pi using AVL lysis buffer (Qiagen). The vRNA was extracted (QiaAMP viral RNA extraction kit, Qiagen) and a reverse transcription reaction carried out on each sample (Taqman kit, Roche) (see section 2.6). QPCR reactions were performed using Taqman PCR mastermix, primers and 6FAM-TAM labelled probes designed to detect FMDV (FMD 3D) and GAPDH. All samples were analysed using a Stratagene MX3000 QPCR machine.

Figure 7.5 (A-B) shows the results for FMDV (A) and GAPDH (B) in IBRS-2 cells infected with a 1 x 10^6 or 0.5 x 10^6 pfu/ml of O1BFS at 0 (T0) and 4 (T4) hours pi. Triplicate samples for each virus dilution were carried out. The upper panel shows the Ct values for the experiment. The Ct value is the cycle number at which fluorescence of the PCR can be detected as positive, and for these experiments the positive threshold was set to intersect the exponential part of the amplification curve. The Ct value is inversely proportional to the log amount of template in the PCR and assuming a 100% effective PCR amplification, a difference of one Ct value corresponds to an approximate 3 fold difference in template amount.

Figure 7.5 (C) shows the mean +/- SD for the samples shown in Fig 7.5 (A-B). In cells infected with a 1 x 10^6 or 0.5 x 10^6 pfu/ml of O1BFS. A difference of ~4-5 Ct values was seen for vRNA from 0 to 4 hours. This equates to an approximate 1.3 log increase in vRNA levels (see above)

FMDV	1×10^6 01BFS			0.5×10^6 01BFS		
Sample	ct value (1)	ct value (2)	ct value (3)	ct value (1)	ct value (2)	ct value (3)
T0	25.5	25.5	25.7	27.8	27.9	27.4
T4	21.3	20.8	21.2	22.9	23.4	24.2

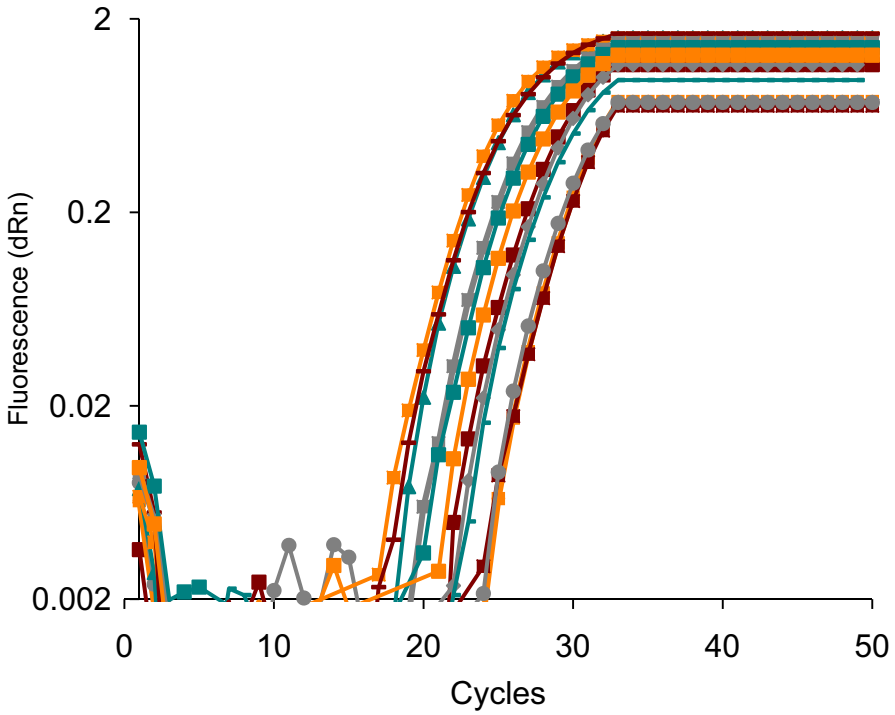


Figure 7.5 (A) The detection of FMDV vRNA in IBRS-2 cells by QPCR IBRS-2 cells were infected with dilutions of FMDV O1BFS. Infected cells were lysed at 0hrs (T0) and 4hrs (T4) post infection, and analysed by QPCR for FMDV vRNA levels. *Upper Table*: shows the Ct values for samples carried out in triplicate at 0hrs and 4hrs pi. *Lower Figure:* The graph shows the amplification plot of each samples fluorescence reading over 50 cycles (Key: each colour and symbol represents the fluorescence reading of one sample)

GAPDH	1 x 10^6 O1BFS			0.5 x 10^6 O1BFS		
Sample	ct value (1)	ct value (2)	ct value (3)	ct value (1)	ct value (2)	ct value (3)
T0	18.4	18.7	18.7	18.5	18.8	18.8
T4	18.3	18.0	19.3	18.5	18.4	19.3

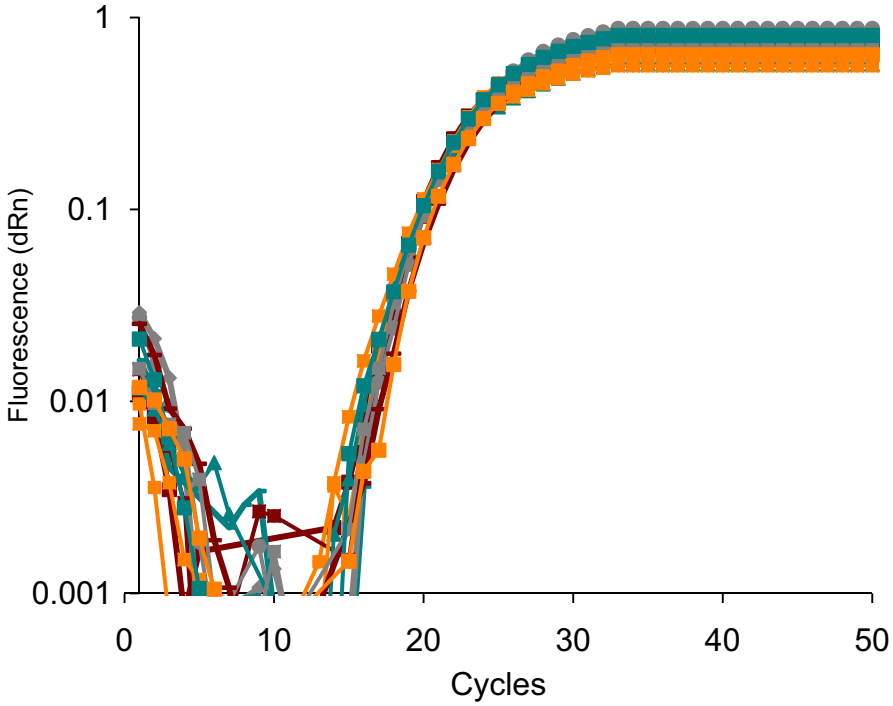


Figure 7.5 (B) The detection of GAPDH mRNA in IBRS-2 cells by QPCR
IBRS-2 cells were infected with dilutions of O1BFS. Infected cells were lysed at 0hrs (T0) and 4hrs (T4) post infection, and analysed by QPCR for GAPDH mRNA levels. *Upper Table*: shows the Ct values for samples carried out in triplicate ay 0hrs and 4hrs pi. *Lower Figure:* The graph shows the amplification plot of each samples fluorescence reading over 50 cycles (Key: each colour and symbol represents the fluorescence reading of one sample)

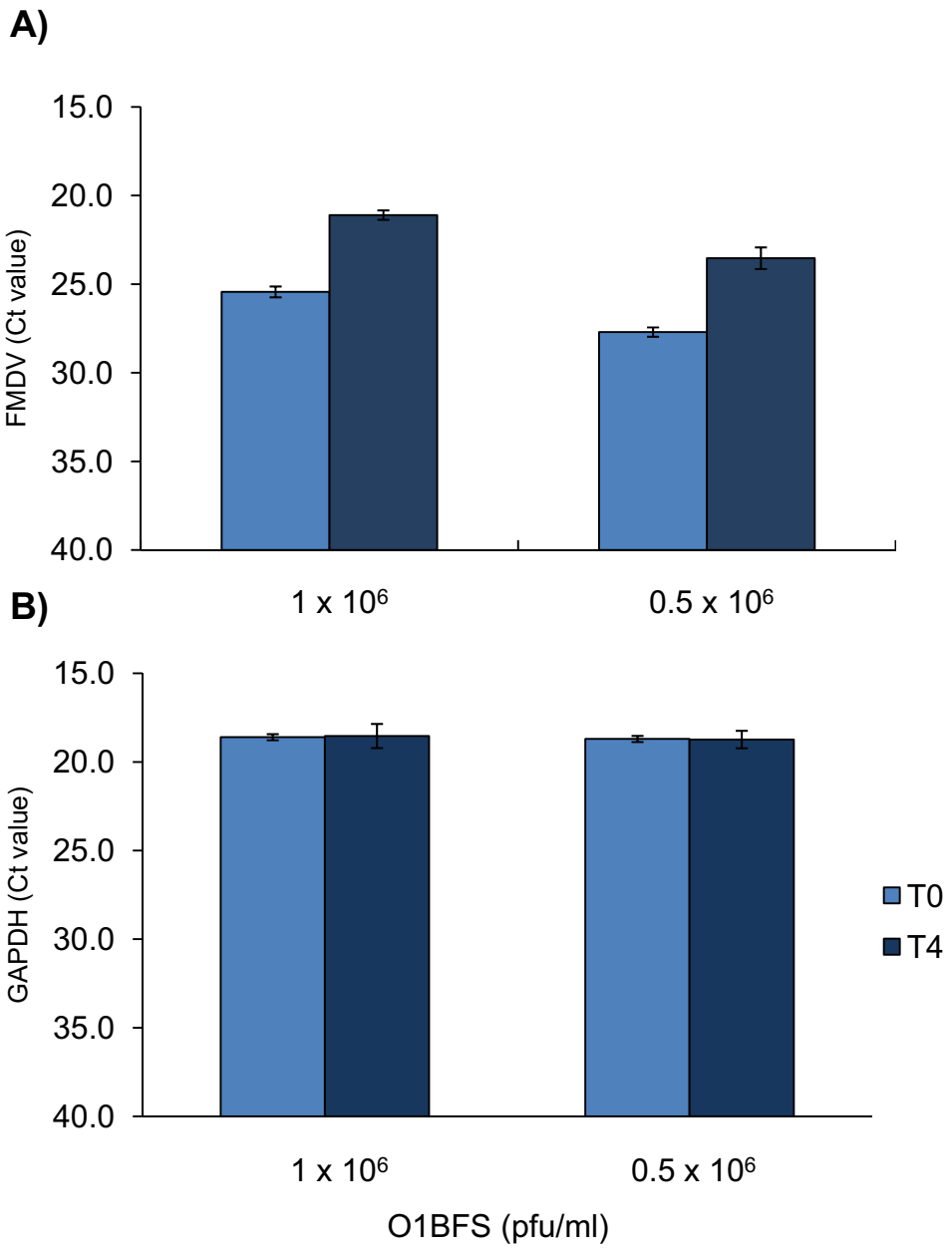


Figure 7.5 (C) The detection of FMDV vRNA and GAPDH mRNA in IBRS-2 cells by QPCR
Shown is the mean +/- SD for the experiments shown in figure 7.5 (A-B). Cells lysed at 0hrs pi are shown in light blue (T0) and cells lysed at 4 hrs pi are shown in dark blue (T4). Panel A shows FMDV vRNA levels. Panel B shows GAPDH mRNA levels.

Fig 7.5, panel A). In contrast to vRNA, the Ct value for GAPDH remained constant throughout the assay (Fig 7.5, panel B). GAPDH is commonly used as an internal control in QPCR assays, therefore it was established if GAPDH mRNA levels remain constant in HeLa cells infected with FMDV. HeLa cells were infected with a serial dilution of O1BFS and analysed by QPCR as described above. Figure 7.6 shows the Ct values for GAPDH mRNA in infected HeLa cells at 0 hours and 4 hours pi. Overall, GAPDH levels in infected cells remains constant during FMDV infection, suggesting that GAPDH is a suitable internal control for QPCR experiments using HeLa cells.

Figure 7.7 shows the Ct values for FMDV vRNA in HeLa cells infected with a serial dilution of O1BFS at 4 hours pi. The Ct values indicated that viral RNA levels are at their highest when the virus is applied at 1 X 10^7 pfu/ml and that the levels progressively decrease with each dilution. Another key observation is that infection with O1BFS (1 X 10^6 pfu/ml) resulted in similar Ct values for both HeLa (Fig 7.7 [A]) and IBRS-2 cells (Fig 7.5C [A]) which demonstrates the efficiency of the assay.

The next experiment established when peak vRNA levels occurred in infected HeLa cells. A time course of infection was carried out in HeLa cells and IBRS-2 cells for comparison. Figure 7.8 shows IBRS-2 cells infected with 0.5 x 10^6 pfu/ml of O1BFS and lysed at 0, 2 and 4 hours pi. Lysates were analysed by QPCR for detection of FMDV (panel A) and GAPDH (panel B) RNA levels. Each reaction was carried out in duplicate. At 2 hours pi, FMDV vRNA only increased by ~1-2 Ct values, which is equivalent to a ~0.3 log increase in virus compared to 0 hours pi; however vRNA increases by ~9 Ct values (~3 logs) by 4 hours pi (Fig 7.8, panel A). Overall, GAPDH mRNA remains constant (Fig 7.8, panel B).

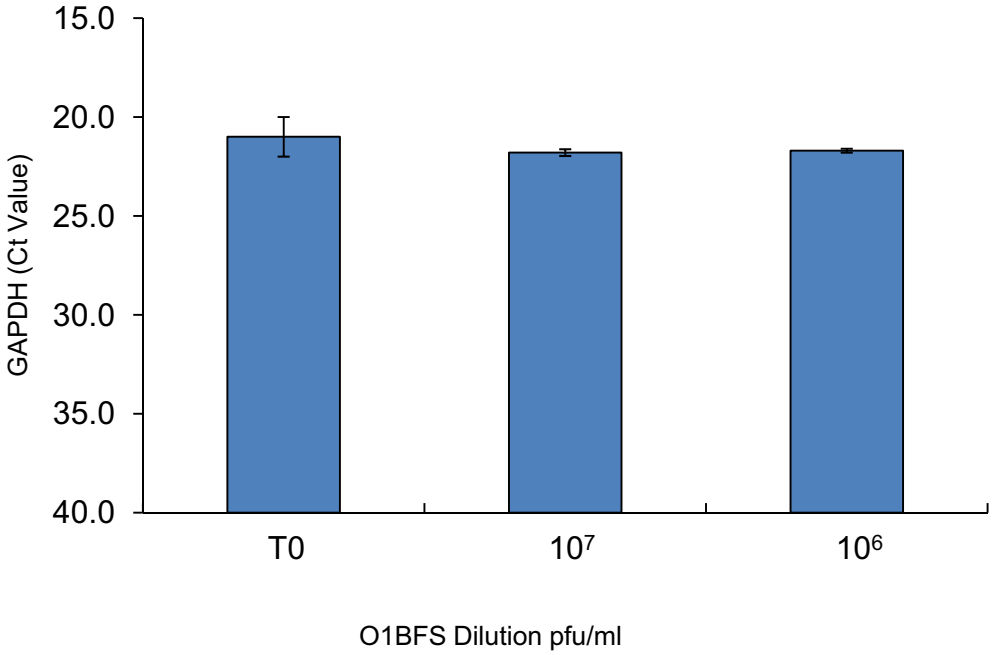


Figure 7.6 GAPDH levels in FMDV infected HeLa cells
Hela cells were infected with O1BFS ($1X10^7$ – $1X10^6$) and cells lysed at 0hrs (T0) and 4hrs pi. GAPDH mRNA levels were determined from cell lysates by QPCR. Shown is the mean +/- SD for triplicate samples.

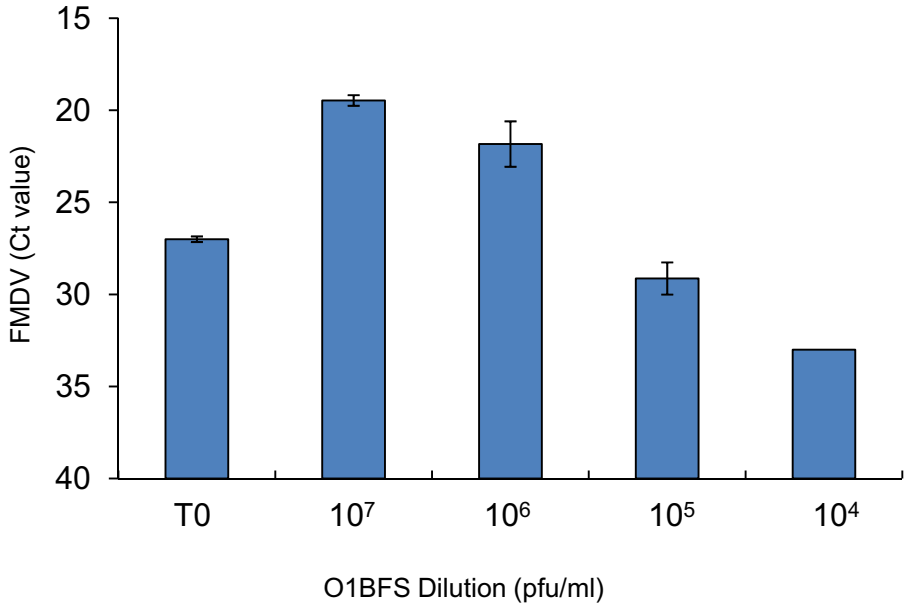


Figure 7.7 QPCR analysis of FMDV infection in HeLa cells
Hela cells were infected with a serial dilution of O1BFS ($1X10^7$ – $1X10^4$) and cells lysed at 0hrs and 4hrs pi. FMDV vRNA levels were determined from cell lysates by QPCR. Shown is the mean +/- SD of triplicate samples.

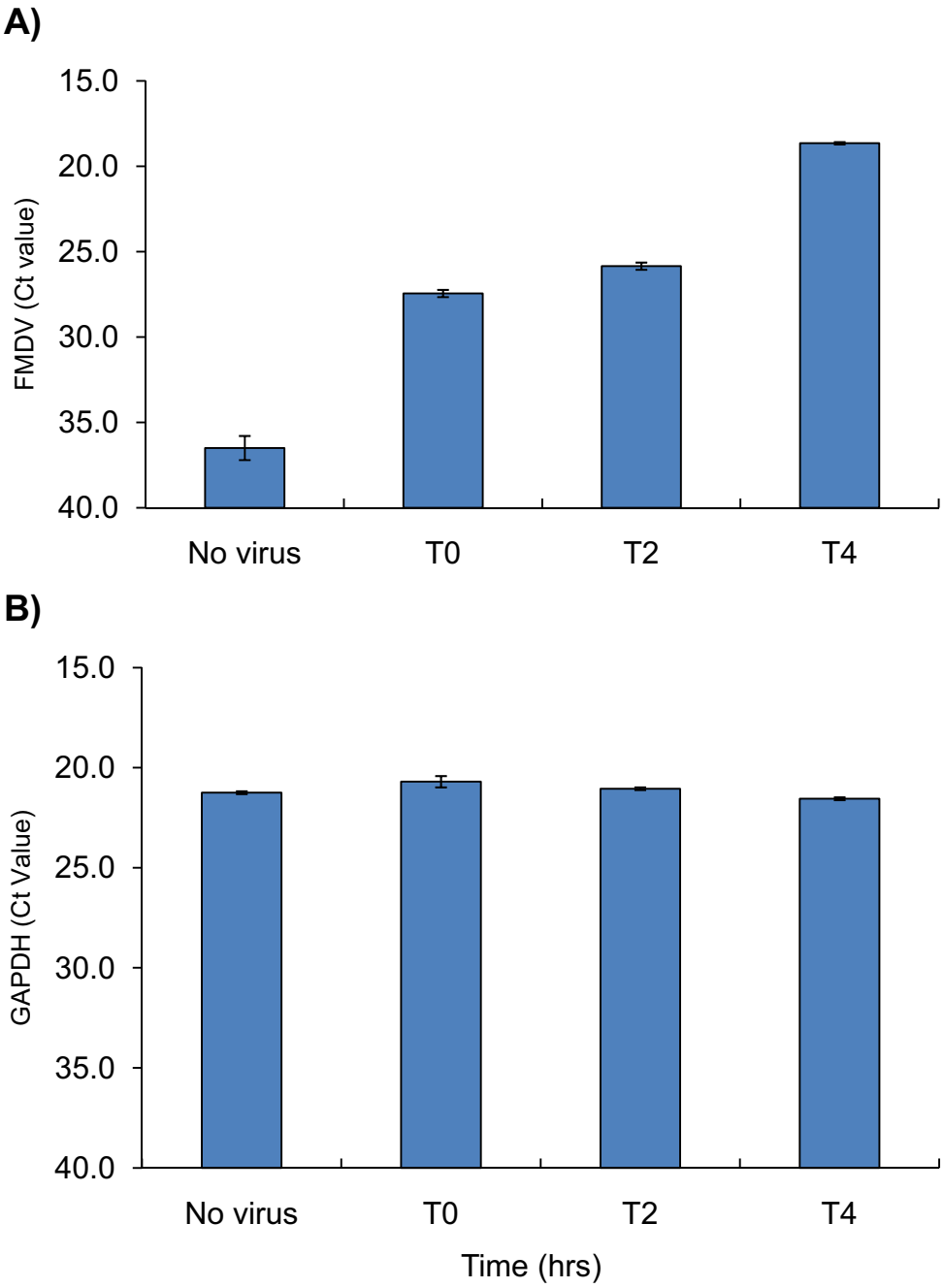


Figure 7.8 Time course of FMDV infection in IBRS-2 cells using QPCR

IBRS-2 cells were infected with a 0.5 x 10^6 pfu/ml of O1BFS and lysed at 0 (T0), 2 (T2) and 4 (T4) hours post infection and analysed by QPCR. Panel A shows FMDV vRNA levels. Panel B shows GAPDH mRNA levels. The mean +/- SD is shown from duplicate samples.

Figure 7.9 shows the same experiment as shown in figure 7.8 for HeLa cells, except that cells were lysed and samples processed for QPCR at 0, 2, 4 and 6 hours pi. Lysates were analysed by QPCR for detection of FMDV (panel A) and GAPDH (panel B) RNA levels. Each reaction was carried out in triplicate. An increase of ~5 Ct values (1.6 log) in FMDV vRNA was detected in HeLa cells at 4 hours pi when compared to the 0 hours pi samples. At 6 hours pi, vRNA levels were around 2 Ct values (0.6 logs) lower than that seen at 4 hours pi (Fig 7.9, panel A). As shown previously, GAPDH mRNA levels remain constant throughout infection (Fig 7.9, panel B). These results indicate that peak FMDV vRNA production is around 4 hours pi in HeLa cells which starts to reduce at 6 hours, most likely due to cell lysis. Further optimisation experiments and observations by IF (see fig 7.3) resulted in a time point of 5 hours pi infection being selected for subsequent QPCR experiments.

The optimal conditions for quantification of FMDV vRNA by QPCR in HeLa cells are using O1BFS at a 0.5 x 10^6 pfu/ml and infecting for 5 hours.

7.4 The effect of Rab depletion by RNAi on FMDV replication

7.4.1 Optimisation of Rab5a knockdown in HeLa cells

The next step was to optimise RNAi conditions for efficient knockdown of Rab proteins in HeLa cells. However, this was not possible for all of the Rab proteins studied, as antibodies to the Rab proteins were not available. Therefore the conditions were optimised for Rab5a siRNA, as antibodies were available. These conditions were then applied to all other Rab proteins. Cells were transfected with Rab5a siRNA (duplexes 78 and 79) (see appendix III), individually or in combination. Transfections were allowed to proceed for 6 hours before media was exchanged for normal cell culture media. After 48

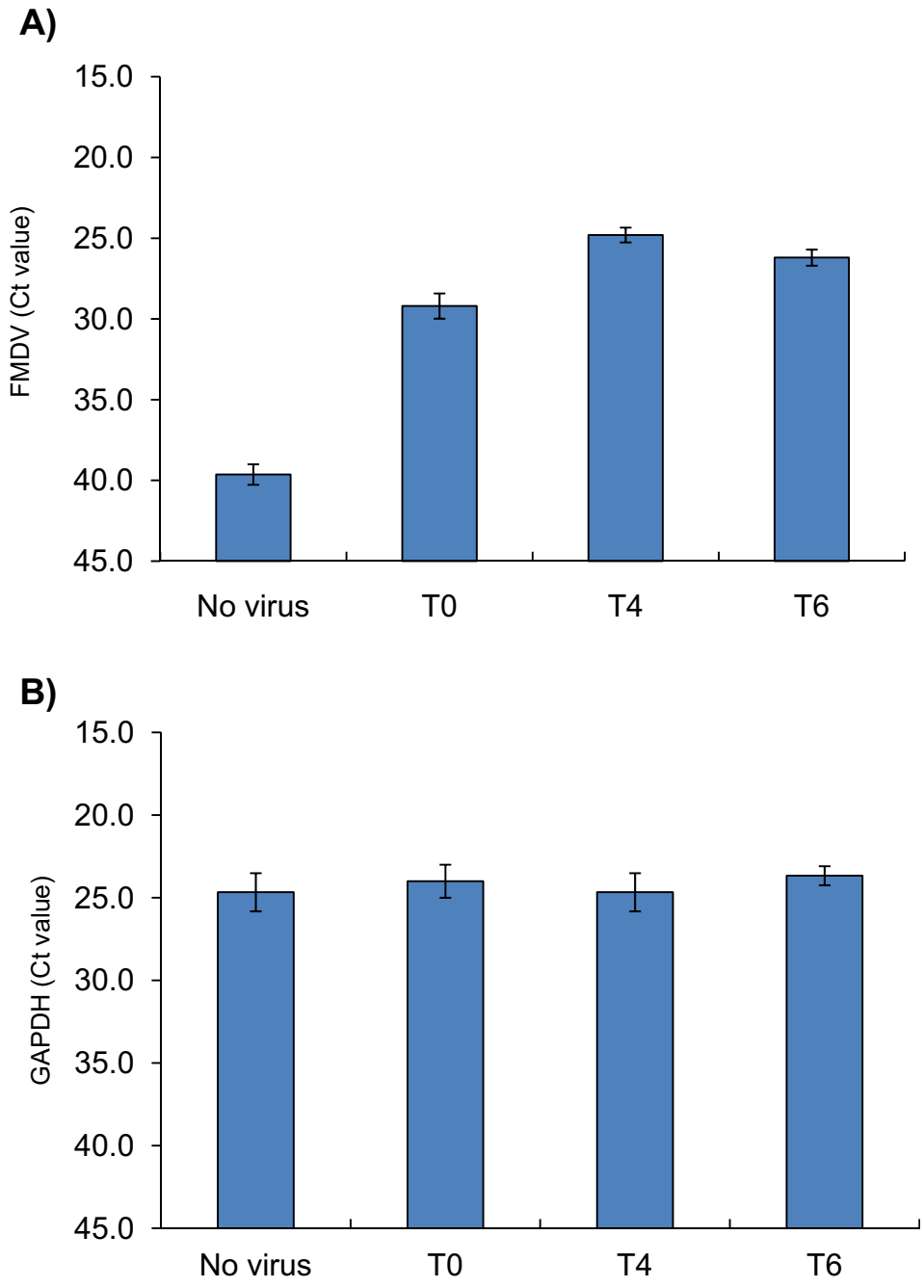
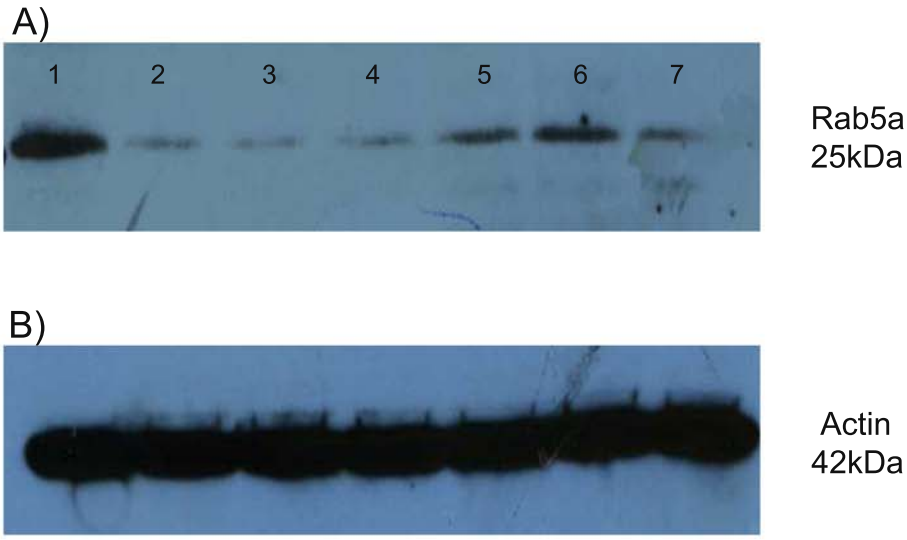


Figure 7.9 Time course of FMDV infection in HeLa cells using QPCR
HeLa cells were infected with a 0.5 x 10^6 pfu/ml of O1BFS and lysed at 0 (T0), 4 (T4) and 6 (T6) hours post infection and analysed by QPCR. Panel A shows FMDV vRNA levels. Panel B shows GAPDH mRNA levels. The mean +/- SD is shown for triplicate samples.

hours incubation, the cells were lysed for western blot analysis (see methods 2.11) to determine the level of Rab5a knockdown. The amount of protein in each sample was quantified using a BCA assay (see methods 2.11) to ensure that equal amounts of protein were loaded onto the gel. In addition, a duplicate western blot was performed on each sample for actin to further ensure the equal loading of protein across the gel. Figure 7.10 shows a western blot of Rab5a in cells transfected with 2.5 or 5pmol of each siRNA duplex (Duplexes 78 and 79), individually or in combination. Lane 1 shows HeLa cell lysate and a 25 kDa band representing Rab5a. Lane's 2-5 show that the transfections of individual siRNAs (78 and 79) reduce Rab5a levels. However, duplex 79 appeared to be less effective at 5pmol when compared to the results obtained with 2.5pmol (see lane 4 and 5). This apparent discrepancy most likely reflects poor transfection efficiency of this particular sample. Lanes 6-7 show that co-transfection of duplexes 78 and 79 reduce Rab5a most efficiently when used at 5pmol. These results indicate that transfection with 5pmol of each siRNA duplex achieved an effective knockdown for Rab5a, however further optimisation indicated a more efficient knockdown of Rab proteins was achieved at 10pmol per duplex and was therefore used for all subsequent experiments.

7.4.2 The effect of the knockdown of Rab proteins on FMDV infection in HeLa cells

Next, the effect on FMDV infection of siRNAs targeted to various Rab proteins was determined. Most Rab proteins exist as multiple isoforms. Therefore cells were co-transfected with Rab siRNAs targeting all the known isoforms for a given Rab. For example Rab1 possesses three isoforms (a, b and c), therefore 10pmol of each Rab isoform siRNA was co-transfected into cells.



1) Cell lysate
2) Rab5a siRNA 78 (2.5pmol)
3) Rab5a siRNA 78 (5pmol)
4) Rab5a siRNA 79 (2.5pmol)
5) Rab5a siRNA 79 (5pmol)
6) Rab5a siRNA 78+79 (2.5pmol each)
7) Rab5a siRNA 78+79 (5pmol each)

Figure 7.10 Knockdown of Rab5a in HeLa cells by siRNA
HeLa cells were transfected with Rab5a siRNA (Duplexes 78 and 79) either individually or in combination for 48hrs. Panel A shows a Western blot for Rab5a. Lane 1 shows untreated cells and lanes 2-5 cells transfected with the individual duplexes (see lane description). Lanes 6-7 show cells co-tranfected with both duplexes (78 and 79) Panel B shows the same samples probed for Actin.

Cells were transfected with non-target siRNA or co-transfected with the various Rab siRNAs in various combinations (Rab1 [a, b and c], Rab2 [a and b], Rab5 [a, b, c], Rab6 [a, b, c] and Rab34) for 48 hours prior to infection with O1BFS FMDV for 5 hours. Supernatants were collected prior to the lysis of cells with AVL buffer (Qiagen) for 10 minutes at room temperature, and the RNA extracted. Reverse transcriptase and QPCR reactions were carried out to detect both FMDV vRNA and GAPDH RNA levels as previously described (see section 7.3). Each reaction was carried out in triplicate.

Figure 7.11 shows the mean +/-SD of Ct values for FMDV vRNA (panel A) and GAPDH mRNA (panel B) in cells transfected with Rab1 (a, b and c), Rab2 (a and b) and Rab5 (a, b, c) siRNA. In cells depleted of Rab1 (a, b and c), an increase of ~3 Ct values (~1 log) in FMDV vRNA was seen, whereas in cells depleted with Rab2 (a and b) or Rab5 (a, b, and c), there did not appear to be any significant effect on vRNA levels when compared to cells transfected with non-target siRNA (Fig 7.11, panel A). Overall, GAPDH mRNA levels remain constant over the experiments (Fig 7.11, panel B). Figure 7.12 shows the results for a similar experiment using cells transfected with siRNA for Rab6 (a, b and c) and Rab34; depletion of Rab6 or Rab34 appeared to have little or no effect on FMDV vRNA levels.

The apparent increase observed in FMDV vRNA in cells depleted of Rab1 (a, b, c) was of interest and was investigated further. The above experiment was repeated with Rab1 (a, b and c) siRNA. Figure 7.13 shows the amount of FMDV vRNA (panel A) and GAPDH mRNA (panel B) in cells transfected with non-target siRNA or co-transfected with Rab1 (a, b and c) siRNA. Similar to the results shown in figure 7.11, an apparent increase of vRNA by ~2 Ct values, which equates to ~0.6-0.7 log of virus, was seen in cells

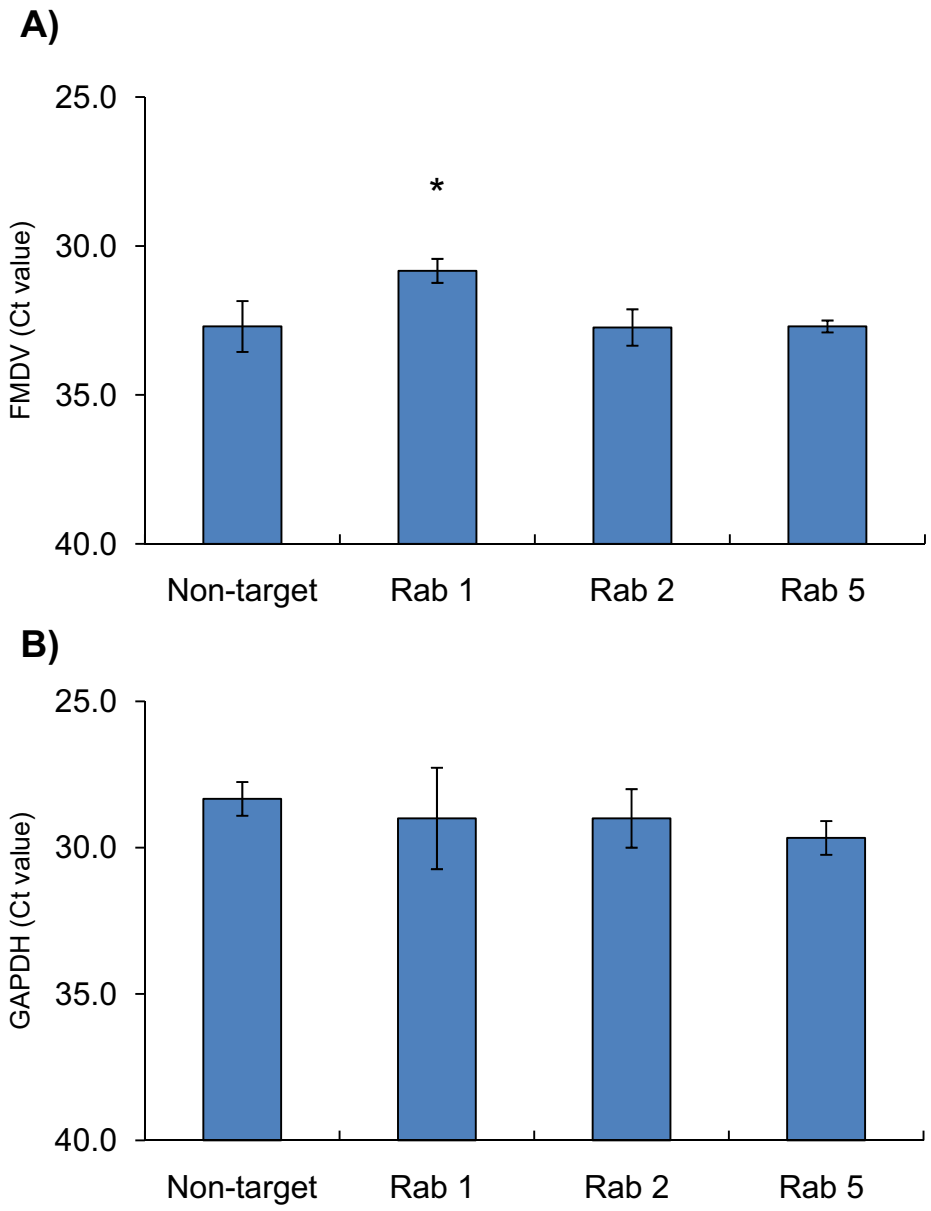


Figure 7.11. The effects of Rab siRNA on FMDV infection in HeLa cells (Experiment A)
HeLa cells were co-transfected with 10pmol of siRNA targeting Rab1 (a ,b and c), Rab2 (a and b) or Rab5 (a, b and c) for 48 hours and then infected with 0.5 X 10^6 pfu/ml of O1BFS . Cell lysates were analysed by QPCR. Panel A shows FMDV vRNA levels. Panel B shows GAPDH mRNA levels. The mean +/- SD is shown for triplicate samples. (*P* value: $*$ < 0.05).

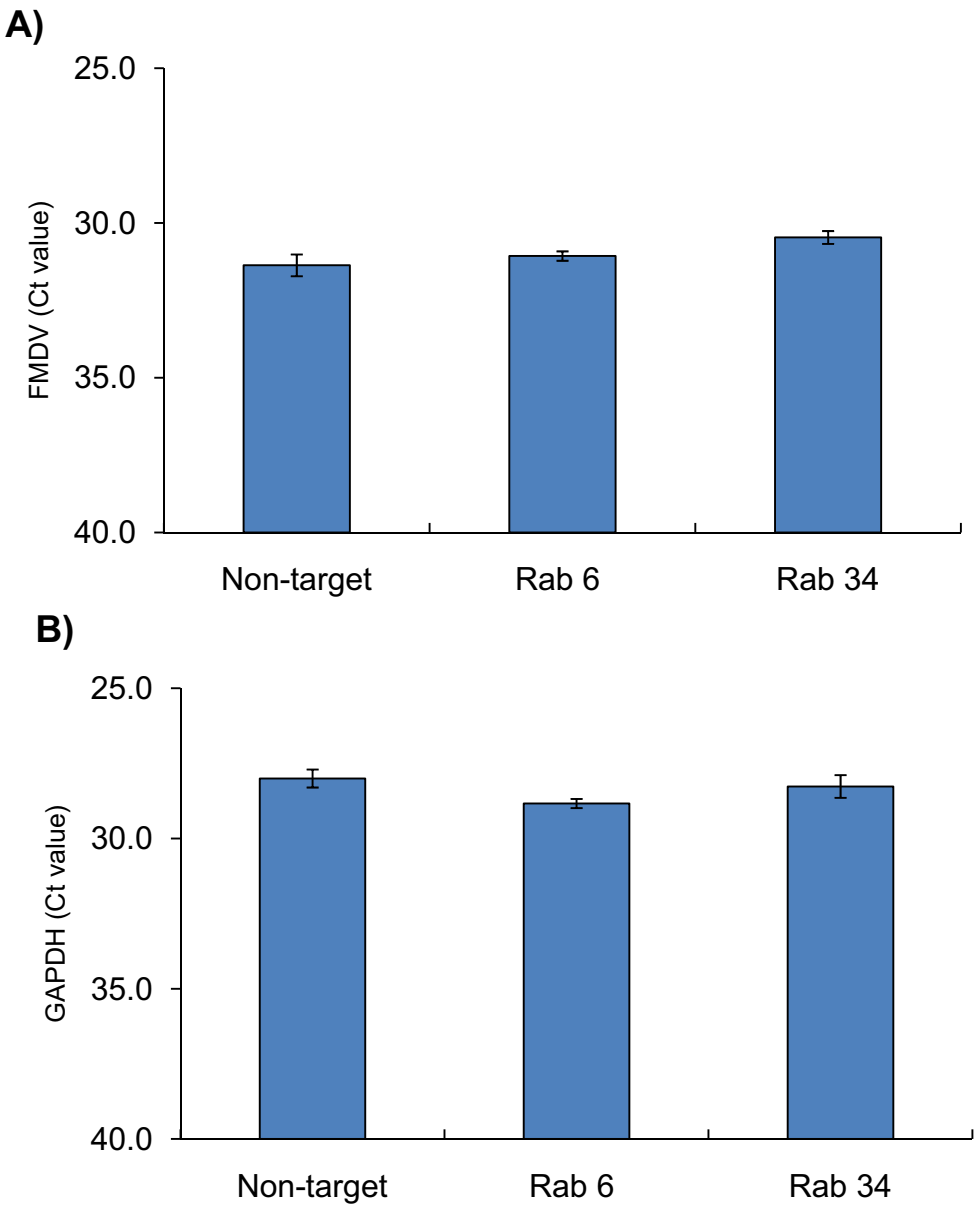


Figure 7.12. The effects of Rab siRNA on FMDV infection in HeLa cells (Experiment B)
HeLa cells were co-transfected 10pmol of siRNA to Rab6 (a ,b and c) or Rab34 for 48 hours and then infected with 0.5 X 10^6 pfu/ml of O1BFS. Cell lysates were analysed by QPCR. Panel A shows FMDV vRNA levels (*P* value >0.05 , non-significant). Panel B shows GAPDH mRNA levels. The mean +/- SD is shown for triplicate samples.

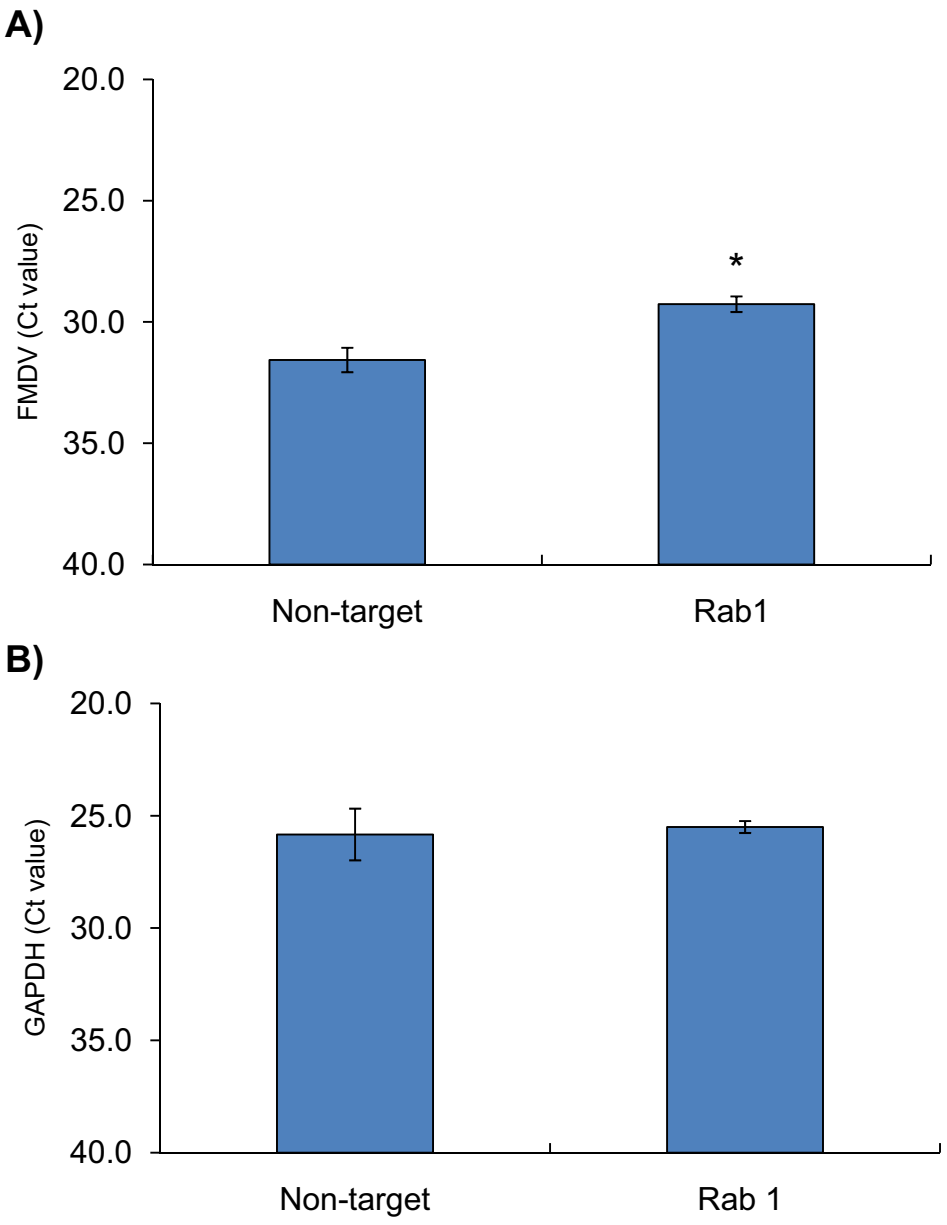


Figure 7.13. The effects of Rab1 siRNA on FMDV infection of HeLa cells.
HeLa cells were co-transfected with 10pmol of siRNA to Rab1 (a ,b and c) for 48 hours and then infected with 0.5 X 10^6 pfu/ml of O1BFS. Cell lysates were analysed by QPCR. Panel A shows FMDV vRNA levels. Panel B shows GAPDH mRNA levels. The mean +/- SD is shown for triplicate samples. (*P value:* $*$ < 0.05).

depleted of Rab1 (a, b and c), in comparison to cells transfected with the non-target siRNA.

Figure 7.14 shows the data for Ct values obtained for cells transfected with Rab1 siRNA normalised to the Ct value of cells transfected with non-target siRNA. For each transfection (Rab1 siRNA or non-target siRNA), the data was normalised using the following equation (Figure 7.14):

Ct = Non-target siRNA (Ct GAPDH – Ct FMDV) – Rab siRNA (Ct GAPDH – Ct FMDV)

This data confirms that Rab1 (a, b and c) knockdown by siRNA produces around a ~1 log increase in the amount of vRNA produced. This result confirms that depletion of Rab1 (a, b and c) increases the amount of vRNA in FMDV infected cells and therefore may enhance replication.

To determine if the observed increase in the amount of vRNA in Rab1 depleted cells translated into an increase in virus yield, the supernatants from the previous experiment were titrated onto BHK21 cells (see methods 2.2.3). Figure 7.15 shows ~3 fold increase in FMDV yield in cells depleted of Rab1 (a, b and c) when compared to cells transfected with non-target siRNA, which confirms the findings from the QPCR experiments.

Taken together this data suggests that Rab1 is not required for FMDV replication, and that the inactivation of the protein maybe advantageous to FMDV replication.

7.5 Discussion

This chapter investigated the role of various Rab proteins in FMDV replication. These experiments were carried out using a human Rab siRNA library. The initial experiments were conducted to establish if HeLa cells could

siRNA target	Non-target siRNA (ct GAPDH-ct FMD)	Rab siRNA (ct GAPDH - ct FMD)	Total (Non-target ct) - (Rab ct)
Rab 1 a, b, c (1st exp)	-4.7	-2.0	-2.7
Rab1 a, b, c (2nd exp)	-5.7	-3.7	-2.0

Figure 7.14 The effects of Rab1 siRNA on FMDV infection (normalised data)
The table shows average Rab1 siRNA Ct values from figures 7.14 and 7.16 normalised to the average ct value for cells transfected with non-target siRNA, using the equation below. Ct values are the mean of samples carried out in triplicate from two separate experiments.

Ct = Non-target (Ct GAPDH – Ct FMDV) – Rab siRNA (Ct GAPDH – Ct FMDV)

	pfu/ml		
Experiment	**Non-target**	**Rab1 siRNA**	**Normalised data**
1	5.6×10^2	1.6×10^3	286%
2	$4.4. \times 10^2$	$1.8. \times 10^3$	417%
3	$5.6.x\ 10^2$	$3.2. \times 10^3$	571%

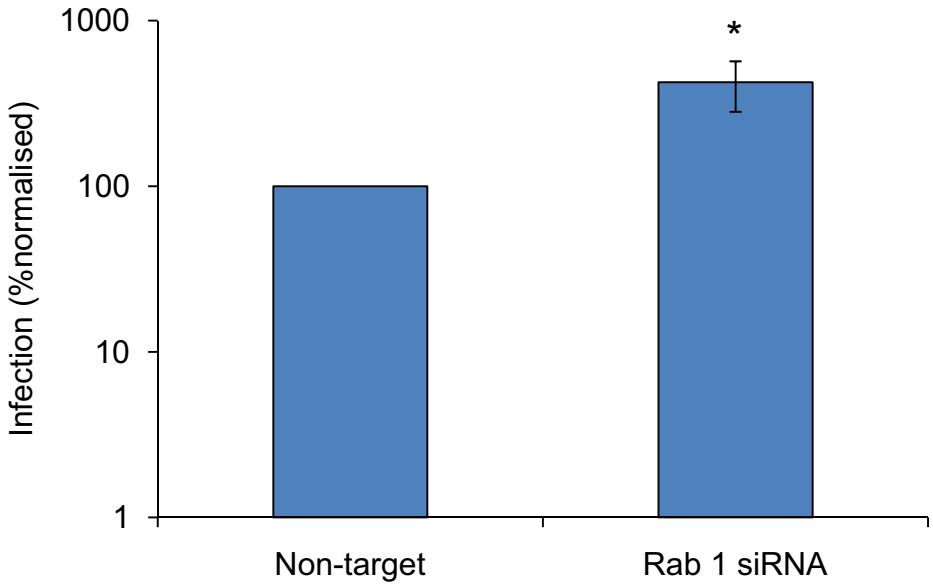


Figure 7.15 The effect of Rab1 siRNA on FMDV virus yield
HeLa cells were transfected with 10pmol of non-target siRNA or Rab1 (a, b, c) siRNA duplexes for 48 hours and then infected with O1BFS. The supernatants were collected at 5 hours pi and titrated onto BHK-21 cells. *Upper Table*: Shows the mean pfu/ml of three independent experiments and the normalised data. *Lower Figure*: The viral yield of cells transfected with Rab1 siRNA was normalised to the yield for cells transfected with non-target siRNA (*P* value: $* < 0.05$).

be productively infected with FMDV (O1BFS). These experiments showed that HeLa cells are productively infected, and that infection results in host cell membrane rearrangements that are similar to those previously observed for BHK and IBRS-2 cells. However, infection did appear to proceed at a slower rate and a lower level of infectious virus was produced when compared to other cell lines that are normally used to study FMDV infection.

The protocols to quantify infection were established using siRNA to Rab5, as antibodies to Rab5 were available to estimate the degree of target protein knockdown. However, antibodies for all the Rab proteins studied were not available, which limits the interpretation of some of the experimental results. Transfection with siRNA to Rab2 (a and b), Rab5 (a, b and c), Rab6 (a, b and c) and Rab34 appeared to result in a slight increase (1Ct; equivalent to 0.3 log) of vRNA, which could suggest that depletion of these proteins may have a slight but positive effect on FMDV replication. However these increases were relatively small and unlikely to be biologically significant. Inhibiting the function of Rab5 using dn proteins has previously been shown to reduce FMDV infection in IBRS-2 cells (Johns et al., 2009); however Rab5 siRNA did not produce an inhibitory effect in HeLa cells. This may be explained by the observation that heparan sulphate binding viruses are not taken up by clathrin-mediated endocytosis (O'Donnell et al., 2008) and therefore, may not rely on Rab5 for infection.

Transfection of cells with siRNA to Rab1 (a, b and c) showed an increase in vRNA (0.6-1.0 log) compared to control cells. This suggests that inactivation of Rab1 (a, b and c) may enhance FMDV replication. Rab1 is the only Rab protein that is known to be involved in transport from the ER to Golgi (Haas 2007). The inactivation of Rab1 is thought to interfere with the docking and

tethering of vesicles that form the ERGIC, and possibly the sequential exchange of the COPII coat to COPI on transport vesicles that exit at ERES.

The apparent increase in FMDV replication caused by siRNA targeting Rab1 (a, b and c) was investigated further. The supernatants from the experiment were collected prior to cell lysis (Rab1 and non-target siRNA) and were titrated on BHK21 cells. These results show that the cells transfected with Rab1 (a, b and c) siRNA showed an increased FMDV yield (~3 fold) when compared to cells transfected with non-target siRNA. This result confirmed the findings in the previous experiment using dn Rab1 and supports the conclusion that inhibiting the function of Rab1 is in some way advantageous for FMDV replication.

In conclusion, it appears the knockdown of the Rab1 (a, b and c) by siRNA results in an increase to FMDV replication which is evident by both an increase in vRNA and virus yield. The main role of Rab1 is to regulate the transport of vesicles between the ER and Golgi and is essential for Golgi integrity (Haas et al., 2007; Nuoffer et al., 1994; Tisdale, 1999). A loss of Rab1 function would result in a block to secretion probably before the ERGIC. Rab1 inhibition has been reported to prevent COPI transport but not affect COPII formation (Alvarez et al., 2003; Tisdale et al., 1992). The recruitment of COPI to vesicles at ERES suggests Rab1 may be responsible for the COPII/COPI exchange on these vesicles. This suggests that FMDV does not require the formation of the ERGIC compartment or the COPII/COPI exchange that allows transport of cargo from the ERGIC into the Golgi, and that a block to this process is actually advantageous to viral replication: Therefore membranes that are generated prior to the COPII/COPI exchange may be required for FMDV replication.

Chapter 8: Discussion

Picornaviruses generate membranous vesicles that provide specialised sites for replication. However, the cellular origin and mechanisms that generate these vesicles, and the properties that make them favourable for replication, are not well understood. During the course of my Thesis it was shown that for enteroviruses (e.g. PV and CVB3) virus-induced vesicles are most likely derived from the early secretory pathway (Hsu et al., 2010).

In my Thesis I investigated the role of the early secretory pathway in FMDV infection. To establish if FMDV requires the early secretory pathway for replication, 3 approaches were used: i) pharmalogical inhibitors that disrupt the secretory pathway, ii) expression of dominant-negative proteins and iii) siRNA's that inhibit the function of key regulatory proteins that, in turn, inhibit the secretory pathway at different stages of transport. The key findings of this study are summarised on Figure 8.1.

FMDV infection of BHK-38 cells has been reported to induce loose clusters of single membrane vesicles. In addition, the cytoplasmic contents become condensed and localised to a region to one side of the nucleus (Monaghan et al., 2004). In my study I used IBRS-2 cells, and established that infection also results in the formation of single membrane vesicles and an internal cellular architecture that was similar to BHK cells, thus confirming that these events take place in cells derived from the natural porcine host of FMDV (Fig 3.1).

It has been reported that on infection of Vero cells, FMDV disrupts the Golgi complex by blocking the secretory pathway through the expression of 2BC. Expression of 2BC alone resulted in a block to protein secretion and

modified the ER compartment (Moffat et al., 2005). Therefore, I labelled in IBRS-2 cells membranes in the early secretory pathway for the ER, ERGIC and Golgi during FMDV infection (Fig 3.3-3.5). The results showed that the Golgi was completely dispersed, and fragmentation of the ERGIC and loss of ER labelling was observed. Previous experiments using the same cell line showed a similar reduction in ER labelling and dispersal of Golgi on FMDV infection of IBRS-2 cells (Martin-Acebes et al., 2008). If both of the ER and Golgi compartments are altered by FMDV infection it would seem likely that the ERGIC would also be affected. However whether the effects seen on the ER and ERGIC are due to the direct action of FMDV, or as a consequence of the loss of the Golgi membranes, was not clear.

Brefeldin A is an inhibitor of membrane transport in the secretory pathway between the ER and Golgi; it prevents the formation of COPI vesicles which are necessary for secretory transport (Doedens and Kirkegaard, 1995; Rothman, 1994). Cells were treated with BfA and labelled for ER, ERGIC and Golgi to determine the effects the drug would have on membranes in the early secretory pathway (Fig 3.6). These experiments showed a loss to Golgi labelling (as expected), plus the peri-nuclear region of the ERGIC also appeared dispersed in some cells and the ER appeared slightly more condensed. Previous studies visualised the effects of BfA on the early secretory pathway and showed that after treatment, the Golgi became tubular and extended through the cytoplasm before emptying its contents into the ER, leaving no Golgi structure behind (Sciaky et al., 1997). This observation explains the loss of the GM130 Golgi labelling and the peri-nuclear region of the ERGIC, which overlaps with the cis-Golgi. The slight concentration of the ER labelling may also be due to the absorption of proteins from the Golgi.

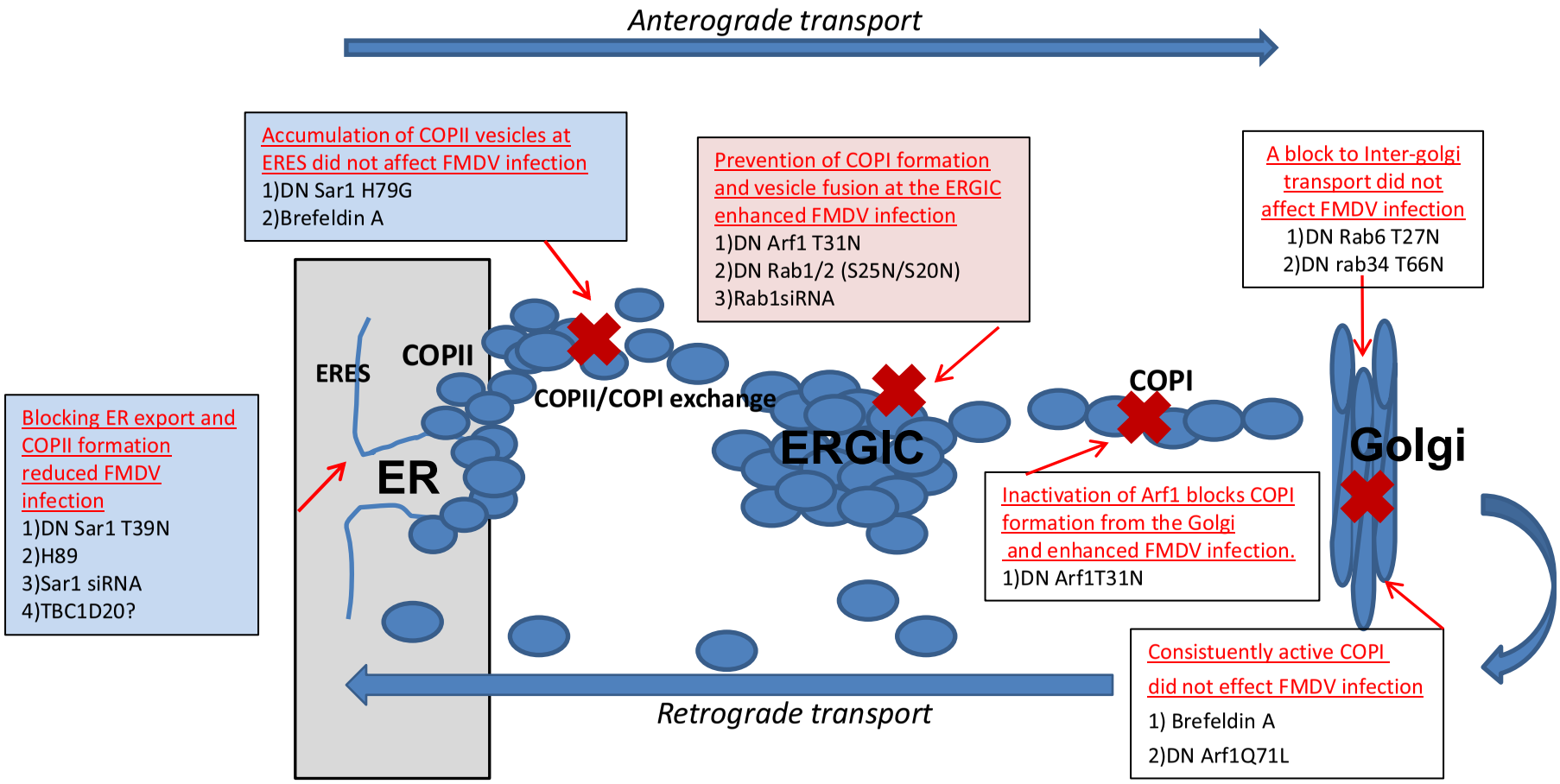


Figure 8.1 Summary: The Role of the early secretory system in FMDV replication
Protein transport begins at the ER at designated ERES where COPII vesicles form, COPII is exchanged for COPI and these vesicles fuse to form the ERGIC which in turn give rise to the Golgi. Proteins are recycled back from the ERGIC and Golgi to the ER. GTPases Sar1, Arf1, & Rab are essential for protein transport.
DN = dominant-negative; Red arrow indicates inhibition; Blue arrow indicates the direct of membrane flow. Red cross indicates membranes not required by FMDV for replication. Grey box indicates possible membranes of the early secretory pathway required for FMDV replication.

An important factor in picornavirus replication is sensitivity to BfA. Infection by PV, EV11 and BEV (bovine enterovirus) are all significantly inhibited by brefeldin A (Maynell et al., 1992), whereas FMDV is not (Martin-Acebes et al., 2008; Monaghan et al., 2004; O'Donnell et al., 2001). This was confirmed by treating IBRS-2 cells with BfA prior to infection with FMDV or BEV; FMDV infection remained unaltered while BEV infection was lost (Fig 3.7). Quantification of the above experiment showed that BfA did not dramatically alter FMDV infection (Fig 3.8). Previous titration experiments using supernatants of cells treated with BfA and infected with FMDV have also shown very little effect on viral yield, suggesting the action of BfA does not have any significant effect on FMDV replication. Brefeldin A prevents the activation and function of Arf1, by inhibiting its GEF, GBF1. The ability of BfA to inhibit PV infection suggests that viral replication relies on Arf-dependant membrane trafficking, however it also suggests FMDV does not require Arf1 function for replication.

The protein kinase inhibitor H89 is thought to prevent the recruitment of Sar1, and therefore COPII complex formation, at ERES which results in a potent block to ER export (Aridor and Balch, 2000). In addition it has been shown that although anterograde transport is blocked by H89, it appears that retrograde transport remains unaffected (Lee and Linstedt, 2000). The effect of H89 treatment on FMDV and BEV infection was investigated (Fig 3.10-3.12). Both FMDV and BEV infection was blocked using 100μm of H89. Importantly, FMDV infection was strongly inhibited when the drug was applied after a period of virus uptake showing that H89 inhibited intracellular virus replication and not cell-entry. As FMDV is unaffected by BfA treatment but is blocked by H89 this may suggest a role for COPII complex formation and the early stages of the

secretory pathway in replication. In comparison BEV infection is blocked by both BfA and H89. This suggests that the loss of ER export may affect the integrity, or protein composition, of other membranes in the secretory pathway (e.g. the Golgi) that BEV may rely on for replication. However, replication of SARS Coronavirus has also been reported to be blocked by H89 and BfA treatment, but is still thought to form RC's from the ER membranes (Knoops et al., 2008; Oostra et al., 2007). Therefore BEV's use of the COPII system/ER for replication cannot be completely ruled out.

The ER possesses quality control machinery to ensure that only correctly folded proteins are exported. Any imbalance in protein homeostasis results in the ER stress response (Patil and Walter, 2001; Schroder and Kaufman, 2005a). It has been reported that ER stress, induced using Thapsigargin (TG), results in a decrease in COPII vesicle formation (Amodio et al., 2009). To determine if ER stress induced by TG affects FMDV infection, cells were treated with TG prior to infection. This treatment did not appear to have any effect on the proportion of FMDV infected cells when compared to the control (Fig 3.15). This would suggest that FMDV infection is not affected by a reduction in COPII formation. However it was reported that that COPII formation was only reduced by 50% in TG treated cells (Amodio et al., 2009) therefore the block may not be potent enough to effect FMDV replication. In addition, the treatment of cells with TG has been shown previously to disrupt both the ERGIC and Golgi labelling, although this was not thought to affect their function (Amodio et al., 2009). In my experiments the Golgi remained largely intact in treated cells (Fig 3.13), suggesting that TG induces a weaker ER stress response in IBRS-2 cells, which along with a functioning ERGIC to Golgi transport system, may also help explain why FMDV remained unaffected by ER stress.

The effects observed on infection using the above inhibitors suggested a role for the early secretory system in FMDV replication. In light of this, the role of the early secretory system in FMDV infection was investigated in more detail using dominant-negative inhibitors of key GTPases that regulate membrane flow through the secretory system. The primary candidate for investigation was Sar1 which is involved in ER to Golgi transport and is required for formation of COPII transport vesicles at ERES. Sar1 activity was blocked by over-expression of dn mutants (Sar1 T39N-CFP or Sar1 H79G-CFP) and the effect on FMDV infection quantified by IFCM. Expression of the wt and dn Sar1 T39N resulted in ~50% decrease to FMDV infection (Fig 4.10). Thus, expression of the wt Sar1 protein appeared to produce a similar effect to that observed in cells expressing the inactive dn Sar1 T39N, suggesting that over-expression of the wt protein may be exerting a dn effect . This conclusion was supported by the observation that a loss to ER labelling was observed in cells expressing the wt protein (Fig 4.2). Sar1 T39N blocks formation of COPII vesicles at ERES thereby preventing export out of the ER. Therefore the decrease in FMDV infection may be due to a reduction in COPII vesicle formation. As dn Sar1 T39N has a high affinity for GDP, and thus cannot be activated by its GEF Sec12 to its GTP-bound form, it will remain in the cytosol and not associate with membranes. It is possible that FMDV may require Sar1 to be recruited directly onto membranes to help form vesicles in a similar manner to that reported for PV 3A which recruits Arf1 onto membranes via GBF1 (Belov and Ehrenfeld, 2007; Belov et al., 2008). Therefore it may be possible that a reduction in “free” Sar1 within the cytosol could result in a reduction to FMDV infection. It should also be noted that expression of dn Sar1 T39N-CFP did not appear to cause a major disruption to Golgi membranes in IBRS-2 cells (Fig 4.5), as previously

described (Altan-Bonnet et al., 2004), which may suggest this particular dn does not completely block protein transport. Perhaps a more potent block would have resulted in a greater decrease to FMDV infection. The above results were confirmed by repeating the experiment in an alternative porcine cell line (MAX) (Fig 4.18); these experiments also showed that expression of the wt or dn T39N resulted in ~50-60% decrease in FMDV infection suggesting a role for Sar1 and COPII in FMDV infection.

Expression of the constituently active dn Sar1 H79G-CFP is thought to allow the recruitment of Sar1 and the COPII components onto ERES and allow transport vesicle formation. However when bound to GTP, Sar1-H79G cannot be hydrolysed by the GAP Sec23 and hence COPII coats are stabilised and COPII components cannot be released back to the cytosol. Thus the fusion of transport vesicles to form the ERGIC is also prevented, resulting in an accumulation of COPII vesicles at ERES (Altan-Bonnet et al., 2004). Experiments carried out in this study show that expression of dn Sar1 H79G-CFP did not appear to effect FMDV infection in IBRS-2 cells (Fig 4.11); however a mild 25% reduction was observed when the protein was expressed in MAX cells (Fig 4.19). The expression of dn Sar1 H79G appeared to produce a potent block on transport through the early secretory system, as the Golgi labelling was dispersed and often absent in IBRS-2 cells (Fig 4.7). In comparison, the Golgi did remain in MAX cells but appeared fragmented (Fig 4.17). In addition, the expression levels of Sar1 proteins appeared higher in IBRS-2 cells. Both of these observed differences may account for the apparent, but small, discrepancy between the two cell lines. Overall, the data suggests that expression of dn Sar1 H79G does not have a dramatic affect on FMDV infection. Therefore these results suggest that blocking formation of COPII

transport vesicles at ERES inhibits FMDV infection, whereas blocking the secretory pathway immediately after the formation of COPII vesicles does not have an inhibitory effect. This would indicate that COPII vesicles are required for virus replication, but events after their formation are not required for productive infection.

Experiments using dn Sar1 were repeated using BEV as an example of a brefeldin A sensitive virus, which is likely to require active Arf1 for replication. It was observed that expression of wt Sar1 and both the dn Sar1 proteins reduced BEV infection by ~25% (Fig 4.13-4.14). This decrease suggests a role for Sar1 in BEV infection, although this does not appear to be essential for replication. Similarly, early studies on PV showed that COPII proteins were present on replication vesicles early on in infection (Rust et al., 2001) however it was later shown that the knockdown of COPII complex proteins by siRNA did not affect PV replication (Cherry et al., 2006). This may be a similar case to BEV infection, as it is also a BfA sensitive. However it is more likely that expression of the Sar1 proteins is affecting membrane flow and the integrity of membranes in the early secretory pathway down-stream from its activity, and this has caused the decrease in infection.

The observed decrease in FMDV infection in cells expressing dn Sar1 proteins, thus blocking COPII formation, prompted further investigation into the role of ERES in infection. The Sec16 protein is reported to localise to, and define ERES where it is thought to act as platform for COPII assembly (Hughes et al., 2009) and stabilise the COPII coat after the hydrolysis of Sar1 (Supek et al., 2002). The dn Sec16 C-terminal mutant is thought to prevent the protein interacting with the COPII protein complex and therefore reduces transport from the ER. Experiments were carried out to investigate the effect of dn Sec16 C-

term expression on FMDV infection. These experiments showed only a mild decrease in infection (Fig 4.23). Hughes et al (Hughes et al., 2009) reported that Sec16 localises to ERES and is thus separate from the other COPII components; it also cycles on and off the membrane at a slower rate than the other COPII components. In addition COPII vesicle formation can be reconstituted in the absence of Sec16 which suggests a role in the formation of ERES, rather than the budding of vesicles (Matsuoka et al., 1998). This would suggest that Sec16 is not essential for COPII formation; it may only reduce ER export rather than block it completely, which would explain why only a small decrease in FMDV infection has occurred.

In an attempt to confirm the requirement of Sar1 and COPII vesicle formation in FMDV infection, the effects of the knockdown of Sar1 was investigated using siRNA targeting both a and b isoforms of the protein. Initially, cells transfected with Sar1 siRNA were infected with FMDV or BEV and the proportion of infected cells determined by IFCM. However, no significant difference to the proportion of infected cells was observed for either virus in cells depleted of Sar1 when compared to the control cells (Fig 4.34). In addition, the supernatants collected from the experiment were titrated to determine the effect of Sar1 knockdown on virus yield. These showed a ~80% decrease in FMDV yield (Fig 4.36). This result also suggests a role for Sar1/COPII in FMDV replication.

The role of Arf1 in FMDV infection was also investigated. Active Arf1 is known to recruit numerous cytosolic proteins to the ERGIC and Golgi membranes. These include COPI vesicles which transport proteins in the early secretory pathway (Altan-Bonnet et al., 2003; De Matteis and Morrow, 2000; Donaldson and Jackson, 2000) and phosphotidylinositol kinases and

phospholipases which create a lipid environment that differs from ER membranes (Brown et al., 2003; De Matteis et al., 2002). It is also thought that Arf1 co-ordinates the transport machinery to help form the ERGIC from ERES, by the fusion of vesicles, which in turn form the Golgi (Altan-Bonnet et al., 2004).

Expression of wt and a constituently active dn form of Arf1 (dn Arf Q71L) did not appear to have an effect on FMDV infection (Fig 5.6-5.7). However over a two fold increase in the number of infected cells was observed in cells expressing the inactive dn Arf1 T31N (Fig 5.6). This was unexpected and suggests that, not only is functional Arf1 and the recruitment of COPI not necessary for FMDV replication (which would be expected as FMDV is insensitive to the Arf1 inhibitor BfA), but that inactivation of Arf1 is in some way advantageous for FMDV replication. As COPII vesicle formation remains unaffected by dn Arf1, it may be possible that the loss of both COPI formation on transport vesicles, and/or the inability of vesicles to fuse to form the ERGIC, are beneficial to FMDV replication. Blocking Arf1 function and recruitment of COPI coats would be likely to result in a collection of “free” vesicles at ERES, causing a similar phenotype to cells expressing the dn Sar1 H79G. It has been reported that the p22 non-structural protein of Norwalk virus mimics an ER export signal which results in its uptake into COPII vesicles, this causes the vesicles to mis-localise and therefore inhibit protein secretion. The alteration to COPII transport then results in disruption of the Golgi (Sharp et al., 2010). Perhaps a similar motif is present in an FMDV non-structural protein that would result in the recruitment of the replication proteins to the COPII vesicle membranes at ERES, however this would require further investigation. Alternatively Sar1 has been implicated in the formation of autophagic vesicles at

ERES in conjunction with Rab1. Both proteins are required for formation and this process is unaffected by BfA treatment (Zoppino et al., 2010). Other picornaviruses such as Poliovirus, Coxsackievirus and Hepatitis C are believed to utilise autophagic vesicles to help form RC's (Guevin et al., 2010; Kemball et al., 2010; Suhy et al., 2000; Taylor and Kirkegaard, 2007; Yoon et al., 2009), so it therefore plausible that FMDV may be doing the same, however a role for Rab1 would also be required. In this study, dn Rab1 protein was shown to enhance FMDV infection (see Chapter 6) which suggests that autophagy is not required for replication. However further investigation is required to determine the exact role for Sar1 in FMDV replication.

Experiments determining the effects of Arf1 on FMDV infection were repeated in MAX cells. In contrast to IBRS-2 cells, a ~50% decrease in FMDV infection was observed in cells expressing wt and the active dn Q71L (Fig 5.15). The observed difference may be due to higher levels of expression of proteins in MAX cells resulting in a greater effect on endogenous Arf1. Arf1 is known to recruit a number of proteins onto membranes, and therefore the constant activation of the protein may not just affect COPI recruitment, but may also affect the recruitment of lipid-modifying enzymes and cytoskeletal proteins. Therefore, even though FMDV is insensitive to BfA, and not thought to require Arf1 activity for activation, it cannot be ruled out that the down-stream effects of the expression of this dn is not affecting membranes in the early secretory pathway, such as their lipid composition. In contrast, an increase in FMDV infection was seen in MAX cells expressing the inactive dn T31N (Fig 5.15), however this was not as great an increase as that observed with IBRS-2 cells (fig 5.6). This discrepancy may be due to varying expression levels between the cell lines. The over-expression of dn T31N was evident in numerous IBRS-

2 cells, which resulted in the localisation of the dn to the plasma membrane (Fig 5.5). However; this expression pattern was rarely seen in MAX cells where it tended to remain diffuse throughout the cell (Fig 5.14). A reduced level of expression may explain the reduced increase observed in MAX cells.

As mentioned previously, BEV is reported to be sensitive to BfA treatment, which inhibits the catalytic activity of GBF1, and in turn prevents the activation of Arf1 and the recruitment of the COPI complex to Golgi membranes (Mossessova et al., 2003; Renault et al., 2003). Expression of wt Arf1, the inactive dn Arf1 T31N and the constituently active dn Arf1 Q71L, all significantly reduced BEV infection. Both Arf1 wt and the active dn Q71L reduced BEV infection by ~50% (Fig 5.10-5.11). The reduction in cells expressing wt Arf1, in combination with the observation that over-expression of this protein results in a slight loss to ER labelling (Fig 5.1), suggests that this protein is producing a dn effect on endogenous Arf1. Expression of the constituently active Arf1 Q71L traps Arf-GTP on the Golgi and ERGIC membranes, making it unavailable for recruitment on to membranes via viral proteins. The continual recruitment of proteins onto membranes, and transport of proteins may also affect the composition and the amount of available membranes to allow efficient replication. In support of this, expression of the inactive dn Arf1 T31N dramatically reduced BEV infection by up to 90% (Fig 5.10). The dn T31N is unable to bind GTP and therefore cannot be recruited to membranes via GBF1, which suggests BEV infection requires the activation of Arf1 for infection. Poliovirus 3A has been found to recruit both GBF1 and Arf1 onto host cell membranes (Belov et al., 2007a; Belov and Ehrenfeld, 2007; Belov et al., 2008), therefore a similar process may be occurring in BEV infection. More recent work on PV has shown that only GBF1 is critical for replication and Arf1 is

expendable (Belov et al., 2010). In light of this, BEV infection may actually differ slightly from PV infection in that both GBF1 and Arf1 activity is required for infection.

The Rab GTPases also regulate key, discrete steps within the early secretory pathway by transporting vesicles to their acceptor membranes, and in some cases, the fusion of the vesicles with the acceptor compartment. The major Rab proteins involved in the secretory pathway are Rab1, Rab2, Rab6, Rab34 and these were investigated using dominant-negative proteins. Also a role for Rab1 in FMDV infection was investigated by over expressing TBC1D20, which is the GAP for Rab1.

The Rab1 protein is reported to be involved in both the initial steps of ER export and in intra-Golgi transport between the cis and medial Golgi stacks, by targeting vesicles to acceptor compartments (Plutner et al., 1991). Essentially, COPII vesicles form at the ERES which leads to the recruitment of Rab1, p115 and SNARE proteins to these sites, and subsequent vesicle fusion events create the ERGIC (Allan et al., 2000; Altan-Bonnet et al., 2004). Rab1 is also known to interact with the Arf1 GEF, GBF1, which results in the recruitment of Arf1 and the COPI complex to transport vesicles, and the ERGIC and Golgi membranes (Monetta et al., 2007). Expression of the dn Rab1 S25N results in the disassembly of the Golgi (Wilson et al., 1994) and a loss of COPI function; however COPII transport continues unaffected (Alvarez et al., 2003). The results in this study show that expression of dn Rab1 S25N enhanced FMDV infection levels by 70% (see Fig 6.4). This increase suggests that inactivation of the Rab1 protein may be beneficial to FMDV infection. A similar enhancement to infection was observed in cells expressing the inactive dn Arf1 T31N (see Fig 5.6). Expression of dn Rab1 S25N results in a loss to COPI

vesicle transport, and as mentioned above, is responsible for the recruitment of Arf1 to ERGIC membranes and ERES. Therefore this data agrees with the observations made in the dn Arf1 experiments, where COPI transport is also arrested. Interestingly, expression of dn Rab1 S25N is not thought to alter COPII vesicle formation (Alvarez et al., 2003; Tisdale et al., 1992), but prevents the COPII/COPI exchange at ERES (Monetta et al., 2007). Together, these observations suggest that FMDV may require membranes from the early secretory pathway that are generated before COPII/COPI exchange. This adds support to the conclusion that transport vesicles formed at ERES are required for FMDV replication. Recently, Rab1 function has been found to be important for the formation of autophagic vesicles at ERES (Zoppino et al., 2010). This gives rise to the possibility that the apparent increase in FMDV infection may be a result of a reduction in autophagic vesicles that may be targeting the virus for degradation. However expression of dn Sar1 proteins are also reported to prevent the formation of autophagic vesicles (Zoppino et al., 2010). The results presented in chapter three report a decrease in FMDV infection, therefore autophagy at ERES is not likely to be the cause for the observed increase in FMDV infection in dn Rab1 expressing cells.

The role of Rab2 in FMDV infection was also investigated as this protein is thought to be responsible for the maturation of the ERGIC vesicles and the recruitment of COPI to the ERGIC (Tisdale and Jackson, 1998). Therefore Rab2 controls ERGIC to Golgi, and ERGIC to ER transport (Tisdale, 1999). Expression of the dn Rab2 S20N interferes with this process by preventing the assembly of the ERGIC and it maturation, thereby blocking protein transport (Tisdale et al., 1992). Experiments investigating the effect of dn Rab2 S20N on FMDV infection showed expression of the protein resulted in ~75% increase in

FMDV infection (Fig 6.8). An increase in FMDV infection (60%) was also observed in cells expressing wt Rab2 suggesting that the over-expression of wt Rab2 may have a dominant-negative effect on endogenous Rab2. Overall, the results suggest the inactivation of Rab2 is also advantageous to FMDV infection. Rab1 and Rab2 are thought to act sequentially within the early secretory pathway, as both are reported to be required to co-ordinate the transport of vesicles between the ER and Golgi, and in the formation of the ERGIC (Altan-Bonnet et al., 2004). These roles may help explain the observed increase in FMDV infection when the function of either Rab is blocked. However they only shared a 40% identity which suggests they are likely to possess separate functions (Tisdale and Balch, 1996). Nonetheless, it appears COPI vesicle transport and the fusion of vesicles to form the ERGIC are not important for FMDV infection. This is supported by the fact that Rab1 also increases infection to a similar level.

Next, transport between the Golgi cisternae and the plasma membrane was investigated, to rule out a role for the Golgi and Golgi transport in FMDV infection. Initially, the effect of Rab6 on infection was investigated. The dn Rab6 T27N blocks transport between the cis/medial and late Golgi compartments and is not thought to affect ER to Golgi or TGN to plasma membrane transport (Martinez et al., 1994). In these experiments, expression of dn Rab6 T27N did not affect FMDV infection (Fig 6.12), suggesting that loss to inter-Golgi transport is not necessary for infection.

Another Golgi associated protein Rab34 was investigated. Rab34 has been reported to be involved in inter-Golgi transport and secretion of proteins to the plasma membrane (Goldenberg et al., 2007). The dn version of this protein blocks TGN to plasma membrane transport but not ER to medial-Golgi transport

(Goldenberg et al., 2007). In the experiments carried out for this study, the expression of dn Rab34 T66N resulted in around a 25% decrease in FMDV infection (Fig 6.16). This is only a slight decrease in infection, which suggests the block to protein transport may not detrimental to FMDV infection. A reduction to protein export from the Golgi to the plasma membrane may reduce the secretion of proteins or receptors required by the virus. In addition Rab34 has been reported to interact with multiple proteins and regulate several processes, including Dynein microtubule motors (Wang and Hong, 2002), apoptosis (Speight and Silverman, 2005), macropinocytosis (Sun et al., 2003) and the translocation of lysosomes (Wang and Hong, 2002). The knockdown of this dn protein may affect any one of these processes, and that may in turn have a slight effect on FMDV infection. For example, a reduction in Rab34 could result in a reduction to endosome and lysosome recycling, which would in turn affect FMDV entry, as endosomes are required for virus up take into the cell. However, if this were the case it does not seem to produce a block potent enough to inhibit FMDV infection, and therefore it can be concluded that the inter-Golgi transport between the TGN and plasma membrane is not essential for FMDV infection.

The role of Rab1 in FMDV infection was also investigated by over-expression of its GTPase activating protein (GAP). This particular GAP has been shown to promote strong GTP hydrolysis for Rab1, suggesting that TBC1D20 regulates the activity of Rab1 (Haas et al., 2007). Over-expression of TBC1D20 is thought to result in the inactivation of Rab1, and result in dispersal of the Golgi by blocking transport at the ER (Haas et al., 2007; Hughes et al., 2009). The catalytically inactive mutant of TBC1D20 (R105A) was not seen to disrupt the Golgi or block transport (Haas et al., 2007; Hughes et al., 2009).

Experiments investigating the effects of these proteins on FMDV infection showed ~40% reduction in infection in cells expressing TBC1D20, and surprisingly, ~60% reduction in infection in cells expressing the catalytically inactive R105A (Fig 6.20). The unexpected decrease in FMDV infection in cells expressing the mutant R105A suggested that over-expression of the protein was resulting in a dn effect on endogenous TBC1D20. This was reinforced by the fact that both ER and ERGIC labelling was altered in cells expressing the inactive protein (Fig 6.17). It may be possible that the inactive mutant is able to bind to active Rab1 on the membrane and prevent its interaction with down-stream effectors. Alternatively, the over-expression of the protein may result in a pool of R105A within the cell that is catalytically inactive and unable to promote GTP hydrolysis, hence Rab1 remains constituently active on the membrane. This scenario would agree with previous data suggesting Rab1 inactivation enhances FMDV infection, and therefore it could be predicted that a constituently active version of the protein would inhibit replication.

Based on the previous data in this study obtained with dn Rab1, the expression of TBC1D20 would be predicted to increase FMDV infection, as it is thought to inactivate Rab1, however a 40% decrease was observed in cells expressing this protein. TBC1D20 has been shown to bind to a reticulon in the ER, and at very high-levels of over-expression, has been reported to disrupt COPII vesicle formation (Haas et al., 2007) by removing Sec23-Sec24 and Sec13-Sec31 from ERES. Additionally, in cells transfected with siRNA targeting TBC1D20, COPII proteins appeared to be dispersed form their normal localisation at ERES (Haas et al., 2007). Therefore it is possible that the observed decrease in FMDV infection may be due to over-expression of the protein blocking COPII vesicle formation, and/or dispersal of COPII proteins,

which strengthens the argument that FMDV may require COPII vesicles for replication. However it cannot be ruled out that TBC1D20 has other binding partners apart from Rab1 such as Rab43 (Haas et al., 2007), and this could result in the inactivation of other proteins required for efficient FMDV replication. It is also worth considering that GAPs along with GEFs are involved in Rab cascades where one GTP-bound Rab recruits the GAP/GEF that inactivates/activates the next Rab along the pathway (Rivera-Molina and Novick, 2009); therefore inactivation of one GAP may have a knock on effect to other Rabs within the early secretory pathway.

The above experiments were repeated in BEV infected cells. These results showed a 40-45% reduction in infection in cells expressing both TBC1D20 and the R105A mutant (Fig 6.22). This data suggests that TBC1D20 or Rab1 activity may have some role in BEV infection. However a loss to the activity of these proteins results in the disruption of the Golgi and ERGIC membranes releasing COPI vesicles into the cytosol, which is a more likely cause for the loss in BEV infection.

To confirm the results of the dn data a QPCR assay was developed to analyse the effects of the knockdown of Rab proteins on FMDV replication using siRNA. An initial screening of Rab1a, b and c, Rab2a and b, Rab5a, b and c, Rab6a, b and c and Rab34 showed a significant increase in vRNA levels (1 log increase) only in cells transfected with Rab1 siRNA (Fig 7.11-7.13). This is in agreement with the results obtained for experiment using dn Rab1, suggesting that inhibiting the function of Rab1 is beneficial for FMDV replication. Based on the results obtained using dn Rab2, an increase in vRNA was also expected in Rab2 depleted cells; however an only a slight increase (0.3 log)

was observed. This may have been due to a relatively poor knockdown of Rab2 as I was unable to confirm the knockdown of Rab2 by western blotting.

The observed increase in vRNA levels in cells transfected with Rab1 siRNA was investigated further by titration of the virus in cell supernatants. Transfection with Rab1 siRNA resulted in ~3 fold increase in FMDV yield, which confirmed the findings of the QPCR data (Fig 7.15). This result also suggested FMDV replication does not require Rab1 activity, and hence, COPI transport, the formation of the ERGIC or the COPII/COPI exchange at ERES. Overall it appears a stage prior to Rab1 activity is required for FMDV replication such as the formation and concentration of COPII vesicles at ERES.

In summary, the knockdown of Sar1 activity using dn Sar1 T39N or siRNA resulted in a reduction to FMDV infection. These observations suggest that FMDV requires Sar1 activity and/or COPII vesicle formation for replication, and hence that transport vesicles formed at ERES may be the source of virus-induced replication vesicles. The expression of the constituently active dn Sar1 H79G had very little effect on FMDV infection, which suggests that the formation of COPII vesicles is sufficient for replication and that downstream membranes of the secretory pathway are not needed for replication. In addition, expression of dn Rab1, dn Rab2 and dn Arf1 all resulted in an apparent increase in FMDV infection. This not only indicates that these proteins are not required for infection but also that their inactivation is in some way advantageous for replication. The loss of Arf1 activity results in loss of COPI vesicle transport; expression of dn Rab2 prevents ERGIC maturation and COPI-mediated transport from the ERGIC; and inactivation of Rab1 also blocks the formation of the ERGIC and COPI vesicles as well as the COPI/COPII exchange at ERES. Therefore it can be assumed FMDV does not require COPI

vesicles for replication, however it is thought COPII vesicle formation proceeds as normal during the expression of all three proteins. Finally, the expression of dn Rab6 and Rab34, which block inter-Golgi transport, did not have a significant effect on FMDV infection, suggesting that neither inter-Golgi transport nor the Golgi membranes are necessary for FMDV Infection.

Therefore a model could be proposed that during FMDV infection, COPII vesicles form at ERES via the activation of Sar1. The COPII coat is then released from the vesicle. If the acquisition of COPI (i.e. COPII/COPI exchange) is prevented, viral replication is enhanced. Together these observations suggest that FMDV may utilise “free” membranes created at ERES, prior to the COPII/COPI exchange, as platforms to form the viral replication complexes.

Chapter 9: Future Work

The results presented in this Thesis indicate that FMDV may use membranes derived from the early secretory pathway for replication, and that Sar1 may play a role in this process. However the exact mechanism for the formation of FMDV-induced vesicles and the membranes for replication remain to be determined.

9.1 Investigate the role of P14P kinases in FMDV replication

Hsu et al (Hsu et al., 2010) identified PI4K as having a role in Poliovirus replication. The PI4P lipids have also been reported to regulate ERES biogenesis and autophagy (Blumental-Perry et al., 2006; Yamashita et al., 2006) and alter membrane curvature (Ishiyama et al., 2002; McMahon and Gallop, 2005) of vesicles. Therefore the role of these lipids in FMDV could be investigated using siRNA etc, to determine if they aid viral replication.

9.2 Investigating the interaction of FMDV NSP with COPII vesicles and ERES

Sar1 and Sec16 are involved in the early process of formation and the recruitment of COPII components at ERES, whereas the Sec 23/24 and Sec13/31 are thought be involved at a later stages of secretory vesicle formation. Co-labelling of various COPII components with viral NSP during FMDV infection may help confirm FMDV interaction with COPII vesicles and which cellular proteins the virus may exploit for formation of the viral RC. The potential interaction of FMDV with ERES could be studied through the use of a model system which uses COPII-coated vesicles formed de novo (Matsuoka et al., 1998).

9.3 Study the effects of the knockdown of Arf1 and other regulatory proteins by siRNA

This Thesis showed evidence that inhibition of Arf1 increases FMDV infection therefore it would be of interest to investigate the role of Arf1 further, using siRNA. In addition, Rab1 siRNA was also shown to enhance FMDV replication when transfected into HeLa cells. These experiments could be repeated in a host cell line such as pig cells to determine if similar effect on FMDV replication is observed.

Bibliography

Abrams, C.C., King, A.M., and Belsham, G.J. (1995). Assembly of foot-and-mouth disease virus empty capsids synthesized by a vaccinia virus expression system. J Gen Virol *76 (Pt 12)*, 3089-3098.

Acharya, R., Fry, E., Stuart, D., Fox, G., Rowlands, D., and Brown, F. (1989). The three-dimensional structure of foot-and-mouth disease virus at 2.9 A resolution. Nature *337*, 709-716.

Al-Awar, O., Radhakrishna, H., Powell, N.N., and Donaldson, J.G. (2000). Separation of membrane trafficking and actin remodeling functions of ARF6 with an effector domain mutant. Mol Cell Biol *20*, 5998-6007.

Alexandersen, S., and Donaldson, A.I. (2002). Further studies to quantify the dose of natural aerosols of foot-and-mouth disease virus for pigs. Epidemiol Infect *128*, 313-323.

Alexandrov, K., Horiuchi, H., Steele-Mortimer, O., Seabra, M.C., and Zerial, M. (1994). Rab escort protein-1 is a multifunctional protein that accompanies newly prenylated rab proteins to their target membranes. EMBO J *13*, 5262-5273.

Allan, B.B., Moyer, B.D., and Balch, W.E. (2000). Rab1 recruitment of p115 into a cis-SNARE complex: programming budding COPII vesicles for fusion. Science *289*, 444-448.

Altan-Bonnet, N., Phair, R.D., Polishchuk, R.S., Weigert, R., and Lippincott-Schwartz, J. (2003). A role for Arf1 in mitotic Golgi disassembly, chromosome segregation, and cytokinesis. Proc Natl Acad Sci U S A *100*, 13314-13319.

Altan-Bonnet, N., Sougrat, R., and Lippincott-Schwartz, J. (2004). Molecular basis for Golgi maintenance and biogenesis. Curr Opin Cell Biol *16*, 364-372.

Alvarez, C., Fujita, H., Hubbard, A., and Sztul, E. (1999). ER to Golgi transport: Requirement for p115 at a pre-Golgi VTC stage. J Cell Biol *147*, 1205-1222.

Alvarez, C., Garcia-Mata, R., Brandon, E., and Sztul, E. (2003). COPI recruitment is modulated by a Rab1b-dependent mechanism. Mol Biol Cell *14*, 2116-2127.

Alvarez, C., Garcia-Mata, R., Hauri, H.P., and Sztul, E. (2001). The p115-interactive proteins GM130 and giantin participate in endoplasmic reticulum-Golgi traffic. J Biol Chem *276*, 2693-2700.

Amodio, G., Renna, M., Paladino, S., Venturi, C., Tacchetti, C., Moltedo, O., Franceschelli, S., Mallardo, M., Bonatti, S., and Remondelli, P. (2009). Endoplasmic reticulum stress reduces the export from the ER and alters the architecture of post-ER compartments. Int J Biochem Cell Biol *41*, 2511-2521.

Anant, J.S., Desnoyers, L., Machius, M., Demeler, B., Hansen, J.C., Westover, K.D., Deisenhofer, J., and Seabra, M.C. (1998). Mechanism of Rab geranylgeranylation: formation of the catalytic ternary complex. Biochemistry *37*, 12559-12568.

Antonny, B., Madden, D., Hamamoto, S., Orci, L., and Schekman, R. (2001). Dynamics of the COPII coat with GTP and stable analogues. Nat Cell Biol *3*, 531-537.

Antony, C., Cibert, C., Geraud, G., Santa Maria, A., Maro, B., Mayau, V., and Goud, B. (1992). The small GTP-binding protein rab6p is distributed from

medial Golgi to the trans-Golgi network as determined by a confocal microscopic approach. J Cell Sci *103 (Pt 3)*, 785-796.
Aoe, T., Cukierman, E., Lee, A., Cassel, D., Peters, P.J., and Hsu, V.W. (1997). The KDEL receptor, ERD2, regulates intracellular traffic by recruiting a GTPase-activating protein for ARF1. EMBO J *16*, 7305-7316.
Aridor, M., and Balch, W.E. (2000). Kinase signaling initiates coat complex II (COPII) recruitment and export from the mammalian endoplasmic reticulum. J Biol Chem *275*, 35673-35676.
Aridor, M., Bannykh, S.I., Rowe, T., and Balch, W.E. (1995). Sequential coupling between COPII and COPI vesicle coats in endoplasmic reticulum to Golgi transport. J Cell Biol *131*, 875-893.
Aridor, M., Fish, K.N., Bannykh, S., Weissman, J., Roberts, T.H., Lippincott-Schwartz, J., and Balch, W.E. (2001). The Sar1 GTPase coordinates biosynthetic cargo selection with endoplasmic reticulum export site assembly. J Cell Biol *152*, 213-229.
Aridor, M., Guzik, A.K., Bielli, A., and Fish, K.N. (2004). Endoplasmic reticulum export site formation and function in dendrites. J Neurosci *24*, 3770-3776.
Aridor, M., Weissman, J., Bannykh, S., Nuoffer, C., and Balch, W.E. (1998). Cargo selection by the COPII budding machinery during export from the ER. J Cell Biol *141*, 61-70.
Arita, M., Koike, S., Aoki, J., Horie, H., and Nomoto, A. (1998). Interaction of poliovirus with its purified receptor and conformational alteration in the virion. J Virol *72*, 3578-3586.
Bailey, D., Kaiser, W.J., Hollinshead, M., Moffat, K., Chaudhry, Y., Wileman, T., Sosnovtsev, S.V., and Goodfellow, I.G. (2010). Feline calicivirus p32, p39 and p30 proteins localize to the endoplasmic reticulum to initiate replication complex formation. J Gen Virol *91*, 739-749.
Baltera, R.F., Jr., and Tershak, D.R. (1989). Guanidine-resistant mutants of poliovirus have distinct mutations in peptide 2C. J Virol *63*, 4441-4444.
Bannykh, S.I., Rowe, T., and Balch, W.E. (1996). The organization of endoplasmic reticulum export complexes. J Cell Biol *135*, 19-35.
Barco, A., and Carrasco, L. (1995). A human virus protein, poliovirus protein 2BC, induces membrane proliferation and blocks the exocytic pathway in the yeast Saccharomyces cerevisiae. EMBO J *14*, 3349-3364.
Barlowe, C. (2000). Traffic COPs of the early secretory pathway. Traffic *1*, 371-377.
Barlowe, C. (2003). Signals for COPII-dependent export from the ER: what's the ticket out? Trends Cell Biol *13*, 295-300.
Barlowe, C., Orci, L., Yeung, T., Hosobuchi, M., Hamamoto, S., Salama, N., Rexach, M.F., Ravazzola, M., Amherdt, M., and Schekman, R. (1994). COPII: a membrane coat formed by Sec proteins that drive vesicle budding from the endoplasmic reticulum. Cell *77*, 895-907.
Barlowe, C., and Schekman, R. (1993). SEC12 encodes a guanine-nucleotide-exchange factor essential for transport vesicle budding from the ER. Nature *365*, 347-349.
Barr, F.A. (2009). Rab GTPase function in Golgi trafficking. Semin Cell Dev Biol *20*, 780-783.
Barton, D.J., O'Donnell, B.J., and Flanegan, J.B. (2001). 5' cloverleaf in poliovirus RNA is a cis-acting replication element required for negative-strand synthesis. EMBO J *20*, 1439-1448.
Baxt, B., and Bachrach, H.L. (1980). Early interactions of foot-and-mouth disease virus with cultured cells. Virology *104*, 42-55.

Baxt, B., and Bachrach, H.L. (1982). The adsorption and degradation of foot-and-mouth disease virus by isolated BHK-21 cell plasma membranes. Virology *116*, 391-405.

Belnap, D.M., McDermott, B.M., Jr., Filman, D.J., Cheng, N., Trus, B.L., Zuccola, H.J., Racaniello, V.R., Hogle, J.M., and Steven, A.C. (2000). Three-dimensional structure of poliovirus receptor bound to poliovirus. Proc Natl Acad Sci U S A *97*, 73-78.

Belov, G.A., Altan-Bonnet, N., Kovtunovych, G., Jackson, C.L., Lippincott-Schwartz, J., and Ehrenfeld, E. (2007a). Hijacking components of the cellular secretory pathway for replication of poliovirus RNA. J Virol *81*, 558-567.

Belov, G.A., and Ehrenfeld, E. (2007). Involvement of cellular membrane traffic proteins in poliovirus replication. Cell Cycle *6*, 36-38.

Belov, G.A., Feng, Q., Nikovics, K., Jackson, C.L., and Ehrenfeld, E. (2008). A critical role of a cellular membrane traffic protein in poliovirus RNA replication. PLoS Pathog *4*, e1000216.

Belov, G.A., Fogg, M.H., and Ehrenfeld, E. (2005). Poliovirus proteins induce membrane association of GTPase ADP-ribosylation factor. J Virol *79*, 7207-7216.

Belov, G.A., Habbersett, C., Franco, D., and Ehrenfeld, E. (2007b). Activation of cellular Arf GTPases by poliovirus protein 3CD correlates with virus replication. J Virol *81*, 9259-9267.

Belov, G.A., Kovtunovych, G., Jackson, C.L., and Ehrenfeld, E. (2010). Poliovirus replication requires the N-terminus but not the catalytic Sec7 domain of ArfGEF GBF1. Cell Microbiol *12*, 1463-1479.

Belsham, G.J. (1993). Distinctive features of foot-and-mouth disease virus, a member of the picornavirus family; aspects of virus protein synthesis, protein processing and structure. Prog Biophys Mol Biol *60*, 241-260.

Belsham, G.J. (2005). Translation and replication of FMDV RNA. Curr Top Microbiol Immunol *288*, 43-70.

Belsham, G.J., and Bostock, C.J. (1988). Studies on the infectivity of foot-and-mouth disease virus RNA using microinjection. J Gen Virol *69 (Pt 2)*, 265-274.

Belsham, G.J., and Brangwyn, J.K. (1990). A region of the 5' noncoding region of foot-and-mouth disease virus RNA directs efficient internal initiation of protein synthesis within cells: involvement with the role of L protease in translational control. J Virol *64*, 5389-5395.

Belsham, G.J., Brangwyn, J.K., Ryan, M.D., Abrams, C.C., and King, A.M. (1990). Intracellular expression and processing of foot-and-mouth disease virus capsid precursors using vaccinia virus vectors: influence of the L protease. Virology *176*, 524-530.

Belsham, G.J., McInerney, G.M., and Ross-Smith, N. (2000). Foot-and-mouth disease virus 3C protease induces cleavage of translation initiation factors eIF4A and eIF4G within infected cells. J Virol *74*, 272-280.

Berinstein, A., Roivainen, M., Hovi, T., Mason, P.W., and Baxt, B. (1995). Antibodies to the vitronectin receptor (integrin alpha V beta 3) inhibit binding and infection of foot-and-mouth disease virus to cultured cells. J Virol *69*, 2664-2666.

Bernards, A. (2003). GAPs galore! A survey of putative Ras superfamily GTPase activating proteins in man and Drosophila. Biochim Biophys Acta *1603*, 47-82.

Berryman, S., Clark, S., Monaghan, P., and Jackson, T. (2005). Early events in integrin alphavbeta6-mediated cell entry of foot-and-mouth disease virus. J Virol *79*, 8519-8534.

Bevis, B.J., Hammond, A.T., Reinke, C.A., and Glick, B.S. (2002). De novo formation of transitional ER sites and Golgi structures in Pichia pastoris. Nat Cell Biol *4*, 750-756.

Bhattacharyya, D., and Glick, B.S. (2007). Two mammalian Sec16 homologues have nonredundant functions in endoplasmic reticulum (ER) export and transitional ER organization. Mol Biol Cell *18*, 839-849.

Bi, X., Corpina, R.A., and Goldberg, J. (2002). Structure of the Sec23/24-Sar1 pre-budding complex of the COPII vesicle coat. Nature *419*, 271-277.

Bienz, K., Egger, D., and Pasamontes, L. (1987). Association of polioviral proteins of the P2 genomic region with the viral replication complex and virus-induced membrane synthesis as visualized by electron microscopic immunocytochemistry and autoradiography. Virology *160*, 220-226.

Bienz, K., Egger, D., Rasser, Y., and Bossart, W. (1980). Kinetics and location of poliovirus macromolecular synthesis in correlation to virus-induced cytopathology. Virology *100*, 390-399.

Bienz, K., Egger, D., Rasser, Y., and Bossart, W. (1983). Intracellular distribution of poliovirus proteins and the induction of virus-specific cytoplasmic structures. Virology *131*, 39-48.

Bienz, K., Egger, D., Troxler, M., and Pasamontes, L. (1990). Structural organization of poliovirus RNA replication is mediated by viral proteins of the P2 genomic region. J Virol *64*, 1156-1163.

Bigay, J., Gounon, P., Robineau, S., and Antonny, B. (2003). Lipid packing sensed by ArfGAP1 couples COPI coat disassembly to membrane bilayer curvature. Nature *426*, 563-566.

Blumental-Perry, A., Haney, C.J., Weixel, K.M., Watkins, S.C., Weisz, O.A., and Aridor, M. (2006). Phosphatidylinositol 4-phosphate formation at ER exit sites regulates ER export. Dev Cell *11*, 671-682.

Bock, J.B., Matern, H.T., Peden, A.A., and Scheller, R.H. (2001). A genomic perspective on membrane compartment organization. Nature *409*, 839-841.

Boehm, J., Letourneur, F., Ballensiefen, W., Ossipov, D., Demolliere, C., and Schmitt, H.D. (1997). Sec12p requires Rer1p for sorting to coatomer (COPI)-coated vesicles and retrieval to the ER. J Cell Sci *110 (Pt 8)*, 991-1003.

Bolten, W.W. (1998). Scientific rationale for specific inhibition of COX-2. J Rheumatol Suppl *51*, 2-7.

Brodsky, F.M., Chen, C.Y., Knuehl, C., Towler, M.C., and Wakeham, D.E. (2001). Biological basket weaving: formation and function of clathrin-coated vesicles. Annu Rev Cell Dev Biol *17*, 517-568.

Brown, F., and Cartwright, B. (1961). Dissociation of foot-and-mouth disease virus into its nucleic acid and protein components. Nature *192*, 1163-1164.

Brown, W.J., Chambers, K., and Doody, A. (2003). Phospholipase A2 (PLA2) enzymes in membrane trafficking: mediators of membrane shape and function. Traffic *4*, 214-221.

Burman, A., Clark, S., Abrescia, N.G., Fry, E.E., Stuart, D.I., and Jackson, T. (2006). Specificity of the VP1 GH loop of Foot-and-Mouth Disease virus for alphav integrins. J Virol *80*, 9798-9810.

Butterworth, B.E., Shimshick, E.J., and Yin, F.H. (1976). Association of the polioviral RNA polymerase complex with phospholipid membranes. J Virol *19*, 457-466.

Caliguiri, L.A., and Tamm, I. (1970). Characterization of poliovirus-specific structures associated with cytoplasmic membranes. Virology *42*, 112-122.

Campanella, M., de Jong, A.S., Lanke, K.W., Melchers, W.J., Willems, P.H., Pinton, P., Rizzuto, R., and van Kuppeveld, F.J. (2004). The coxsackievirus 2B protein suppresses apoptotic host cell responses by manipulating intracellular Ca2+ homeostasis. J Biol Chem *279*, 18440-18450.

Chantalat, S., Courbeyrette, R., Senic-Matuglia, F., Jackson, C.L., Goud, B., and Peyroche, A. (2003). A novel Golgi membrane protein is a partner of the ARF exchange factors Gea1p and Gea2p. Mol Biol Cell *14*, 2357-2371.

Chantalat, S., Park, S.K., Hua, Z., Liu, K., Gobin, R., Peyroche, A., Rambourg, A., Graham, T.R., and Jackson, C.L. (2004). The Arf activator Gea2p and the P-type ATPase Drs2p interact at the Golgi in Saccharomyces cerevisiae. J Cell Sci *117*, 711-722.

Charcosset, M., Sassolas, A., Peretti, N., Roy, C.C., Deslandres, C., Sinnett, D., Levy, E., and Lachaux, A. (2008). Anderson or chylomicron retention disease: molecular impact of five mutations in the SAR1B gene on the structure and the functionality of Sar1b protein. Mol Genet Metab *93*, 74-84.

Chavrier, P., and Goud, B. (1999). The role of ARF and Rab GTPases in membrane transport. Curr Opin Cell Biol *11*, 466-475.

Chen, W., Feng, Y., Chen, D., and Wandinger-Ness, A. (1998). Rab11 is required for trans-golgi network-to-plasma membrane transport and a preferential target for GDP dissociation inhibitor. Mol Biol Cell *9*, 3241-3257.

Cherry, S., Kunte, A., Wang, H., Coyne, C., Rawson, R.B., and Perrimon, N. (2006). COPI activity coupled with fatty acid biosynthesis is required for viral replication. PLoS Pathog *2*, e102.

Chinsangaram, J., Piccone, M.E., and Grubman, M.J. (1999). Ability of foot-and-mouth disease virus to form plaques in cell culture is associated with suppression of alpha/beta interferon. J Virol *73*, 9891-9898.

Cho, M.W., Teterina, N., Egger, D., Bienz, K., and Ehrenfeld, E. (1994). Membrane rearrangement and vesicle induction by recombinant poliovirus 2C and 2BC in human cells. Virology *202*, 129-145.

Choe, S.S., Dodd, D.A., and Kirkegaard, K. (2005). Inhibition of cellular protein secretion by picornaviral 3A proteins. Virology *337*, 18-29.

Claude, A., Zhao, B.P., Kuziemsky, C.E., Dahan, S., Berger, S.J., Yan, J.P., Armold, A.D., Sullivan, E.M., and Melancon, P. (1999). GBF1: A novel Golgi-associated BFA-resistant guanine nucleotide exchange factor that displays specificity for ADP-ribosylation factor 5. J Cell Biol *146*, 71-84.

Cornell, C.T., Kiosses, W.B., Harkins, S., and Whitton, J.L. (2006). Inhibition of protein trafficking by coxsackievirus b3: multiple viral proteins target a single organelle. J Virol *80*, 6637-6647.

Cosson, P., and Letourneur, F. (1994). Coatomer interaction with di-lysine endoplasmic reticulum retention motifs. Science *263*, 1629-1631.

Cox, S.J.a.B., P.V. (2000). Longevity of antibody response in pigs and sheep following single administartion of high potency emergency FMD vaccines. Paper presented at: European commission for the control of foot and

mouth disease session of the research group of the standing techincal committee (Bulgaria).
Crotty, S., Saleh, M.C., Gitlin, L., Beske, O., and Andino, R. (2004). The poliovirus replication machinery can escape inhibition by an antiviral drug that targets a host cell protein. J Virol *78*, 3378-3386.
Cukierman, E., Huber, I., Rotman, M., and Cassel, D. (1995). The ARF1 GTPase-activating protein: zinc finger motif and Golgi complex localization. Science *270*, 1999-2002.
Curry, S., Abrams, C.C., Fry, E., Crowther, J.C., Belsham, G.J., Stuart, D.I., and King, A.M. (1995). Viral RNA modulates the acid sensitivity of foot-and-mouth disease virus capsids. J Virol *69*, 430-438.
Curry, S., Chow, M., and Hogle, J.M. (1996). The poliovirus 135S particle is infectious. J Virol *70*, 7125-7131.
Curry, S., Fry, E., Blakemore, W., Abu-Ghazaleh, R., Jackson, T., King, A., Lea, S., Newman, J., and Stuart, D. (1997). Dissecting the roles of VP0 cleavage and RNA packaging in picornavirus capsid stabilization: the structure of empty capsids of foot-and-mouth disease virus. J Virol *71*, 9743-9752.
Dales, S. (1965). Replication of Animal Viruses as Studied by Electron Microscopy. Am J Med *38*, 699-715.
Dancourt, J., and Barlowe, C. (2010). Protein sorting receptors in the early secretory pathway. Annu Rev Biochem *79*, 777-802.
Danthi, P., Tosteson, M., Li, Q.H., and Chow, M. (2003). Genome delivery and ion channel properties are altered in VP4 mutants of poliovirus. J Virol *77*, 5266-5274.
Dascher, C., and Balch, W.E. (1994). Dominant inhibitory mutants of ARF1 block endoplasmic reticulum to Golgi transport and trigger disassembly of the Golgi apparatus. J Biol Chem *269*, 1437-1448.
De Matteis, M., Godi, A., and Corda, D. (2002). Phosphoinositides and the golgi complex. Curr Opin Cell Biol *14*, 434-447.
De Matteis, M.A., and Morrow, J.S. (2000). Spectrin tethers and mesh in the biosynthetic pathway. J Cell Sci *113 (Pt 13)*, 2331-2343.
de Renzis, S., Sonnichsen, B., and Zerial, M. (2002). Divalent Rab effectors regulate the sub-compartmental organization and sorting of early endosomes. Nat Cell Biol *4*, 124-133.
Deitz, S.B., Dodd, D.A., Cooper, S., Parham, P., and Kirkegaard, K. (2000). MHC I-dependent antigen presentation is inhibited by poliovirus protein 3A. Proc Natl Acad Sci U S A *97*, 13790-13795.
Dicara, D., Burman, A., Clark, S., Berryman, S., Howard, M.J., Hart, I.R., Marshall, J.F., and Jackson, T. (2008). Foot-and-mouth disease virus forms a highly stable, EDTA-resistant complex with its principal receptor, integrin alphavbeta6: implications for infectiousness. J Virol *82*, 1537-1546.
Dirac-Svejstrup, A.B., Sumizawa, T., and Pfeffer, S.R. (1997). Identification of a GDI displacement factor that releases endosomal Rab GTPases from Rab-GDI. EMBO J *16*, 465-472.
Dodd, D.A., Giddings, T.H., Jr., and Kirkegaard, K. (2001). Poliovirus 3A protein limits interleukin-6 (IL-6), IL-8, and beta interferon secretion during viral infection. J Virol *75*, 8158-8165.
Doedens, J.R., and Kirkegaard, K. (1995). Inhibition of cellular protein secretion by poliovirus proteins 2B and 3A. EMBO J *14*, 894-907.

Domingo, E., Escarmis, C., Baranowski, E., Ruiz-Jarabo, C.M., Carrillo, E., Nunez, J.I., and Sobrino, F. (2003). Evolution of foot-and-mouth disease virus. Virus Res *91*, 47-63.

Doms, R.W., Russ, G., and Yewdell, J.W. (1989). Brefeldin A redistributes resident and itinerant Golgi proteins to the endoplasmic reticulum. J Cell Biol *109*, 61-72.

Donaldson, A.I., Gibson, C.F., Oliver, R., Hamblin, C., and Kitching, R.P. (1987). Infection of cattle by airborne foot-and-mouth disease virus: minimal doses with O1 and SAT 2 strains. Res Vet Sci *43*, 339-346.

Donaldson, J.G., Finazzi, D., and Klausner, R.D. (1992). Brefeldin A inhibits Golgi membrane-catalysed exchange of guanine nucleotide onto ARF protein. Nature *360*, 350-352.

Donaldson, J.G., Honda, A., and Weigert, R. (2005). Multiple activities for Arf1 at the Golgi complex. Biochim Biophys Acta *1744*, 364-373.

Donaldson, J.G., and Jackson, C.L. (2000). Regulators and effectors of the ARF GTPases. Curr Opin Cell Biol *12*, 475-482.

Donnelly, M.L., Hughes, L.E., Luke, G., Mendoza, H., ten Dam, E., Gani, D., and Ryan, M.D. (2001). The 'cleavage' activities of foot-and-mouth disease virus 2A site-directed mutants and naturally occurring '2A-like' sequences. J Gen Virol *82*, 1027-1041.

Dorsch-Hasler, K., Yogo, Y., and Wimmer, E. (1975). Replication of picornaviruses. I. Evidence from in vitro RNA synthesis that poly(A) of the poliovirus genome is genetically coded. J Virol *16*, 1512-1517.

E.K.Wagner, M.J.H. (2004). Basic Virology, 3rd edn (Blackwell Science).

Echard, A., Jollivet, F., Martinez, O., Lacapere, J.J., Rousselet, A., Janoueix-Lerosey, I., and Goud, B. (1998). Interaction of a Golgi-associated kinesin-like protein with Rab6. Science *279*, 580-585.

Echeverri, A., Banerjee, R., and Dasgupta, A. (1998). Amino-terminal region of poliovirus 2C protein is sufficient for membrane binding. Virus Res *54*, 217-223.

Echeverri, A.C., and Dasgupta, A. (1995). Amino terminal regions of poliovirus 2C protein mediate membrane binding. Virology *208*, 540-553.

Ellard, F.M., Drew, J., Blakemore, W.E., Stuart, D.I., and King, A.M. (1999). Evidence for the role of His-142 of protein 1C in the acid-induced disassembly of foot-and-mouth disease virus capsids. J Gen Virol *80 (Pt 8)*, 1911-1918.

Escarmis, C., Toja, M., Medina, M., and Domingo, E. (1992). Modifications of the 5' untranslated region of foot-and-mouth disease virus after prolonged persistence in cell culture. Virus Res *26*, 113-125.

Espenshade, P., Gimeno, R.E., Holzmacher, E., Teung, P., and Kaiser, C.A. (1995). Yeast SEC16 gene encodes a multidomain vesicle coat protein that interacts with Sec23p. J Cell Biol *131*, 311-324.

Falk, M.M., Grigera, P.R., Bergmann, I.E., Zibert, A., Multhaup, G., and Beck, E. (1990). Foot-and-mouth disease virus protease 3C induces specific proteolytic cleavage of host cell histone H3. J Virol *64*, 748-756.

Farsad, K., and De Camilli, P. (2003). Mechanisms of membrane deformation. Curr Opin Cell Biol *15*, 372-381.

Forss, S., Strebel, K., Beck, E., and Schaller, H. (1984). Nucleotide sequence and genome organization of foot-and-mouth disease virus. Nucleic Acids Res *12*, 6587-6601.

Futai, E., Hamamoto, S., Orci, L., and Schekman, R. (2004). GTP/GDP exchange by Sec12p enables COPII vesicle bud formation on synthetic liposomes. EMBO J *23*, 4146-4155.

Gamarnik, A.V., and Andino, R. (1997). Two functional complexes formed by KH domain containing proteins with the 5' noncoding region of poliovirus RNA. RNA *3*, 882-892.

Gamarnik, A.V., and Andino, R. (1998). Switch from translation to RNA replication in a positive-stranded RNA virus. Genes Dev *12*, 2293-2304.

Garcia-Mata, R., and Sztul, E. (2003). The membrane-tethering protein p115 interacts with GBF1, an ARF guanine-nucleotide-exchange factor. EMBO Rep *4*, 320-325.

Garland, A.J.M.a.D., A.I. (1990). Foot and mouth disease. Surveillance *17*, 6-8.

Gazina, E.V., Mackenzie, J.M., Gorrell, R.J., and Anderson, D.A. (2002). Differential requirements for COPI coats in formation of replication complexes among three genera of Picornaviridae. J Virol *76*, 11113-11122.

Gerber, K., Wimmer, E., and Paul, A.V. (2001). Biochemical and genetic studies of the initiation of human rhinovirus 2 RNA replication: identification of a cis-replicating element in the coding sequence of 2A(pro). J Virol *75*, 10979-10990.

Gimeno, R.E., Espenshade, P., and Kaiser, C.A. (1996). COPII coat subunit interactions: Sec24p and Sec23p bind to adjacent regions of Sec16p. Mol Biol Cell *7*, 1815-1823.

Gingras, A.C., Raught, B., and Sonenberg, N. (1999). eIF4 initiation factors: effectors of mRNA recruitment to ribosomes and regulators of translation. Annu Rev Biochem *68*, 913-963.

Girod, A., Storrie, B., Simpson, J.C., Johannes, L., Goud, B., Roberts, L.M., Lord, J.M., Nilsson, T., and Pepperkok, R. (1999). Evidence for a COP-I-independent transport route from the Golgi complex to the endoplasmic reticulum. Nat Cell Biol *1*, 423-430.

Godi, A., Di Campli, A., Konstantakopoulos, A., Di Tullio, G., Alessi, D.R., Kular, G.S., Daniele, T., Marra, P., Lucocq, J.M., and De Matteis, M.A. (2004). FAPPs control Golgi-to-cell-surface membrane traffic by binding to ARF and PtdIns(4)P. Nat Cell Biol *6*, 393-404.

Goldberg, J. (1999). Structural and functional analysis of the ARF1-ARFGAP complex reveals a role for coatomer in GTP hydrolysis. Cell *96*, 893-902.

Goldenberg, N.M., Grinstein, S., and Silverman, M. (2007). Golgi-bound Rab34 is a novel member of the secretory pathway. Mol Biol Cell *18*, 4762-4771.

Gommel, D.U., Memon, A.R., Heiss, A., Lottspeich, F., Pfannstiel, J., Lechner, J., Reinhard, C., Helms, J.B., Nickel, W., and Wieland, F.T. (2001). Recruitment to Golgi membranes of ADP-ribosylation factor 1 is mediated by the cytoplasmic domain of p23. EMBO J *20*, 6751-6760.

Gonzalez, L., Jr., and Scheller, R.H. (1999). Regulation of membrane trafficking: structural insights from a Rab/effector complex. Cell *96*, 755-758.

Goodfellow, I., Chaudhry, Y., Richardson, A., Meredith, J., Almond, J.W., Barclay, W., and Evans, D.J. (2000). Identification of a cis-acting replication element within the poliovirus coding region. J Virol *74*, 4590-4600.

Goodfellow, I.G., Kerrigan, D., and Evans, D.J. (2003a). Structure and function analysis of the poliovirus cis-acting replication element (CRE). RNA *9*, 124-137.

Goodfellow, I.G., Polacek, C., Andino, R., and Evans, D.J. (2003b). The poliovirus 2C cis-acting replication element-mediated uridylylation of VPg is not required for synthesis of negative-sense genomes. J Gen Virol *84*, 2359-2363.

Gosert, R., Egger, D., and Bienz, K. (2000). A cytopathic and a cell culture adapted hepatitis A virus strain differ in cell killing but not in intracellular membrane rearrangements. Virology *266*, 157-169.

Gosert, R., Egger, D., Lohmann, V., Bartenschlager, R., Blum, H.E., Bienz, K., and Moradpour, D. (2003). Identification of the hepatitis C virus RNA replication complex in Huh-7 cells harboring subgenomic replicons. J Virol *77*, 5487-5492.

Gosert, R., Kanjanahaluethai, A., Egger, D., Bienz, K., and Baker, S.C. (2002). RNA replication of mouse hepatitis virus takes place at double-membrane vesicles. J Virol *76*, 3697-3708.

Goud, B., Zahraoui, A., Tavitian, A., and Saraste, J. (1990). Small GTP-binding protein associated with Golgi cisternae. Nature *345*, 553-556.

Grosshans, B.L., Ortiz, D., and Novick, P. (2006). Rabs and their effectors: achieving specificity in membrane traffic. Proc Natl Acad Sci U S A *103*, 11821-11827.

Grubman, M.J., and Bachrach, H.L. (1979). Isolation of foot-and-mouth disease virus messenger RNA from membrane-bound polyribosomes and characterization of its 5' and 3' termini. Virology *98*, 466-470.

Grubman, M.J., Morgan, D.O., Kendall, J., and Baxt, B. (1985). Capsid intermediates assembled in a foot-and-mouth disease virus genome RNA-programmed cell-free translation system and in infected cells. J Virol *56*, 120-126.

Grubman, M.J., Zellner, M., Bablanian, G., Mason, P.W., and Piccone, M.E. (1995). Identification of the active-site residues of the 3C proteinase of foot-and-mouth disease virus. Virology *213*, 581-589.

Guevin, C., Manna, D., Belanger, C., Konan, K.V., Mak, P., and Labonte, P. (2010). Autophagy protein ATG5 interacts transiently with the hepatitis C virus RNA polymerase (NS5B) early during infection. Virology *405*, 1-7.

Guttman, N., and Baltimore, D. (1977). Morphogenesis of poliovirus. IV. existence of particles sedimenting at 150S and having the properties of provirion. J Virol *23*, 363-367.

Haas, A.K., Yoshimura, S., Stephens, D.J., Preisinger, C., Fuchs, E., and Barr, F.A. (2007). Analysis of GTPase-activating proteins: Rab1 and Rab43 are key Rabs required to maintain a functional Golgi complex in human cells. J Cell Sci *120*, 2997-3010.

Harber, J.J., Bradley, J., Anderson, C.W., and Wimmer, E. (1991). Catalysis of poliovirus VP0 maturation cleavage is not mediated by serine 10 of VP2. J Virol *65*, 326-334.

Harris, T.J., and Brown, F. (1977). Biochemical analysis of a virulent and an avirulent strain of foot-and-mouth disease virus. J Gen Virol *34*, 87-105.

He, Y., Bowman, V.D., Mueller, S., Bator, C.M., Bella, J., Peng, X., Baker, T.S., Wimmer, E., Kuhn, R.J., and Rossmann, M.G. (2000). Interaction of the poliovirus receptor with poliovirus. Proc Natl Acad Sci U S A *97*, 79-84.

Hellen, C.U., and Sarnow, P. (2001). Internal ribosome entry sites in eukaryotic mRNA molecules. Genes Dev *15*, 1593-1612.

Helms, J.B., and Rothman, J.E. (1992). Inhibition by brefeldin A of a Golgi membrane enzyme that catalyses exchange of guanine nucleotide bound to ARF. Nature *360*, 352-354.

Herold, J., and Andino, R. (2000). Poliovirus requires a precise 5' end for efficient positive-strand RNA synthesis. J Virol *74*, 6394-6400.
Herold, J., and Andino, R. (2001). Poliovirus RNA replication requires genome circularization through a protein-protein bridge. Mol Cell *7*, 581-591.
Hershey, J.I.a.M., W.C (2000). Pathway and mechanism of initiation of protein synthesis. In Translational control of gene expression, H.a.M. Sonenberg, ed. (Cold Spring Harbour Laboratory Press), pp. 33-88.
Hinton, T.M., Ross-Smith, N., Warner, S., Belsham, G.J., and Crabb, B.S. (2002). Conservation of L and 3C proteinase activities across distantly related aphthoviruses. J Gen Virol *83*, 3111-3121.
Hofer, F., Gruenberger, M., Kaualski, E., Machat, H., Huettinger, M., Kuechler, E., Blaas, D. (1994). Members of the low-density lipoprotein receptor family mediate cell entry of a minor-group common cold virus. Proc Natl Acad Sci USA. *1:91*(5), 1839-42.
Hogle, J.M., Chow, M., and Filman, D.J. (1985). Three-dimensional structure of poliovirus at 2.9 A resolution. Science *229*, 1358-1365.
Hsu, N.Y., Ilnytska, O., Belov, G., Santiana, M., Chen, Y.H., Takvorian, P.M., Pau, C., van der Schaar, H., Kaushik-Basu, N., Balla, T.*, et al.* (2010). Viral reorganization of the secretory pathway generates distinct organelles for RNA replication. Cell *141*, 799-811.
Huang, M., Weissman, J.T., Beraud-Dufour, S., Luan, P., Wang, C., Chen, W., Aridor, M., Wilson, I.A., and Balch, W.E. (2001). Crystal structure of Sar1-GDP at 1.7 A resolution and the role of the NH2 terminus in ER export. J Cell Biol *155*, 937-948.
Huber, I., Cukierman, E., Rotman, M., Aoe, T., Hsu, V.W., and Cassel, D. (1998). Requirement for both the amino-terminal catalytic domain and a noncatalytic domain for in vivo activity of ADP-ribosylation factor GTPase-activating protein. J Biol Chem *273*, 24786-24791.
Huber, L.A., Pimplikar, S., Parton, R.G., Virta, H., Zerial, M., and Simons, K. (1993). Rab8, a small GTPase involved in vesicular traffic between the TGN and the basolateral plasma membrane. J Cell Biol *123*, 35-45.
Hughes, H., Budnik, A., Schmidt, K., Palmer, K.J., Mantell, J., Noakes, C., Johnson, A., Carter, D.A., Verkade, P., Watson, P.*, et al.* (2009). Organisation of human ER-exit sites: requirements for the localisation of Sec16 to transitional ER. J Cell Sci *122*, 2924-2934.
Hyslop, N.S. (1965). Secretion of Foot-and-Mouth Disease Virus and Antibody in the Saliva of Infected and Immunized Cattle. J Comp Pathol *75*, 111-117.
Iinuma, T., Shiga, A., Nakamoto, K., O'Brien, M.B., Aridor, M., Arimitsu, N., Tagaya, M., and Tani, K. (2007). Mammalian Sec16/p250 plays a role in membrane traffic from the endoplasmic reticulum. J Biol Chem *282*, 17632-17639.
Ishiyama, N., Hill, C.M., Bates, I.R., and Harauz, G. (2002). The formation of helical tubular vesicles by binary monolayers containing a nickel-chelating lipid and phosphoinositides in the presence of basic polypeptides. Chem Phys Lipids *114*, 103-111.
Itoh, T., Satoh, M., Kanno, E., and Fukuda, M. (2006). Screening for target Rabs of TBC (Tre-2/Bub2/Cdc16) domain-containing proteins based on their Rab-binding activity. Genes Cells *11*, 1023-1037.
Jackson, C.L., and Casanova, J.E. (2000). Turning on ARF: the Sec7 family of guanine-nucleotide-exchange factors. Trends Cell Biol *10*, 60-67.

Jackson, T., Clark, S., Berryman, S., Burman, A., Cambier, S., Mu, D., Nishimura, S., and King, A.M. (2004). Integrin alphavbeta8 functions as a receptor for foot-and-mouth disease virus: role of the beta-chain cytodomain in integrin-mediated infection. J Virol *78*, 4533-4540.

Jackson, T., King, A.M., Stuart, D.I., and Fry, E. (2003). Structure and receptor binding. Virus Res *91*, 33-46.

Jackson, T., Mould, A.P., Sheppard, D., and King, A.M. (2002). Integrin alphavbeta1 is a receptor for foot-and-mouth disease virus. J Virol *76*, 935-941.

Jackson, T., Sheppard, D., Denyer, M., Blakemore, W., and King, A.M. (2000). The epithelial integrin alphavbeta6 is a receptor for foot-and-mouth disease virus. J Virol *74*, 4949-4956.

Jahn, R., and Grubmuller, H. (2002). Membrane fusion. Curr Opin Cell Biol *14*, 488-495.

Jezequel, A.M., and Steiner, J.W. (1966). Some ultrastructural and histochemical aspects of Coxsackie virus-cell interactions. Lab Invest *15*, 1055-1083.

Johns, H.L., Berryman, S., Monaghan, P., Belsham, G.J., and Jackson, T. (2009). A dominant-negative mutant of rab5 inhibits infection of cells by foot-and-mouth disease virus: implications for virus entry. J Virol *83*, 6247-6256.

Kano, F., Yamauchi, S., Yoshida, Y., Watanabe-Takahashi, M., Nishikawa, K., Nakamura, N., and Murata, M. (2009). Yip1A regulates the COPI-independent retrograde transport from the Golgi complex to the ER. J Cell Sci *122*, 2218-2227.

Kawamoto, K., Yoshida, Y., Tamaki, H., Torii, S., Shinotsuka, C., Yamashina, S., and Nakayama, K. (2002). GBF1, a guanine nucleotide exchange factor for ADP-ribosylation factors, is localized to the cis-Golgi and involved in membrane association of the COPI coat. Traffic *3*, 483-495.

Kemball, C.C., Alirezaei, M., Flynn, C.T., Wood, M.R., Harkins, S., Kiosses, W.B., and Whitton, J.L. (2010). Coxsackievirus infection induces autophagy-like vesicles and megaphagosomes in pancreatic acinar cells in vivo. J Virol *84*, 12110-12124.

King, A.M., Sangar, D.V., Harris, T.J., and Brown, F. (1980). Heterogeneity of the genome-linked protein of foot-and-mouth disease virus. J Virol *34*, 627-634.

Klausner, R.D., Donaldson, J.G., and Lippincott-Schwartz, J. (1992). Brefeldin A: insights into the control of membrane traffic and organelle structure. J Cell Biol *116*, 1071-1080.

Klein, M., Eggers, H.J., and Nelsen-Salz, B. (2000). Echovirus-9 protein 2C binds single-stranded RNA unspecifically. J Gen Virol *81*, 2481-2484.

Knipe, T., Rieder, E., Baxt, B., Ward, G., and Mason, P.W. (1997). Characterization of synthetic foot-and-mouth disease virus provirions separates acid-mediated disassembly from infectivity. J Virol *71*, 2851-2856.

Knoops, K., Kikkert, M., Worm, S.H., Zevenhoven-Dobbe, J.C., van der Meer, Y., Koster, A.J., Mommaas, A.M., and Snijder, E.J. (2008). SARS-coronavirus replication is supported by a reticulovesicular network of modified endoplasmic reticulum. PLoS Biol *6*, e226.

Knoops, K., Swett-Tapia, C., van den Worm, S.H., Te Velthuis, A.J., Koster, A.J., Mommaas, A.M., Snijder, E.J., and Kikkert, M. (2010). Integrity of the early secretory pathway promotes, but is not required for, severe acute

respiratory syndrome coronavirus RNA synthesis and virus-induced remodeling of endoplasmic reticulum membranes. J Virol *84*, 833-846.
Knox, C., Moffat, K., Ali, S., Ryan, M., and Wileman, T. (2005). Foot-and-mouth disease virus replication sites form next to the nucleus and close to the Golgi apparatus, but exclude marker proteins associated with host membrane compartments. J Gen Virol *86*, 687-696.
Kolatkar, P.R., Bella, J., Olson, N.H., Bator, C.M., Baker, T.S., and Rossmann, M.G. (1999). Structural studies of two rhinovirus serotypes complexed with fragments of their cellular receptor. EMBO J *18*, 6249-6259.
Kozak, M. (1989). The scanning model for translation: an update. J Cell Biol *108*, 229-241.
Kuehn, M.J., Herrmann, J.M., and Schekman, R. (1998). COPII-cargo interactions direct protein sorting into ER-derived transport vesicles. Nature *391*, 187-190.
Kuge, O., Dascher, C., Orci, L., Rowe, T., Amherdt, M., Plutner, H., Ravazzola, M., Tanigawa, G., Rothman, J.E., and Balch, W.E. (1994). Sar1 promotes vesicle budding from the endoplasmic reticulum but not Golgi compartments. J Cell Biol *125*, 51-65.
Kuhn, R., Luz, N., and Beck, E. (1990). Functional analysis of the internal translation initiation site of foot-and-mouth disease virus. J Virol *64*, 4625-4631.
Kusov, Y.Y., Probst, C., Jecht, M., Jost, P.D., and Gauss-Muller, V. (1998). Membrane association and RNA binding of recombinant hepatitis A virus protein 2C. Arch Virol *143*, 931-944.
Lama, J., Sanz, M.A., and Carrasco, L. (1998). Genetic analysis of poliovirus protein 3A: characterization of a non-cytopathic mutant virus defective in killing Vero cells. J Gen Virol *79 (Pt 8)*, 1911-1921.
Lea, S., Hernandez, J., Blakemore, W., Brocchi, E., Curry, S., Domingo, E., Fry, E., Abu-Ghazaleh, R., King, A., Newman, J.*, et al.* (1994). The structure and antigenicity of a type C foot-and-mouth disease virus. Structure *2*, 123-139.
Lederkremer, G.Z., Cheng, Y., Petre, B.M., Vogan, E., Springer, S., Schekman, R., Walz, T., and Kirchhausen, T. (2001). Structure of the Sec23p/24p and Sec13p/31p complexes of COPII. Proc Natl Acad Sci U S A *98*, 10704-10709.
Lee, M.C., Orci, L., Hamamoto, S., Futai, E., Ravazzola, M., and Schekman, R. (2005). Sar1p N-terminal helix initiates membrane curvature and completes the fission of a COPII vesicle. Cell *122*, 605-617.
Lee, M.C.S.M., E.A.; Goldberg, J.; Orci, L.; Schekman, R. (2004). Bi-Directional protein transport between the ER and Golgi. In Annuual review of Cell developmental biology, pp. 87-123.
Lee, T.H., and Linstedt, A.D. (2000). Potential role for protein kinases in regulation of bidirectional endoplasmic reticulum-to-Golgi transport revealed by protein kinase inhibitor H89. Mol Biol Cell *11*, 2577-2590.
Lee, W.M., Monroe, S.S., and Rueckert, R.R. (1993). Role of maturation cleavage in infectivity of picornaviruses: activation of an infectosome. J Virol *67*, 2110-2122.
Letourneur, F., Gaynor, E.C., Hennecke, S., Demolliere, C., Duden, R., Emr, S.D., Riezman, H., and Cosson, P. (1994). Coatomer is essential for retrieval of dilysine-tagged proteins to the endoplasmic reticulum. Cell *79*, 1199-1207.

Lewis, S.M., Poon, P.P., Singer, R.A., Johnston, G.C., and Spang, A. (2004). The ArfGAP Glo3 is required for the generation of COPI vesicles. Mol Biol Cell *15*, 4064-4072.

Lippincott-Schwartz, J. (2001). The secretory membrane system studied in real-time. Robert Feulgen Prize Lecture, 2001. Histochem Cell Biol *116*, 97-107.

Lippincott-Schwartz, J., Donaldson, J.G., Schweizer, A., Berger, E.G., Hauri, H.P., Yuan, L.C., and Klausner, R.D. (1990). Microtubule-dependent retrograde transport of proteins into the ER in the presence of brefeldin A suggests an ER recycling pathway. Cell *60*, 821-836.

Lippincott-Schwartz, J., Yuan, L.C., Bonifacino, J.S., and Klausner, R.D. (1989). Rapid redistribution of Golgi proteins into the ER in cells treated with brefeldin A: evidence for membrane cycling from Golgi to ER. Cell *56*, 801-813.

Liu, Y., Wang, C., Mueller, S., Paul, A.V., Wimmer, E., and Jiang, P. (2010). Direct interaction between two viral proteins, the nonstructural protein 2C and the capsid protein VP3, is required for enterovirus morphogenesis. PLoS Pathog *6*.

Lloyd, R.E. (2000). Translational control by viral proteinases. Virus Research *119 vol1*, 330-335.

Lobert, P.E., Escriou, N., Ruelle, J., and Michiels, T. (1999). A coding RNA sequence acts as a replication signal in cardioviruses. Proc Natl Acad Sci U S A *96*, 11560-11565.

Lopez de Quinto, S., and Martinez-Salas, E. (2000). Interaction of the eIF4G initiation factor with the aphthovirus IRES is essential for internal translation initiation in vivo. Rna *6*, 1380-1392.

Lopez de Quinto, S., Saiz, M., de la Morena, D., Sobrino, F., and Martinez-Salas, E. (2002). IRES-driven translation is stimulated separately by the FMDV 3'-NCR and poly(A) sequences. Nucleic Acids Res *30*, 4398-4405.

Luo, M., Vriend, G., Kamer, G., Minor, I., Arnold, E., Rossmann, M.G., Boege, U., Scraba, D.G., Duke, G.M., and Palmenberg, A.C. (1987). The atomic structure of Mengo virus at 3.0 A resolution. Science *235*, 182-191.

Luz, N., and Beck, E. (1991). Interaction of a cellular 57-kilodalton protein with the internal translation initiation site of foot-and-mouth disease virus. J Virol *65*, 6486-6494.

Lyons, T., Murray, K.E., Roberts, A.W., and Barton, D.J. (2001). Poliovirus 5'-terminal cloverleaf RNA is required in cis for VPg uridylylation and the initiation of negative-strand RNA synthesis. J Virol *75*, 10696-10708.

Mackenzie, J.M., Khromykh, A.A., Jones, M.K., and Westaway, E.G. (1998). Subcellular localization and some biochemical properties of the flavivirus Kunjin nonstructural proteins NS2A and NS4A. Virology *245*, 203-215.

Majoul, I., Straub, M., Hell, S.W., Duden, R., and Soling, H.D. (2001). KDEL-cargo regulates interactions between proteins involved in COPI vesicle traffic: measurements in living cells using FRET. Dev Cell *1*, 139-153.

Mallard, F., Tang, B.L., Galli, T., Tenza, D., Saint-Pol, A., Yue, X., Antony, C., Hong, W., Goud, B., and Johannes, L. (2002). Early/recycling endosomes-to-TGN transport involves two SNARE complexes and a Rab6 isoform. J Cell Biol *156*, 653-664.

Mansour, M., Lee, S.Y., and Pohajdak, B. (2002). The N-terminal coiled coil domain of the cytohesin/ARNO family of guanine nucleotide exchange factors interacts with the scaffolding protein CASP. J Biol Chem *277*, 32302-32309.

Marc, D., Girard, M., and van der Werf, S. (1991). A Gly1 to Ala substitution in poliovirus capsid protein VP0 blocks its myristoylation and prevents viral assembly. J Gen Virol *72 (Pt 5)*, 1151-1157.

Marlovits, T.C., Abrahamsberg, C., Blaas, D. (1998). Very low-density lipoprotein receptor fragment shed from HeLa cells inhibit human rhinovirus infection. J Virol *72,* 10246-50.

Martin-Acebes, M.A., Gonzalez-Magaldi, M., Rosas, M.F., Borrego, B., Brocchi, E., Armas-Portela, R., and Sobrino, F. (2008). Subcellular distribution of swine vesicular disease virus proteins and alterations induced in infected cells: a comparative study with foot-and-mouth disease virus and vesicular stomatitis virus. Virology *374*, 432-443.

Martinez-Salas, E., Ramos, R., Lafuente, E., and Lopez de Quinto, S. (2001). Functional interactions in internal translation initiation directed by viral and cellular IRES elements. J Gen Virol *82*, 973-984.

Martinez-Salas, E., Saiz, J.C., Davila, M., Belsham, G.J., and Domingo, E. (1993). A single nucleotide substitution in the internal ribosome entry site of foot-and-mouth disease virus leads to enhanced cap-independent translation in vivo. J Virol *67*, 3748-3755.

Martinez, O., and Goud, B. (1998). Rab proteins. Biochim Biophys Acta *1404*, 101-112.

Martinez, O., Schmidt, A., Salamero, J., Hoflack, B., Roa, M., and Goud, B. (1994). The small GTP-binding protein rab6 functions in intra-Golgi transport. J Cell Biol *127*, 1575-1588.

Mason, P.W., Bezborodova, S.V., and Henry, T.M. (2002). Identification and characterization of a cis-acting replication element (cre) adjacent to the internal ribosome entry site of foot-and-mouth disease virus. J Virol *76*, 9686-9694.

Mason, P.W., Grubman, M.J., and Baxt, B. (2003). Molecular basis of pathogenesis of FMDV. Virus Res *91*, 9-32.

Matsuoka, K., Orci, L., Amherdt, M., Bednarek, S.Y., Hamamoto, S., Schekman, R., and Yeung, T. (1998). COPII-coated vesicle formation reconstituted with purified coat proteins and chemically defined liposomes. Cell *93*, 263-275.

Maynell, L.A., Kirkegaard, K., and Klymkowsky, M.W. (1992). Inhibition of poliovirus RNA synthesis by brefeldin A. J Virol *66*, 1985-1994.

McKnight, K.L., and Lemon, S.M. (1996). Capsid coding sequence is required for efficient replication of human rhinovirus 14 RNA. J Virol *70*, 1941-1952.

McMahon, H.T., and Gallop, J.L. (2005). Membrane curvature and mechanisms of dynamic cell membrane remodelling. Nature *438*, 590-596.

Medina, M., Domingo, E., Brangwyn, J.K., and Belsham, G.J. (1993). The two species of the foot-and-mouth disease virus leader protein, expressed individually, exhibit the same activities. Virology *194*, 355-359.

Meerovitch, K., Svitkin, Y.V., Lee, H.S., Lejbkowicz, F., Kenan, D.J., Chan, E.K., Agol, V.I., Keene, J.D., and Sonenberg, N. (1993). La autoantigen enhances and corrects aberrant translation of poliovirus RNA in reticulocyte lysate. J Virol *67*, 3798-3807.

Melia, T.J., Weber, T., McNew, J.A., Fisher, L.E., Johnston, R.J., Parlati, F., Mahal, L.K., Sollner, T.H., and Rothman, J.E. (2002). Regulation of membrane fusion by the membrane-proximal coil of the t-SNARE during zippering of SNAREpins. J Cell Biol *158*, 929-940.

Mesmin, B., Drin, G., Levi, S., Rawet, M., Cassel, D., Bigay, J., and Antonny, B. (2007). Two lipid-packing sensor motifs contribute to the sensitivity of ArfGAP1 to membrane curvature. Biochemistry *46*, 1779-1790.

Meyer, K., Petersen, A., Niepmann, M., and Beck, E. (1995). Interaction of eukaryotic initiation factor eIF-4B with a picornavirus internal translation initiation site. J Virol *69*, 2819-2824.

Michelsen, K., Schmid, V., Metz, J., Heusser, K., Liebel, U., Schwede, T., Spang, A., and Schwappach, B. (2007). Novel cargo-binding site in the beta and delta subunits of coatomer. J Cell Biol *179*, 209-217.

Miller, E.A., Beilharz, T.H., Malkus, P.N., Lee, M.C., Hamamoto, S., Orci, L., and Schekman, R. (2003). Multiple cargo binding sites on the COPII subunit Sec24p ensure capture of diverse membrane proteins into transport vesicles. Cell *114*, 497-509.

Miller, S., Kastner, S., Krijnse-Locker, J., Buhler, S., and Bartenschlager, R. (2007). The non-structural protein 4A of dengue virus is an integral membrane protein inducing membrane alterations in a 2K-regulated manner. J Biol Chem *282*, 8873-8882.

Miller, S., and Krijnse-Locker, J. (2008). Modification of intracellular membrane structures for virus replication. Nat Rev Microbiol *6*, 363-374.

Moffat, K., Howell, G., Knox, C., Belsham, G.J., Monaghan, P., Ryan, M.D., and Wileman, T. (2005). Effects of foot-and-mouth disease virus nonstructural proteins on the structure and function of the early secretory pathway: 2BC but not 3A blocks endoplasmic reticulum-to-Golgi transport. J Virol *79*, 4382-4395.

Moffat, K., Knox, C., Howell, G., Clark, S.J., Yang, H., Belsham, G.J., Ryan, M., and Wileman, T. (2007). Inhibition of the secretory pathway by foot-and-mouth disease virus 2BC protein is reproduced by coexpression of 2B with 2C, and the site of inhibition is determined by the subcellular location of 2C. J Virol *81*, 1129-1139.

Monaghan, P., Cook, H., Jackson, T., Ryan, M., and Wileman, T. (2004). The ultrastructure of the developing replication site in foot-and-mouth disease virus-infected BHK-38 cells. J Gen Virol *85*, 933-946.

Monetta, P., Slavin, I., Romero, N., and Alvarez, C. (2007). Rab1b interacts with GBF1 and modulates both ARF1 dynamics and COPI association. Mol Biol Cell *18*, 2400-2410.

Morasco, B.J., Sharma, N., Parilla, J., and Flanegan, J.B. (2003). Poliovirus cre(2C)-dependent synthesis of VPgpUpU is required for positive- but not negative-strand RNA synthesis. J Virol *77*, 5136-5144.

Mossessova, E., Corpina, R.A., and Goldberg, J. (2003). Crystal structure of ARF1*Sec7 complexed with Brefeldin A and its implications for the guanine nucleotide exchange mechanism. Mol Cell *12*, 1403-1411.

Moyer, B.D., Allan, B.B., and Balch, W.E. (2001). Rab1 interaction with a GM130 effector complex regulates COPII vesicle cis--Golgi tethering. Traffic *2*, 268-276.

Muckelbauer, J.K., Kremer, M., Minor, I., Diana, G., Dutko, F.J., Groarke, J., Pevear, D.C., and Rossmann, M.G. (1995). The structure of coxsackievirus B3 at 3.5 A resolution. Structure *3*, 653-667.

Munro, S. (2002). More than one way to replicate the Golgi apparatus. Nat Cell Biol *4*, E223-224.

Murray, K.E., and Barton, D.J. (2003). Poliovirus CRE-dependent VPg uridylylation is required for positive-strand RNA synthesis but not for negative-strand RNA synthesis. J Virol *77*, 4739-4750.

Murray, K.E., Roberts, A.W., and Barton, D.J. (2001). Poly(rC) binding proteins mediate poliovirus mRNA stability. Rna *7*, 1126-1141.

Murray, L., Luke, G.A., Ryan, M.D., Wileman, T., and Knox, C. (2009). Amino acid substitutions within the 2C coding sequence of Theiler's Murine Encephalomyelitis virus alter virus growth and affect protein distribution. Virus Res *144*, 74-82.

Nakano, A., Brada, D., and Schekman, R. (1988). A membrane glycoprotein, Sec12p, required for protein transport from the endoplasmic reticulum to the Golgi apparatus in yeast. J Cell Biol *107*, 851-863.

Nayak, A., Goodfellow, I.G., and Belsham, G.J. (2005). Factors required for the Uridylylation of the foot-and-mouth disease virus 3B1, 3B2, and 3B3 peptides by the RNA-dependent RNA polymerase (3Dpol) in vitro. J Virol *79*, 7698-7706.

Nayak, A., Goodfellow, I.G., Woolaway, K.E., Birtley, J., Curry, S., and Belsham, G.J. (2006). Role of RNA structure and RNA binding activity of foot-and-mouth disease virus 3C protein in VPg uridylylation and virus replication. J Virol *80*, 9865-9875.

Nie, Z., Hirsch, D.S., and Randazzo, P.A. (2003). Arf and its many interactors. Curr Opin Cell Biol *15*, 396-404.

Niu, T.K., Pfeifer, A.C., Lippincott-Schwartz, J., and Jackson, C.L. (2005). Dynamics of GBF1, a Brefeldin A-sensitive Arf1 exchange factor at the Golgi. Mol Biol Cell *16*, 1213-1222.

Nomoto, A., Kitamura, N., Golini, F., and Wimmer, E. (1977). The 5'-terminal structures of poliovirion RNA and poliovirus mRNA differ only in the genome-linked protein VPg. Proc Natl Acad Sci U S A *74*, 5345-5349.

Novak, J.E., and Kirkegaard, K. (1991). Improved method for detecting poliovirus negative strands used to demonstrate specificity of positive-strand encapsidation and the ratio of positive to negative strands in infected cells. J Virol *65*, 3384-3387.

Nugent, C.I., Johnson, K.L., Sarnow, P., and Kirkegaard, K. (1999). Functional coupling between replication and packaging of poliovirus replicon RNA. J Virol *73*, 427-435.

Nuoffer, C., Davidson, H.W., Matteson, J., Meinkoth, J., and Balch, W.E. (1994). A GDP-bound of rab1 inhibits protein export from the endoplasmic reticulum and transport between Golgi compartments. J Cell Biol *125*, 225-237.

O'Donnell, V., Larocco, M., and Baxt, B. (2008). Heparan sulfate-binding foot-and-mouth disease virus enters cells via caveola-mediated endocytosis. J Virol *82*, 9075-9085.

O'Donnell, V., LaRocco, M., Duque, H., and Baxt, B. (2005). Analysis of foot-and-mouth disease virus internalization events in cultured cells. J Virol *79*, 8506-8518.

O'Donnell, V.K., Pacheco, J.M., Henry, T.M., and Mason, P.W. (2001). Subcellular distribution of the foot-and-mouth disease virus 3A protein in cells infected with viruses encoding wild-type and bovine-attenuated forms of 3A. Virology *287*, 151-162.

Ochs, K., Rust, R.C., and Niepmann, M. (1999). Translation initiation factor eIF4B interacts with a picornavirus internal ribosome entry site in both 48S and 80S initiation complexes independently of initiator AUG location. J Virol *73*, 7505-7514.

Oka, T., and Nakano, A. (1994). Inhibition of GTP hydrolysis by Sar1p causes accumulation of vesicles that are a functional intermediate of the ER-to-Golgi transport in yeast. J Cell Biol *124*, 425-434.

Oostra, M., te Lintelo, E.G., Deijs, M., Verheije, M.H., Rottier, P.J., and de Haan, C.A. (2007). Localization and membrane topology of coronavirus nonstructural protein 4: involvement of the early secretory pathway in replication. J Virol *81*, 12323-12336.

Orci, L., Brown, D., Amherdt, M., and Perrelet, A. (1982). Distribution of intramembrane particles and filipin-sterol complexes in plasma membranes of kidney. I. Corpuscle of Malpighi. Lab Invest *46*, 545-553.

Orci, L., Perrelet, A., Ravazzola, M., Wieland, F.T., Schekman, R., and Rothman, J.E. (1993). "BFA bodies": a subcompartment of the endoplasmic reticulum. Proc Natl Acad Sci U S A *90*, 11089-11093.

Orci, L., Tagaya, M., Amherdt, M., Perrelet, A., Donaldson, J.G., Lippincott-Schwartz, J., Klausner, R.D., and Rothman, J.E. (1991). Brefeldin A, a drug that blocks secretion, prevents the assembly of non-clathrin-coated buds on Golgi cisternae. Cell *64*, 1183-1195.

Pacheco, J.M., Piccone, M.E., Rieder, E., Pauszek, S.J., Borca, M.V., Rodriguez, L.L. (2010). Doamin disruptions of individual 3B proteins of foot-and-mouth disease virus do not alter growth in cell culture or virulence in cattle. Virology *405*, 149-56.

Palokangas, H., Ying, M., Vaananen, K., and Saraste, J. (1998). Retrograde transport from the pre-Golgi intermediate compartment and the Golgi complex is affected by the vacuolar H+-ATPase inhibitor bafilomycin A1. Mol Biol Cell *9*, 3561-3578.

Parsley, T.B., Towner, J.S., Blyn, L.B., Ehrenfeld, E., and Semler, B.L. (1997). Poly (rC) binding protein 2 forms a ternary complex with the 5'-terminal sequences of poliovirus RNA and the viral 3CD proteinase. Rna *3*, 1124-1134.

Patil, C., and Walter, P. (2001). Intracellular signaling from the endoplasmic reticulum to the nucleus: the unfolded protein response in yeast and mammals. Curr Opin Cell Biol *13*, 349-355.

Paul, A.V., Molla, A., and Wimmer, E. (1994). Studies of a putative amphipathic helix in the N-terminus of poliovirus protein 2C. Virology *199*, 188-199.

Paul, A.V., Rieder, E., Kim, D.W., van Boom, J.H., and Wimmer, E. (2000). Identification of an RNA hairpin in poliovirus RNA that serves as the primary template in the in vitro uridylylation of VPg. J Virol *74*, 10359-10370.

Paul, A.V., van Boom, J.H., Filippov, D., and Wimmer, E. (1998). Protein-primed RNA synthesis by purified poliovirus RNA polymerase. Nature *393*, 280-284.

Peters, P.J., Hsu, V.W., Ooi, C.E., Finazzi, D., Teal, S.B., Oorschot, V., Donaldson, J.G., and Klausner, R.D. (1995). Overexpression of wild-type and mutant ARF1 and ARF6: distinct perturbations of nonoverlapping membrane compartments. J Cell Biol *128*, 1003-1017.

Peyroche, A., Paris, S., and Jackson, C.L. (1996). Nucleotide exchange on ARF mediated by yeast Gea1 protein. Nature *384*, 479-481.

Pfeffer, S.R. (2001). Rab GTPases: specifying and deciphering organelle identity and function. Trends Cell Biol *11*, 487-491.

Pfister, T., and Wimmer, E. (1999). Characterization of the nucleoside triphosphatase activity of poliovirus protein 2C reveals a mechanism by

which guanidine inhibits poliovirus replication. J Biol Chem *274*, 6992-7001.

Pilipenko, E.V., Blinov, V.M., Chernov, B.K., Dmitrieva, T.M., and Agol, V.I. (1989). Conservation of the secondary structure elements of the 5'-untranslated region of cardio- and aphthovirus RNAs. Nucleic Acids Res *17*, 5701-5711.

Pilipenko, E.V., Gmyl, A.P., Maslova, S.V., Svitkin, Y.V., Sinyakov, A.N., and Agol, V.I. (1992). Prokaryotic-like cis elements in the cap-independent internal initiation of translation on picornavirus RNA. Cell *68*, 119-131.

Pilipenko, E.V., Pestova, T.V., Kolupaeva, V.G., Khitrina, E.V., Poperechnaya, A.N., Agol, V.I., and Hellen, C.U. (2000). A cell cycle-dependent protein serves as a template-specific translation initiation factor. Genes Dev *14*, 2028-2045.

Plutner, H., Cox, A.D., Pind, S., Khosravi-Far, R., Bourne, J.R., Schwaninger, R., Der, C.J., and Balch, W.E. (1991). Rab1b regulates vesicular transport between the endoplasmic reticulum and successive Golgi compartments. J Cell Biol *115*, 31-43.

Plutner, H., Schwaninger, R., Pind, S., and Balch, W.E. (1990). Synthetic peptides of the Rab effector domain inhibit vesicular transport through the secretory pathway. EMBO J *9*, 2375-2383.

Powell, R.M., Ward, T., Evans, D.J., and Almond, J.W. (1997). Interaction between echovirus 7 and its receptor, decay-accelerating factor (CD55): evidence for a secondary cellular factor in A-particle formation. J Virol *71*, 9306-9312.

Prchla, E., Plank, C., Wagner, E., Blaas, D., and Fuchs, R. (1995). Virus-mediated release of endosomal content in vitro: different behavior of adenovirus and rhinovirus serotype 2. J Cell Biol *131*, 111-123.

Puri, S., and Linstedt, A.D. (2003). Capacity of the golgi apparatus for biogenesis from the endoplasmic reticulum. Mol Biol Cell *14*, 5011-5018.

Rein, U., Andag, U., Duden, R., Schmitt, H.D., and Spang, A. (2002). ARF-GAP-mediated interaction between the ER-Golgi v-SNAREs and the COPI coat. J Cell Biol *157*, 395-404.

Ren, M., Xu, G., Zeng, J., De Lemos-Chiarandini, C., Adesnik, M., and Sabatini, D.D. (1998). Hydrolysis of GTP on rab11 is required for the direct delivery of transferrin from the pericentriolar recycling compartment to the cell surface but not from sorting endosomes. Proc Natl Acad Sci U S A *95*, 6187-6192.

Renault, L., Guibert, B., and Cherfils, J. (2003). Structural snapshots of the mechanism and inhibition of a guanine nucleotide exchange factor. Nature *426*, 525-530.

Richards, O.C., and Ehrenfeld, E. (1990). Poliovirus RNA replication. Curr Top Microbiol Immunol *161*, 89-119.

Richter, S., Geldner, N., Schrader, J., Wolters, H., Stierhof, Y.D., Rios, G., Koncz, C., Robinson, D.G., and Jurgens, G. (2007). Functional diversification of closely related ARF-GEFs in protein secretion and recycling. Nature *448*, 488-492.

Rieder, E., Bunch, T., Brown, F., and Mason, P.W. (1993). Genetically engineered foot-and-mouth disease viruses with poly(C) tracts of two nucleotides are virulent in mice. J Virol *67*, 5139-5145.

Rivera-Molina, F.E., and Novick, P.J. (2009). A Rab GAP cascade defines the boundary between two Rab GTPases on the secretory pathway. Proc Natl Acad Sci U S A *106*, 14408-14413.

Rodriguez, P.L., and Carrasco, L. (1993). Poliovirus protein 2C has ATPase and GTPase activities. J Biol Chem *268*, 8105-8110.
Rodriguez, P.L., and Carrasco, L. (1995). Poliovirus protein 2C contains two regions involved in RNA binding activity. J Biol Chem *270*, 10105-10112.
Roosendaal, J., Westaway, E.G., Khromykh, A., and Mackenzie, J.M. (2006). Regulated cleavages at the West Nile virus NS4A-2K-NS4B junctions play a major role in rearranging cytoplasmic membranes and Golgi trafficking of the NS4A protein. J Virol *80*, 4623-4632.
Rossmann, M.G., Arnold, E., Erickson, J.W., Frankenberger, E.A., Griffith, J.P., Hecht, H.J., Johnson, J.E., Kamer, G., Luo, M., Mosser, A.G.*, et al.* (1985). Structure of a human common cold virus and functional relationship to other picornaviruses. Nature *317*, 145-153.
Rothman, J.E. (1994). Intracellular membrane fusion. Adv Second Messenger Phosphoprotein Res *29*, 81-96.
Rust, R.C., Landmann, L., Gosert, R., Tang, B.L., Hong, W., Hauri, H.P., Egger, D., and Bienz, K. (2001). Cellular COPII proteins are involved in production of the vesicles that form the poliovirus replication complex. J Virol *75*, 9808-9818.
Rust, R.C., Ochs, K., Meyer, K., Beck, E., and Niepmann, M. (1999). Interaction of eukaryotic initiation factor eIF4B with the internal ribosome entry site of foot-and-mouth disease virus is independent of the polypyrimidine tract-binding protein. J Virol *73*, 6111-6113.
Sa-Carvalho, D., Rieder, E., Baxt, B., Rodarte, R., Tanuri, A., and Mason, P.W. (1997). Tissue culture adaptation of foot-and-mouth disease virus selects viruses that bind to heparin and are attenuated in cattle. J Virol *71*, 5115-5123.
Saiz, M., Gomez, S., Martinez-Salas, E., and Sobrino, F. (2001). Deletion or substitution of the aphthovirus 3' NCR abrogates infectivity and virus replication. J Gen Virol *82*, 93-101.
Salama, N.R., Yeung, T., and Schekman, R.W. (1993). The Sec13p complex and reconstitution of vesicle budding from the ER with purified cytosolic proteins. EMBO J *12*, 4073-4082.
Saleh, L., Rust, R.C., Fullkrug, R., Beck, E., Bassili, G., Ochs, K., and Niepmann, M. (2001). Functional interaction of translation initiation factor eIF4G with the foot-and-mouth disease virus internal ribosome entry site. J Gen Virol *82*, 757-763.
Salonen, A., Ahola, T., and Kaariainen, L. (2005). Viral RNA replication in association with cellular membranes. Curr Top Microbiol Immunol *285*, 139-173.
Sandoval, I.V., and Carrasco, L. (1997). Poliovirus infection and expression of the poliovirus protein 2B provoke the disassembly of the Golgi complex, the organelle target for the antipoliovirus drug Ro-090179. J Virol *71*, 4679-4693.
Sangar, D.V., Newton, S.E., Rowlands, D.J., and Clarke, B.E. (1987). All foot and mouth disease virus serotypes initiate protein synthesis at two separate AUGs. Nucleic Acids Res *15*, 3305-3315.
Sanz-Parra, A., Sobrino, F., and Ley, V. (1998). Infection with foot-and-mouth disease virus results in a rapid reduction of MHC class I surface expression. J Gen Virol *79 (Pt 3)*, 433-436.
Saraste, J., Lahtinen, U., and Goud, B. (1995). Localization of the small GTP-binding protein rab1p to early compartments of the secretory pathway. J Cell Sci *108 (Pt 4)*, 1541-1552.

Sato, K., Ueda, T., and Nakano, A. (1999). The Arabidopsis thaliana RER1 gene family: its potential role in the endoplasmic reticulum localization of membrane proteins. Plant Mol Biol *41*, 815-824.
Sato, M., Sato, K., and Nakano, A. (1996). Endoplasmic reticulum localization of Sec12p is achieved by two mechanisms: Rer1p-dependent retrieval that requires the transmembrane domain and Rer1p-independent retention that involves the cytoplasmic domain. J Cell Biol *134*, 279-293.
Saunders, K., and King, A.M. (1982). Guanidine-resistant mutants of aphthovirus induce the synthesis of an altered nonstructural polypeptide, P34. J Virol *42*, 389-394.
Scales, S.J., Pepperkok, R., and Kreis, T.E. (1997). Visualization of ER-to-Golgi transport in living cells reveals a sequential mode of action for COPII and COPI. Cell *90*, 1137-1148.
Schindler, C., and Spang, A. (2007). Interaction of SNAREs with ArfGAPs precedes recruitment of Sec18p/NSF. Mol Biol Cell *18*, 2852-2863.
Schlegel, A., Giddings, T.H., Jr., Ladinsky, M.S., and Kirkegaard, K. (1996). Cellular origin and ultrastructure of membranes induced during poliovirus infection. J Virol *70*, 6576-6588.
Schroder, M., and Kaufman, R.J. (2005a). ER stress and the unfolded protein response. Mutat Res *569*, 29-63.
Schroder, M., and Kaufman, R.J. (2005b). The mammalian unfolded protein response. Annu Rev Biochem *74*, 739-789.
Sciaky, N., Presley, J., Smith, C., Zaal, K.J., Cole, N., Moreira, J.E., Terasaki, M., Siggia, E., and Lippincott-Schwartz, J. (1997). Golgi tubule traffic and the effects of brefeldin A visualized in living cells. J Cell Biol *139*, 1137-1155.
Segev, N. (2001). Ypt/rab gtpases: regulators of protein trafficking. Sci STKE *2001*, re11.
Sellars, R.F. (1971). Quantitative aspects of the spread of foot and mouth disease. The veterinary bulletin *41*, 504-506.
Serrano, P., Pulido, M.R., Saiz, M., and Martinez-Salas, E. (2006). The 3' end of the foot-and-mouth disease virus genome establishes two distinct long-range RNA-RNA interactions with the 5' end region. J Gen Virol *87*, 3013-3022.
Sharp, T.M., Guix, S., Katayama, K., Crawford, S.E., and Estes, M.K. (2010). Inhibition of cellular protein secretion by norwalk virus nonstructural protein p22 requires a mimic of an endoplasmic reticulum export signal. PLoS One *5*, e13130.
Shatkin, A.J. (1976). Capping of eucaryotic mRNAs. Cell *9*, 645-653.
Sheetz, M.P., and Singer, S.J. (1974). Biological membranes as bilayer couples. A molecular mechanism of drug-erythrocyte interactions. Proc Natl Acad Sci U S A *71*, 4457-4461.
Shima, D.T., Scales, S.J., Kreis, T.E., and Pepperkok, R. (1999). Segregation of COPI-rich and anterograde-cargo-rich domains in endoplasmic-reticulum-to-Golgi transport complexes. Curr Biol *9*, 821-824.
Shin, H.W., Morinaga, N., Noda, M., and Nakayama, K. (2004). BIG2, a guanine nucleotide exchange factor for ADP-ribosylation factors: its localization to recycling endosomes and implication in the endosome integrity. Mol Biol Cell *15*, 5283-5294.
Shinotsuka, C., Yoshida, Y., Kawamoto, K., Takatsu, H., and Nakayama, K. (2002). Overexpression of an ADP-ribosylation factor-guanine nucleotide

exchange factor, BIG2, uncouples brefeldin A-induced adaptor protein-1 coat dissociation and membrane tubulation. J Biol Chem *277*, 9468-9473.
Skinner, M.S., Halperen, S., and Harkin, J.C. (1968). Cytoplasmic membrane-bound vesicles in echovirus 12-infected cells. Virology *36*, 241-253.
Sklan, E.H., Serrano, R.L., Einav, S., Pfeffer, S.R., Lambright, D.G., and Glenn, J.S. (2007a). TBC1D20 is a Rab1 GTPase-activating protein that mediates hepatitis C virus replication. J Biol Chem *282*, 36354-36361.
Sklan, E.H., Staschke, K., Oakes, T.M., Elazar, M., Winters, M., Aroeti, B., Danieli, T., and Glenn, J.S. (2007b). A Rab-GAP TBC domain protein binds hepatitis C virus NS5A and mediates viral replication. J Virol *81*, 11096-11105.
Sollner, T.H. (2004). Intracellular and viral membrane fusion: a uniting mechanism. Curr Opin Cell Biol *16*, 429-435.
Spang, A. (2002). ARF1 regulatory factors and COPI vesicle formation. Curr Opin Cell Biol *14*, 423-427.
Spang, A., Herrmann, J.M., Hamamoto, S., and Schekman, R. (2001). The ADP ribosylation factor-nucleotide exchange factors Gea1p and Gea2p have overlapping, but not redundant functions in retrograde transport from the Golgi to the endoplasmic reticulum. Mol Biol Cell *12*, 1035-1045.
Speight, P., and Silverman, M. (2005). Diacylglycerol-activated Hmunc13 serves as an effector of the GTPase Rab34. Traffic *6*, 858-865.
Stagg, S.M., Gurkan, C., Fowler, D.M., LaPointe, P., Foss, T.R., Potter, C.S., Carragher, B., and Balch, W.E. (2006). Structure of the Sec13/31 COPII coat cage. Nature *439*, 234-238.
Stearns, T., Willingham, M.C., Botstein, D., and Kahn, R.A. (1990). ADP-ribosylation factor is functionally and physically associated with the Golgi complex. Proc Natl Acad Sci U S A *87*, 1238-1242.
Stephens, D.J. (2003). De novo formation, fusion and fission of mammalian COPII-coated endoplasmic reticulum exit sites. EMBO Rep *4*, 210-217.
Stephens, D.J., and Pepperkok, R. (2002). Imaging of procollagen transport reveals COPI-dependent cargo sorting during ER-to-Golgi transport in mammalian cells. J Cell Sci *115*, 1149-1160.
Suhy, D.A., Giddings, T.H., Jr., and Kirkegaard, K. (2000). Remodeling the endoplasmic reticulum by poliovirus infection and by individual viral proteins: an autophagy-like origin for virus-induced vesicles. J Virol *74*, 8953-8965.
Sun, P., Yamamoto, H., Suetsugu, S., Miki, H., Takenawa, T., and Endo, T. (2003). Small GTPase Rah/Rab34 is associated with membrane ruffles and macropinosomes and promotes macropinosome formation. J Biol Chem *278*, 4063-4071.
Supek, F., Madden, D.T., Hamamoto, S., Orci, L., and Schekman, R. (2002). Sec16p potentiates the action of COPII proteins to bud transport vesicles. J Cell Biol *158*, 1029-1038.
Sutmoller, P., and McVicar, J.W. (1976). Pathogenesis of foot-and-mouth disease: clearance of the virus from the circulation of cattle and goats during experimental viraemia. J Hyg (Lond) *77*, 245-253.
Sutmoller, P., McVicar, J.W., and Cottral, G.E. (1968). The epizootiological importance of foot-and-mouth disease carriers. I. Experimentally produced foot-and-mouth disease carriers in susceptible and immune cattle. Arch Gesamte Virusforsch *23*, 227-235.
Sweeney, T.R., Cisnetto, V., Bose, D., Bailey, M., Wilson, J.R., Zhang, X., Belsham, G.J., and Curry, S. (2010). Foot-and-mouth disease virus 2C is a

hexameric AAA+ protein with a coordinated ATP hydrolysis mechanism. J Biol Chem *285*, 24347-24359.

Tanigawa, G., Orci, L., Amherdt, M., Ravazzola, M., Helms, J.B., and Rothman, J.E. (1993). Hydrolysis of bound GTP by ARF protein triggers uncoating of Golgi-derived COP-coated vesicles. J Cell Biol *123*, 1365-1371.

Taylor, M.P., and Kirkegaard, K. (2007). Modification of cellular autophagy protein LC3 by poliovirus. J Virol *81*, 12543-12553.

Tesar, M., Berger, H.G., and Marquardt, O. (1989). Serological probes for some foot-and-mouth disease virus nonstructural proteins. Virus Genes *3*, 29-44.

Teterina, N.L., Egger, D., Bienz, K., Brown, D.M., Semler, B.L., and Ehrenfeld, E. (2001). Requirements for assembly of poliovirus replication complexes and negative-strand RNA synthesis. J Virol *75*, 3841-3850.

Tisdale, E.J. (1999). A Rab2 mutant with impaired GTPase activity stimulates vesicle formation from pre-Golgi intermediates. Mol Biol Cell *10*, 1837-1849.

Tisdale, E.J. (2000). Rab2 requires PKC iota/lambda to recruit beta-COP for vesicle formation. Traffic *1*, 702-712.

Tisdale, E.J., and Balch, W.E. (1996). Rab2 is essential for the maturation of pre-Golgi intermediates. J Biol Chem *271*, 29372-29379.

Tisdale, E.J., Bourne, J.R., Khosravi-Far, R., Der, C.J., and Balch, W.E. (1992). GTP-binding mutants of rab1 and rab2 are potent inhibitors of vesicular transport from the endoplasmic reticulum to the Golgi complex. J Cell Biol *119*, 749-761.

Tisdale, E.J., and Jackson, M.R. (1998). Rab2 protein enhances coatomer recruitment to pre-Golgi intermediates. J Biol Chem *273*, 17269-17277.

Tomassini, J.E., Graham, D., Dewitt, C.M., Lineberger, D.W, Rodkey, J.A., Colonno, R.J. (1989). cDNA cloning reveals that the major group rhinovirus receptor on HeLa cells is intercellular adhesion molecule 1. Proc Natl Acad Sci USA *86*, 4907-11.

Towner, J.S., Ho, T.V., and Semler, B.L. (1996). Determinants of membrane association for poliovirus protein 3AB. J Biol Chem *271*, 26810-26818.

Tsuchiya, M., Price, S.R., Tsai, S.C., Moss, J., and Vaughan, M. (1991). Molecular identification of ADP-ribosylation factor mRNAs and their expression in mammalian cells. J Biol Chem *266*, 2772-2777.

Tuthill, T.J., Bubeck, D., Rowlands, D.J., and Hogle, J.M. (2006). Characterization of early steps in the poliovirus infection process: receptor-decorated liposomes induce conversion of the virus to membrane-anchored entry-intermediate particles. J Virol *80*, 172-180.

Ullrich, O., Stenmark, H., Alexandrov, K., Huber, L.A., Kaibuchi, K., Sasaki, T., Takai, Y., and Zerial, M. (1993). Rab GDP dissociation inhibitor as a general regulator for the membrane association of rab proteins. J Biol Chem *268*, 18143-18150.

van Kuppeveld, F.J., Galama, J.M., Zoll, J., van den Hurk, P.J., and Melchers, W.J. (1996). Coxsackie B3 virus protein 2B contains cationic amphipathic helix that is required for viral RNA replication. J Virol *70*, 3876-3886.

van Ooij, M.J., Polacek, C., Glaudemans, D.H., Kuijpers, J., van Kuppeveld, F.J., Andino, R., Agol, V.I., and Melchers, W.J. (2006). Polyadenylation of genomic RNA and initiation of antigenomic RNA in a positive-strand RNA virus are controlled by the same cis-element. Nucleic Acids Res *34*, 2953-2965.

Verheije, M.H., Raaben, M., Mari, M., Te Lintelo, E.G., Reggiori, F., van Kuppeveld, F.J., Rottier, P.J., and de Haan, C.A. (2008). Mouse hepatitis coronavirus RNA replication depends on GBF1-mediated ARF1 activation. PLoS Pathog *4*, e1000088.

Verlinden, Y., Cuconati, A., Wimmer, E., and Rombaut, B. (2000). Cell-free synthesis of poliovirus: 14S subunits are the key intermediates in the encapsidation of poliovirus RNA. J Gen Virol *81*, 2751-2754.

Wang, T., and Hong, W. (2002). Interorganellar regulation of lysosome positioning by the Golgi apparatus through Rab34 interaction with Rab-interacting lysosomal protein. Mol Biol Cell *13*, 4317-4332.

Ward, T.H., Polishchuk, R.S., Caplan, S., Hirschberg, K., and Lippincott-Schwartz, J. (2001). Maintenance of Golgi structure and function depends on the integrity of ER export. J Cell Biol *155*, 557-570.

Waters, M.G., Serafini, T., and Rothman, J.E. (1991). 'Coatomer': a cytosolic protein complex containing subunits of non-clathrin-coated Golgi transport vesicles. Nature *349*, 248-251.

Wessels, E., Duijsings, D., Lanke, K.H., Melchers, W.J., Jackson, C.L., and van Kuppeveld, F.J. (2007). Molecular determinants of the interaction between coxsackievirus protein 3A and guanine nucleotide exchange factor GBF1. J Virol *81*, 5238-5245.

Wessels, E., Duijsings, D., Lanke, K.H., van Dooren, S.H., Jackson, C.L., Melchers, W.J., and van Kuppeveld, F.J. (2006a). Effects of picornavirus 3A Proteins on Protein Transport and GBF1-dependent COP-I recruitment. J Virol *80*, 11852-11860.

Wessels, E., Duijsings, D., Niu, T.K., Neumann, S., Oorschot, V.M., de Lange, F., Lanke, K.H., Klumperman, J., Henke, A., Jackson, C.L.*, et al.* (2006b). A viral protein that blocks Arf1-mediated COP-I assembly by inhibiting the guanine nucleotide exchange factor GBF1. Dev Cell *11*, 191-201.

Wilson, B.S., Nuoffer, C., Meinkoth, J.L., McCaffery, M., Feramisco, J.R., Balch, W.E., and Farquhar, M.G. (1994). A Rab1 mutant affecting guanine nucleotide exchange promotes disassembly of the Golgi apparatus. J Cell Biol *125*, 557-571.

Wimmer, E. (1982). Genome-linked proteins of viruses. Cell *28*, 199-201.

Xiao, C., Bator, C.M., Bowman, V.D., Rieder, E., He, Y., Hebert, B., Bella, J., Baker, T.S., Wimmer, E., Kuhn, R.J.*, et al.* (2001). Interaction of coxsackievirus A21 with its cellular receptor, ICAM-1. J Virol *75*, 2444-2451.

Yafal, A.G., and Palma, E.L. (1979). Morphogenesis of foot-and-mouth disease virus. I. Role of procapsids as virion Precursors. J Virol *30*, 643-649.

Yamashita, S., Oku, M., Wasada, Y., Ano, Y., and Sakai, Y. (2006). PI4P-signaling pathway for the synthesis of a nascent membrane structure in selective autophagy. J Cell Biol *173*, 709-717.

Yang, J.S., Lee, S.Y., Gao, M., Bourgoin, S., Randazzo, P.A., Premont, R.T., and Hsu, V.W. (2002). ARFGAP1 promotes the formation of COPI vesicles, suggesting function as a component of the coat. J Cell Biol *159*, 69-78.

Yang, X., Matern, H.T., and Gallwitz, D. (1998). Specific binding to a novel and essential Golgi membrane protein (Yip1p) functionally links the transport GTPases Ypt1p and Ypt31p. EMBO J *17*, 4954-4963.

Yoon, S.Y., Ha, Y.E., Choi, J.E., Ahn, J., Lee, H., and Kim, D.H. (2009). Autophagy in coxsackievirus-infected neurons. Autophagy *5*, 388-389.

Yoshihisa, T., Barlowe, C., and Schekman, R. (1993). Requirement for a GTPase-activating protein in vesicle budding from the endoplasmic reticulum. Science *259*, 1466-1468.

Young, J., Stauber, T., del Nery, E., Vernos, I., Pepperkok, R., and Nilsson, T. (2005). Regulation of microtubule-dependent recycling at the trans-Golgi network by Rab6A and Rab6A'. Mol Biol Cell *16*, 162-177.

Ypma-Wong, M.F., Dewalt, P.G., Johnson, V.H., Lamb, J.G., and Semler, B.L. (1988). Protein 3CD is the major poliovirus proteinase responsible for cleavage of the P1 capsid precursor. Virology *166*, 265-270.

Yu, S., and Roth, M.G. (2002). Casein kinase I regulates membrane binding by ARF GAP1. Mol Biol Cell *13*, 2559-2570.

Zaal, K.J., Smith, C.L., Polishchuk, R.S., Altan, N., Cole, N.B., Ellenberg, J., Hirschberg, K., Presley, J.F., Roberts, T.H., Siggia, E.*, et al.* (1999). Golgi membranes are absorbed into and reemerge from the ER during mitosis. Cell *99*, 589-601.

Zerial, M., and McBride, H. (2001). Rab proteins as membrane organizers. Nat Rev Mol Cell Biol *2*, 107-117.

Zhao, X., Lasell, T.K., and Melancon, P. (2002). Localization of large ADP-ribosylation factor-guanine nucleotide exchange factors to different Golgi compartments: evidence for distinct functions in protein traffic. Mol Biol Cell *13*, 119-133.

Zoppino, F.C., Militello, R.D., Slavin, I., Alvarez, C., and Colombo, M.I. (2010). Autophagosome formation depends on the small GTPase Rab1 and functional ER exit sites. Traffic *11*, 1246-1261.

Appendix I

10% SDS-PAGE gel (10ml)

Resolving Gel

30% Acrylamide (Sigma)	3.3ml
1.5 M Tris pH 8.8	2.5ml
dH_20	4ml
10% SDS	100µl
10% Ammonium persulphate (APS)	100µl
TEMED (Invitrogen)	10µl

2.5% Stacking gel

30% Acrylamide	1.7ml
1M Tris pH 6.8	1.2ml
dH_20	6.8ml
10% SDS	100µl
10% Ammonium persulphate (APS)	100µl
TEMED	15µl

Running Buffer (2L)

deionised water (dH_20)	2L
Glycine	28.8g
Trizma base	6g
SDS	2g

Transfer Buffer (2L)

dH_20	1.6L
Glycine	28.8g
Trizma base	6g
Methanol	400ml

Eagles Overlay (100ml)

Eagles overlay	75 ml
TPB	5ml
FCS	1ml
100 U/ml penicillin, 100 µg/ml streptomycin (IAH)	1ml

dH_20	25ml
Indubiose	0.6g

Acid wash pH 5 (1L)

0.85% Saline	1L
Citric acid	7.6g
Sodium citrate	18.6g

Appendix II

Thermocycler programmes

RT

Step1	48°C	45 min
Step 2	95°C	5 min
Step 3	20°C	20 min

PCR

Step 1	94°C	5 min
Step 2	55°C	2 min
Step 3	72°C	30 secs
Step 4	94°C	30secs
Step 5	55°C	30 secs
Step 6	72°C	10 min

30 cycles

QPCR

Step 1	60°C	30 min	
Step 2	95°C	10 min	
Step 3	95°C	15 secs	50 cycles
Step 4	60°C	96 secs	

Sequencing

Step 1	96°C	1 min	
Step 2	96°C	10 secs	25 cycles
Step 3	50°C	5 secs	
Step 4	60°C	4 min	

Appendix III

shRNA constructs

GAPDH shRNA in plasmid pLKO.1: Open biosystems

clone ID:
TRCN0000041754 (GC3)
TRCN0000041284 (GC4)
TRCN0000041755 (GC5)

Sar1 shRNA in plasmid pLKO.1: Open Biosystems

	Sar1A clone ID	Sense	Loop	Anti-sense
D5	TRCN0000048083	GCAATTAATGGGATTGTCTTT	CTCGAG	AAAGACAATCCCATTAATTGC
D7	TRCN0000048085	CGTGAGATATTTGGGCTTTAT	CTCGAG	ATAAAGCCCAAATATCTCACG
E9	TRCN0000048369	GCCAATCCTTATCTTGGGTAA	CTCGAG	TTACCCAAGATAAGGATTGGC

	Sar1B clone ID	Sense	Loop	Anti-sense
C3	TRCN0000100805	GCTCTTTGTGAAAGTGGTTTA	CTCGAG	TAAACCACTTTCACAAAGAGC
C4	V2HS_164893	GGTGAGATATTTGGGCTTTAT	TAGTGAA GCCACAG ATGTA	ATAAAGCCCAAATATCTCACC

siRNA duplexes

Dharmacon (custom made)

siRNA ID	Sense	Anti-sense
Sar1a (duplex C)	*CUACAAGAAAUCCGGAAAAUU*	*UUUUCCGGAUUUCUUGUAGUU*
Sar1a (duplex D)	*AGUCGAGCUUAAUGCUUUAUU*	*UAAAGCAUUAAGCUCGACUUU*
Sar1b (duplex E)	*CAUGAAAGGCUGUUAGAAUUU*	*AUUCUAACAGCCUUUCAUGUU*
Sar1b (duplex G)	*GCUCGGAGAGUGUGGAAAAUU*	*UUUUCCACACUCUCCGAGCUU*